



Role of the novel protein tyrosine phosphatase AUM for cell adhesion

Dissertation zur Erlangung des naturwissenschaftlichen Doktorgrades
der Fakultät für Biologie,
Julius-Maximilians-Universität Würzburg

Vorgelegt von

Amrish Saxena

aus

Rewa (Indien)

Würzburg, 2011

Eingereicht am: 16.08.2011
Mitglieder der Promotionskomitees:

Vorsitzender: Prof. Dr. Thomas Dandekar

1. Betreuer: Prof. Dr. Antje Gohla

2. Betreuer: Prof. Dr. Jörg Schultz

Tag der Promotionskolloquiums :
Doktorurkunde ausgehändigt am :

Contents

1	INTRODUCTION	1
1.1	CLASSIFICATION OF PHOSPHATASES	2
	HAD-SUPERFAMILY OF PHOSPHATASES	3
	CHRONOPHIN	3
1.2	IDENTIFICATION AND CHARACTERIZATION OF NOVEL HAD-PHOSPHATASE AUM	3
1.3	REGULATION OF CELL ADHESION BY PHOSPHATASES AND KINASES	6
1.4	CELL ADHESION ON EXTRACELLULAR MATRIX	8
	FIBRONECTIN	8
1.5	INTEGRINS	9
	INTEGRIN ACTIVATION	10
	BIDIRECTIONAL SIGNALING THROUGH INTEGRINS	11
	INTEGRIN BINDING PROTEINS	14
1.6	FOCAL ADHESIONS	15
1.7	ROLE OF ACTIN DYNAMICS FOR CELL ADHESION ON EXTRACELLULAR MATRIX	17
1.8	REGULATION OF ADHESION DYNAMICS BY RHO GTPASES	18
	DOWNSTREAM EFFECTORS OF RHOA	19
	REGULATION OF RHOA	20
	ROLE OF INTEGRINS IN RHOA ACTIVATION	21
2	AIM OF THE STUDY	22
3	MATERIALS	23
3.1	LIST OF MANUFACTURERS AND DISTRIBUTORS	23
3.2	CHEMICALS	24
3.3	NUCLEOTIDES, NUCLEIC ACIDS AND PRIMERS	25
3.4	PLASMIDS	25
3.5	ANTIBODIES	25
3.6	BACTERIAL STRAIN AND CELL LINES	26
3.7	TISSUE CULTURE REAGENTS AND MATERIALS	27
3.8	OTHER MATERIALS	27
3.9	COMMERCIAL KITS	28
3.10	SOFTWARE AND DATABASES	28
3.11	RNA INTERFERENCE TOOLS	28
3.12	SOLUTIONS & BUFFERS	29
4	METHODS	34
4.1	CELL BIOLOGY METHODS	34
	CELL LINES	34
	TRANSIENT TRANSFECTION	34
	IMMUNOCYTOCHEMISTRY	35
	CONFOCAL LASER-SCANNING MICROSCOPY	36
	RNA INTERFERENCE	36
	VALIDATION OF THE RNAI TOOLS	37
4.2	CELL BIOLOGICAL ASSAYS	39
	CELL SPREADING ON FIBRONECTIN	39
	CELL AREA DETERMINATION OF FIXED CELLS	39
	CELL- ECM ADHESION ASSAY	39
4.3	FLOW CYTOMETRY	41

4.4 MOLECULAR BIOLOGY METHODS	42
PLASMID PREPARATION	42
QUANTIFICATION OF NUCLEIC ACIDS BY PHOTOMETRIC MEASUREMENT	43
RESTRICTION DIGESTS OF PLASMID DNA	43
DNA GEL ELECTROPHORESIS	43
SITE-DIRECTED MUTAGENESIS	43
4.5 PROTEIN BIOCHEMICAL METHODS	44
SAMPLE PREPARATION FOR IMMUNOBLOT ANALYSIS	44
ESTIMATION OF PROTEIN CONCENTRATION	44
SDS-POLYACRYLAMIDE GEL ELECTROPHORESIS (SDS-PAGE)	44
IMMUNOBLOT ANALYSIS	45
REPROBING OF NITROCELLULOSE MEMBRANES	46
4.6 RHOA/RAC1 ACTIVITY ASSAY	46
ACTIVE RHO/RAC PULL-DOWN ASSAY	47
ACTIVE RHOA/RAC1 G-LISA ASSAY	47
5 RESULTS	48
<hr/>	
5.1 AUM KNOCKDOWN BY RNA INTERFERENCE	48
STABLE AUM DEPLETION	48
TRANSIENT AUM DEPLETION	49
5.2 AUM IS INVOLVED IN EARLY CELL SPREADING	50
5.3 AUM REGULATES EARLY CELL-ECM ADHESION	52
GC-1 CELLS PREFERENTIALLY ADHERE TO FN	52
EFFECT OF AUM ON CELL-FN ADHESION	52
5.4 ACUTE AUM DEPLETION ALSO LEADS TO INCREASED CELL ADHESION ON FN	55
5.5 RE-EXPRESSION OF AUM NORMALIZES CELL ADHESION	56
5.6 ACCELERATED ADHESION DUE TO AUM-DEPLETION IS INTEGRIN DEPENDENT	60
5.7 CELL SURFACE EXPRESSION OF INTEGRINS	61
5.8 AUM-DEPLETED CELLS HAVE MORE ACTIVE β1-INTEGRIN ON CELL SURFACE	64
β 1-INTEGRIN ACTIVATION IS FN-DEPENDENT	65
5.9 AUM INFLUENCES ACTIN DYNAMICS DURING ADHESION AND SPREADING	67
5.10 AUM IS A NEGATIVE REGULATOR OF RHOA	68
INCREASED ADHESION DUE TO AUM-DEPLETION IS RHOA/ROCK DEPENDENT	70
5.11 AUM-DEPLETION INDUCES FASTER FOCAL ADHESION MATURATION	73
5.12 AUM-DEPLETED CELLS HAVE MORE PHOSPHOR-TYROSINE CONTENT	75
6 DISCUSSION	77
<hr/>	
6.1 EFFECT OF AUM ON CELL ADHESION AND SPREADING	78
6.2 EFFECT OF AUM DEPLETION ON CELL ADHESION CAN BE RESCUED	79
6.3 INTEGRINS ARE INVOLVED IN AUM MEDIATED CELL ADHESION	80
6.4 EFFECT OF AUM ON INTEGRIN ACTIVATION	81
6.5 AUM MODULATES ACTIN DYNAMICS MEDIATED BY ITS EFFECT ON RHOA	82
6.6 ROLE OF AUM IN FOCAL ADHESION FORMATION AND MATURATION	83
6.7 POSSIBLE MODEL FOR ROLE OF AUM IN CELL ADHESION AND SPREADING	84
7 SUMMARY	86
<hr/>	
8 ZUSAMMENFASSUNG	88
<hr/>	
9 REFERENCES	90
<hr/>	

Contents III

10 CURRICULUM VITAE 107

11 ERKLÄRUNG 109

12 ACKNOWLEDGEMENTS 110

Figure Index

Figure 1: Schematic representation of AUM showing characteristic HAD-motifs and active site.....	4
Figure 2: The “switchblade” model of integrin activation.....	11
Figure 3: Biological consequences of bi-directional integrin signaling.....	13
Figure 4: Integrin binding and activating proteins.....	14
Figure 5: Scheme of migrating cell with focal adhesion initiation and maturation.....	15
Figure 6: Focal adhesion components and assembly.....	17
Figure 7: Schematic diagram showing actin dynamics during cell spreading.....	18
Figure 8: Role of RhoA, Rac1 and Cdc42 in actin dynamics.....	19
Figure 9: Signaling pathways of RhoA and its effectors.....	20
Figure 10: A model for gene inactivation <i>via</i> RNA interference.....	37
Figure 11: Localization of the mAUM siRNA/shRNA in open reading frame of mouse AUM.....	38
Figure 12: Schematic diagram showing conversion of Calcein AM to Calcein by intracellular esterases.....	40
Figure 13: Analysis of AUM expression in mouse tissues.....	48
Figure 14: Stable AUM depletion by shRNA.....	49
Figure 15: Transient AUM depletion by siRNA.....	50
Figure 16: AUM depletion accelerates cell spreading on FN.....	51
Figure 17: GC-1 cells preferentially adhere to Fibronectin.....	52
Figure 18: Adhesion of AUM depleted cells to fibronectin.....	53
Figure 19: AUM depletion accelerates cell adhesion on FN.....	54
Figure 20: AUM depletion accelerates cell adhesion on FN.....	55
Figure 21: Acute AUM depletion also leads to increased cell adhesion on FN.....	56
Figure 22: Re-expression of AUM to rescue AUM depletion.....	58
Figure 23: Re-expression of AUM normalizes increase in cell adhesion due to AUM depletion.....	59
Figure 24: Accelerated adhesion due to AUM-depletion is integrin-dependent.....	61
Figure 25: Cell surface expression of various fibronectin binding integrin subunits..	63
Figure 26: Monoclonal antibody 9EG7 recognizes active conformation of β 1 integrin.....	64
Figure 27: AUM depleted cells have more active β 1 integrin receptors.....	65
Figure 28: β 1 integrin receptor activation is AUM dependent.....	66
Figure 29: AUM depleted cells have more actin stress fibers.....	67
Figure 30: AUM depleted cells have more active RhoA.....	69
Figure 31: AUM depleted cells have more active RhoA.....	70
Figure 32: C3-transferase effectively reduces active RhoA levels in AUM depleted cells.....	71
Figure 33: Increased adhesion of AUM-depleted cells on fibronectin is due to increased active RhoA.....	72
Figure 34: Increased adhesion of AUM-depleted cells on fibronectin is due to increased ROCK activity.....	73
Figure 35: AUM-depletion influences focal adhesion elongation and maturation.....	75
Figure 36: AUM depleted cells have increased phospho-tyrosine content in focal adhesions.....	76
Figure 37: Flow diagram showing possible role of AUM in early cell adhesion to FN.....	84

Abbreviations

µg	Microgram
µl	Microliter
ADP	adenosine diphosphate
APS	ammonium peroxide sulphate
ATP	adenosine triphosphate
mAUM, hAUM	murine or human aspartate based, ubiquitously expressed, magnesium-dependent phosphatase hAUM (NM_001042371), mAUM (NM_025954)
BCA	bicinchoninic acid
BLAST	basic local alignment search tool
BPB	bromophenol blue
cDNA	complementary deoxyribonucleic acid
CIN	Chronophin
CIP	calf intestinal phosphatase
DAB	3,3'-diaminobenzidine tetrahydrochloride
DAPI	4,6-diamidino 2-phenylindole
DEPC	Diethylpyrocarbonate
DMEM	Dulbecco's modified Eagle's minimal essential medium
DMSO	Dimethylsulfoxide
DNA	deoxyribonucleic acid
DTT	Dithiothreitol
E. coli	<i>Escherichia coli</i>
EB	elution buffer
EDTA	ethylene diamine-N,N,N',N'-tetraacetic acid
EGF	epidermal growth factor
EK	Enterokinase
F-actin	filamentous actin
FAK	focal adhesion kinase
FCS/FBS	fetal calf/bovine serum
FN	Fibronectin
FITC	fluorescein-5-isothiocyanate
G-actin	globular actin
GAPDH	glyceraldehyde-3-phosphate dehydrogenase
GC1-spg	mouse spermatogonial cell line
GFP	green fluorescent protein from the jellyfish <i>Aequoria Victoria</i>
HAD	haloacid dehalogenase

HEPES	N-(2-hydroxyethyl)piperazine-N'-(2-ethanesulfonic acid)
HRP	horseradish peroxidase
Ig	Immunoglobulin
Kbp	kilo basepair
kDa	kilo Dalton
LB medium	Luria-Bertani medium
LIMK	LIM kinase (acronym for Lin-11, Isl-1 and Mec-3)
LSM	laser scanning microscopy
MCS	multiple cloning site
mM	Millimolar
NCBI	National Centre for Biotechnology Information
nm	Nanometer
ORF	open reading frame
PCR	polymerase chain reaction
PFA	<i>para</i> -formaldehyde
pH	negative decadic logarithm of the hydrogen ion concentration
Pi	inorganic phosphate
pI	isoelectric point
PLP	pyridoxal 5'-phosphate
<i>p</i> -NPP	<i>para</i> -nitrophenylphosphate
PMSF	phenylmethyl sulfonylfluoride
PTP	protein tyrosine phosphatase
PPM	phosphoprotein phosphatase, magnesium-dependent
PPP	phosphoprotein phosphatase
RE	restriction enzyme
RIPA	radioimmunoprecipitation assay
RNA	ribonucleic acid
RNAi	RNA interference
RT	room temperature
ROCK	Rho associated coiled coil kinase
SDS-PAGE	sodium dodecylsulphate polyacrylamide gel electrophoresis
shRNA	short hairpin RNA
siRNA	short interfering RNA
SOC	super optimal broth with catabolic repression
TBS	Tris-buffered saline
TEMED	N,N,N',N'- tetramethylethylenediamine
Tris	tris (hydroxymethyl)-aminomethane

Triton X-100	t-octylphenoxypolyethoxyethanol
Tween-20	polyoxyethylen-(20)-monolaurate
UV	ultra violet (light)
v/v	volume per volume
w/v	weight per volume
wt	wild type
x g	acceleration due to gravity (9.81 m/s ²)
YFP	yellow fluorescent protein

1 Introduction

Cell adhesion is critical for development, tissue repair and normal homeostasis and its proper regulation is extremely important for sustaining life in multicellular organisms. Adhesion of cells to each other and to the extracellular matrix (ECM) forms the basis of tissue homeostasis. A number of proteins work in a concerted manner to bring about this complex regulation. Three broad classes of macromolecules: the adhesion receptors, the extracellular matrix molecules, and the adhesion proteins act in well orchestrated manner to regulate this complex and critical process of cell adhesion (Gumbiner, 1996). Cell adhesion receptors are transmembrane glycoproteins present on cell surface and mediate binding of cells to ECM molecules and also determine the specificity of cell-ECM interaction. The ECM members are fibrous proteins that provide a platform for cell-ECM adhesion and act as 'molecular glue' for the cell clusters. Though this might sound simple, cell-ECM adhesion is an extremely complex process that is stringently regulated by adhesion proteins. These proteins are not just static architectural entities but are rather capable of sensing and integrating signals from extracellular stimuli for further downstream signaling. This property of adhesion proteins allows them to act as master regulators of cell-ECM adhesion. This is made possible by the capability of these proteins to exist in a functionally active or inactive state. Cell adhesion regulating proteins are able to transmit signal specific information by repeated events of phosphorylation or dephosphorylation, respectively, which also dictates the role of these proteins in signaling specific information to its downstream effectors.

Protein phosphorylation refers to the process of addition of phosphate $[(\text{PO}_4)^{3-}]$ residues to selected amino acids. This is made possible by the action of "Protein Kinases". Phosphorylation of protein by kinase is highly specific given the fact that every kinase has its own choice of substrates/target proteins. In majority of instances a phosphorylated protein is considered active as it can convey essential signaling information further downstream the signaling cascade. The "active" signaling protein must be reverted back to its "inactive" state once it has signaled the information downstream. This is accomplished by protein dephosphorylation. "Protein Phosphatases" have the capability to "dephosphorylate" the same signaling protein which was phosphorylated by the kinase before. Like kinases the dephosphorylation reaction by protein phosphatases is also highly specific in terms of substrate/target protein. This cycling of the phosphate moiety by kinases and phosphatases constitutes the basics of "on and off switch" in cellular/adhesion signaling that in turn governs the precise timing and action of an adhesion event.

Addition of the phosphate moiety on signaling proteins is only possible on 9 different amino acid residues. This includes tyrosine (tyr), serine (ser), threonine (thr), cystine (cys), arginine (arg), lysine (lys) aspartate (asp), glutamate (glu) and histidine (his), with phosphorylation of

tyr, ser and thr being the most prominent in eukaryotic cell signaling (Hunter, 2004). In humans majority of protein phosphorylation occurs on serine residues (86.4% of all protein phosphorylation) followed by thr (11.8%) or tyr (1.8%), respectively.

1.1 Classification of Phosphatases

Protein phosphorylation is a primary means for the regulation of most cellular processes (Hunter, 2007). This is underlined by the fact that protein kinases and phosphatases constitute 2-4% of all cellular proteins encoded by the human genome (Hunter, 2004). As per estimates, 500 different phosphatases are encoded within the human genome alone (Hooft van Huijsduijnen, 1998).

Phosphatases are broadly classified into 2 categories based on their substrate specificity (dephosphorylation of phospho-ser/thr or phospho-tyr residues). The classical and most well studied phospho-ser/thr specific phosphatases in this class fall in the phosphoprotein phosphatase (PPP family) subfamily. This includes extensively studied and well characterized phosphatases like PP1 and PP2A among others.

Other major and relatively new class of phosphatase is involved in dephosphorylation of phospho-tyrosine residues. This superfamily of phosphatases is also referred to as "Phospho-tyrosine phosphatases" (PTPs). PTPs are further divided into 2 subclasses based on their cellular location. Phosphatases that are present in cell membrane are called receptor protein tyrosine phosphatases (RPTPs). As the name signifies, members of this class can regulate cell signaling by ligand-mediated phospho-tyr dephosphorylation. The other subclass of PTPs is the non-transmembrane, cytoplasmic PTPs. These phosphatases have a distinct regulatory sequence flanked by the catalytic domain. Most of the enzymes in this category use their active site to interact with other effector protein/s which in-turn modulates their enzymatic activity. The non-catalytic motif in these phosphatases also dictates the exact localization of the enzyme in cytosol. This mechanism is of critical importance for sustained bioavailability of PTPs for their respective substrates.

So far the above mentioned classification of phosphatases is based on their substrate specificity. This classification cannot be considered complete in itself given the vast diversity of phosphatases. Most phosphatases have cys at their active site which serves as the nucleophile for the dephosphorylation reaction.

Recently a novel group of asp-based phosphatases have begun to emerge. These phosphatases have asp instead of cysteine acting as the nucleophile at their active site and are collectively referred to as HAD (haloacid dehalogenase) family phosphatases.

HAD-superfamily of phosphatases

The HAD-family of phosphatases is a highly conserved archaic family of proteins. Although other families of phosphatases are being studied for more than 3 decades, those utilizing asp-based catalytic mechanism have emerged recently. One of the well studied members of this family is the Eya (eyes absent) phosphatase. Eya derives its name from studies on drosophila where it was shown to be essential for proper eye formation (Bonini et al., 1993). Recent studies have shown important roles for eya in tumor cell migration and invasion (Pandey et al., 2010). Also eya phosphatase has been implicated in transcription control (Jung et al., 2010). Another well known member of HAD-phosphatase family is phosphoserine phosphatase (PSP). As the name suggests PSP is involved in the final step of L-serine biosynthesis (Snell and Fell, 1990). Moreover, recently PSP was shown to be essential for neural stem and progenitor cell proliferation (Nakano et al., 2007).

These examples clearly show the functional importance of this class of enzymes. Our research group is involved in identification and functional characterization of novel HAD-phosphatases. To this end we have successfully identified and characterized two novel members of this family.

Chronophin

Chronophin (CIN) is perhaps the youngest member of this expanding family and was identified in our lab (Gohla et al., 2005). The name chronophin is derived from the Greek word "Chronos" meaning time in Greek as chronophin was shown to regulate cofilin dependent actin dynamics spatially and temporally. CIN, an asp-based phosphatase can directly dephosphorylate ser-3-phospho-cofilin. Moreover CIN was shown to be essential for actin filament reorganization and proper cell division (Gohla et al., 2005). Later work showed that cofilin dephosphorylation by CIN was stimulated by the protease-activated receptor-2(PAR-2) which has been proposed as a therapeutic target for inflammation and cancer (Zoudilova et al., 2007). Additionally, CIN was shown to be actively involved in modulating actin dynamics during epileptogenesis (Kim et al., 2008) and also during induction of long term potentiation (Kim et al., 2009).

1.2 Identification and characterization of novel HAD-phosphatase AUM

The apparent biological importance of CIN prompted us to look for a CIN homologue or a splice variant. By database mining and phylogenetic analysis of human HAD phosphatases, our laboratory identified a previously unknown enzyme with homology to CIN. This novel enzyme was cloned and after initial biochemical characterization was named as AUM, for aspartate based, ubiquitously expressed, magnesium-dependent HAD phosphatase. Murine

AUM is a 34 kDa protein consisting of 321 amino acids. It has 3 characteristic domains of HAD-phosphatases and domain I harbors the characteristic catalytic site DXDX(V/T) (Fig. 1).

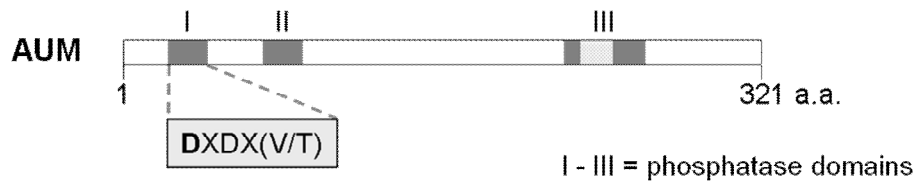


Figure 1: Schematic representation of AUM showing characteristic HAD-motifs and active site

As this work investigates the role of AUM in cell adhesion, its enzymatic and known cellular characteristics will be discussed in details below. In spite of the fact that CIN and AUM are 45% identical and 61% similar at the amino acid level, results of the enzymatic characterization of AUM clearly showed its distinct characteristics in comparison to CIN. By comparing the results from work on the characterization of the serine-directed phosphatase CIN (Gohla, Birkenfeld et al. 2005) and experimental evidence from the initial work on AUM, AUM emerged as a novel tyrosine phosphatase in spite of being the closest CIN homolog (Duraphe, 2009).

P. Duraphe from this lab has shown previously that AUM is an efficient tyrosine-phosphatase. AUM was cloned and successfully overexpressed and recombinant AUM was purified from bacteria. Recombinantly purified AUM was also shown to be biologically active as it efficiently dephosphorylated *para*-nitrophenyl phosphate (*p*-NPP). *p*-NPP is a widely used artificial substrate for tyrosine-phosphatases which can be enzymatically dephosphorylated thereby resulting in release of inorganic phosphate (P_i) and the yellow-colored *p*-nitrophenol. This change in color can be spectrophotometrically measured over time. AUM dephosphorylates *p*-NPP (preferred substrate for tyrosine –phosphatase) much more efficiently than CIN which is a serine-phosphatase.

As mentioned before AUM is a novel HAD phosphatase and therefore must have aspartate at its active site which should act as a nucleophile. To confirm that AUM is an aspartate-based phosphatase, the aspartate at position 34 in the HAD motif I of murine AUM (Fig. 1), (which is predicted to act as a nucleophile), was mutated to asparagine (AUM^{D34N}). The mutant and the wildtype AUM were then expressed in bacteria and purified by affinity chromatography. Subsequently, the *in vitro* phosphatase activities of AUM^{D34N} and AUM^{wt} were analyzed against *p*-NPP. In contrast to AUM^{wt}, which efficiently dephosphorylated *p*-NPP in a concentration-dependent manner, even the highest employed concentration of mutated AUM demonstrated only 1-2% of residual activity against *p*-NPP as compared to the same concentration of AUM^{wt}. Although the biological substrate of AUM remains unknown to-

date, early attempts were made to identify the substrate by conducting a phosphopeptide screen with recombinant AUM. More than 700 phosphopeptides (174 pSer peptides, 58 pThr peptides and 488 pTyr peptides) derived from human proteins were tested. Interestingly, AUM dephosphorylated only pTyr peptides and that too with a high specificity. This establishes AUM as a highly specific tyrosine phosphatase (Duraphe, 2009).

In order to study the role of AUM at protein level, our lab also successfully raised and purified AUM specific polyclonal antibody in rabbit. This antibody was used to screen different mouse organs for the expression analysis of AUM. Although AUM was ubiquitously expressed in all the tissues tested, testis showed highest expression of AUM. Therefore GC-1 (mouse spermatogonia derived cell line) cells were used to study the cellular function of AUM. These cells were stably depleted of AUM using AUM-targeting shRNA and this was confirmed by western blotting.

AUM was also established as tyrosine-phosphatase at the cellular level. To this end, control and AUM-depleted GC-1 cells were stimulated with the epidermal growth factor (EGF) to induce EGF receptor-mediated tyrosine phosphorylation for different time points and probed for global changes in tyrosine-phosphorylated proteins using a phosphor-tyr specific antibody. AUM-depleted GC-1 cells clearly showed increased tyrosine phosphorylation after EGF stimulation. These results clearly show that AUM acts as a tyrosine-phosphatase even at cellular levels.

On a cellular level, AUM-depleted cells are characterized by altered actin cytoskeletal dynamics and adhesion, as indicated by stabilized actin filaments, enlarged focal adhesions, a marked increase in cell area of spreading cells, as well as accelerated cell spreading on fibronectin. Cells treated with latrunculin A (a G-actin sequestering drug) showed a stabilization of actin stress fibers in cells overexpressing AUM^{D34N} as well as in AUM depleted cells. In contrast, AUM^{wt} overexpressing cells showed fewer F-actin structures than control cells. These data strongly supports the hypothesis that AUM is involved in the regulation of actin filament turnover in cells. Also, AUM^{wt} overexpressing cells were less adherent to the substratum and smaller in size when spread on fibronectin. In contrast, AUM^{D34N} expressing cells were found to be advanced in spreading under similar conditions (Duraphe 2009). So far discussed identification and initial characterization of AUM is currently being prepared for publication as a part of doctoral thesis of P. Duraphe.

The above observations regarding involvement of AUM in cell-matrix adhesion prompted us to study role of AUM in details with respect to AUM-dependent cellular interaction and signaling involved in cell adhesion and spreading. This aspect is the main emphasis of this work. Therefore, regulation of cell adhesion and various components involved in this process will be discussed in detail.

1.3 Regulation of cell adhesion by phosphatases and kinases

Almost four decades back striking micrographs from electron microscope facilitated the first visualization of focal adhesion structures (Abercrombie et. al., 1971). Here focal adhesions were described as dense, pointed objects in close proximity to plasma membrane. Since then our understanding of focal adhesions formation and function has increased enormously. Focal adhesions are actually complexes of more than 50 proteins involved directly or indirectly in cell adhesion. Most of these proteins interact with integrin heterodimer present on cell surface either directly or interact with proteins that bind directly to the integrin receptor. The composition and characteristic of focal adhesion and their link to integrins will be discussed in details in later section.

One of the major functions of focal adhesion complex is to provide mechanical stability to the adhering cells. Apart from this they also serve as origins for biochemical signaling. Focal adhesions are capable of performing these functions as a result of tightly regulated interplay of phosphatases and kinases. Well orchestrated and sequential events of phosphorylation and de-phosphorylation of scaffold proteins by kinases and phosphatases are responsible for cell-matrix adhesion and subsequently cell migration.

One of the key signaling events at focal adhesions is the tyrosine phosphorylation. Many important and well studied components of focal adhesions like FAK (focal adhesion kinase), Src, vinculin and paxillin are all phosphorylated before recruitment to the focal adhesions. Tyrosine phosphorylation at focal adhesion sites is majorly enforced by kinases like Src and FAK. Both these kinases bind specifically to their interactors to regulate focal adhesion dynamics and cell behavior.

As the name implies FAK is an important signaling component of focal adhesion complex. FAK is a high molecular weight tyrosine kinase known to be localized in focal adhesions (Schaller et al., 1992). It has been proven beyond doubt that localization of FAK to focal adhesion is absolutely critical for its function as mutants lacking c-terminal FAT (focal adhesion targeting) domain of FAK fail to localize at focal adhesions and are unable to phosphorylate down-stream FAK substrates post cell-matrix adhesion (Shen and Scheller, 1999). Interestingly, FAK is capable of auto-phosphorylation thereby rendering itself capable for self activation. Autophosphorylation of FAK at tyr397 (Y397) is believed to be responsible for FAK activation (Schaller et al., 1994). The phosphorylated Y397 acts as a binding site for another tyrosine kinase, Src, which in turn phosphorylates FAK at Y576 and Y577. These two subsequent phosphorylations by Src further enhance FAK activity (Calalb et al., 1995). Also Src plays a critical role in phosphorylating Y861 and Y925 in FAK and this is believed to create new docking sites for SH-2 domain containing components of focal adhesions like Grb2. Grb2 is capable of connecting Ras and MAPK signaling to FAK (Schlaepfer et al., 1998).

Interestingly, Src is also activated when its SH2 (Src homology) domain binds to FAK pY397 (Hanks et al., 1997). Once Src is activated it is rendered capable of phosphorylating various components of focal complex like FAK, p130cas and paxillin. Proper targeting of Src to focal adhesion complex is absolutely essential for its regulation and function (Li et al., 2002). Apart from this, Src and its family of kinases (SFK) are known to bind directly to β integrin cytoplasmic tails. The enzymatic activity of Src is critical for proper execution of various cellular processes like cell-matrix adhesion and overall focal adhesion turnover (Aria-Salgado et al., 2003).

One can envisage that if phosphorylation is important in regulation of focal adhesion complex formation, dephosphorylation of its components is equally important. Phosphatases present in focal adhesion complexes are responsible for regulating signals originating from focal complexes. Also phosphatases can disassemble focal complexes resulting in overall focal adhesion turnover, eventually leading to altered cell migration. One such phosphatase found at focal complex is PTP-PEST. Importance of PTP-PEST in focal complexes can be assessed by the fact that cells lacking PTP-PEST show increased number of focal adhesions and decreased cell migration (Angers-Loustau et al., 1999). On the contrary, overexpression of PTP-PEST leads to a strong increase in p130Cas phosphorylation, thereby rendering p130Cas unable to redistribute at focal complexes. Aberrant p130cas phosphorylation in the absence of PTP-PEST results in inefficient binding of p130cas to its interactors (Garton and Tonks, 1999). However cell migration is inhibited by both deletion and overexpression of PTP-PEST.

Depletion or overexpression of PTP-1B leads to decreases in cell adhesion, motility and focal adhesion formation (Hassid et al., 1999; Liu et al., 1998). PTP-1B is believed to be a negative regulator of adhesion signaling by directly dephosphorylating p130cas (Liu et al., 1998).

SHP-2 is another ubiquitously expressed phosphatase localized in focal adhesions and has been implicated in growth factor signaling and integrin signaling (Neel et al., 2003). Reports suggest that post-cell adhesion, integrin engagement leads to pp60^{Src}-dependent phosphorylation of SHPS-1. SHPS-1 is the known biological substrate of SHP-2. Phosphorylated SHPS-1 recruits SHP-2 which leads to further activation of pp60^{Src} (Zhang et al., 2004). Active pp60^{Src} in turn is responsible for FAK activation. Although this mechanism remains controversial, still role of SHP-2 in FAK activation is absolutely certain.

The above examples of phosphatases and kinases in focal adhesion assembly and signaling clearly emphasize the fact that involvement of a tight regulation of tyrosine phosphorylation and dephosphorylation is of critical importance in focal adhesion complexes. This also indicates that a proper balance of focal adhesion components is a key regulator of basal cellular processes like adhesion and migration.

1.4 Cell adhesion on extracellular matrix

Maintenance of cellular adhesive interactions is critical for sustenance of eukaryotic life. Cell adhesions exist between adjacent cells and also with the extracellular matrix (ECM), while the earlier type being classified as “Cell-cell adhesion” and later as “Cell-ECM adhesion”. Cell-ECM adhesion is the basic process through which cells interact and communicate with the extracellular environment. This also enables cells to receive and subsequently transduce vital signaling information in response to various extracellular stimuli.

Cell migration is essential for embryonic development, inflammatory immune response, wound repair and tumor formation and metastasis (Costa and Parsons, 2010). Cell migration essentially follows cell-ECM adhesion. After receiving migratory cues, adhering cells show initial protrusion at the leading edge of the cells. These protrusions referred to as lamelliopodia are driven by the polymerization of actin filaments and are stabilized by the formation of focal adhesion complexes (Wolfenson et al., 2009). As cells migrate, the nascent adhesion complex tends to mature into larger and more organized focal adhesions. Focal adhesions serve as a site of traction over which the cell body moves further (Shattil et al., 2010).

As a result, there is a constant formation and maturation of focal adhesion sites. This turnover is inevitable for continued movement of cells. However, at the rear end of the migrating cell older adhesion contacts need to be released for the cell body to move forward resulting in “focal adhesion turnover”. This dynamic turnover is tightly controlled by well orchestrated interplay of kinases and phosphatases. Therefore it can be concluded that kinase and phosphatase mediated control of cell-ECM adhesion is a pre-requisite for effective cell migration. This is evident by the fact that alterations of cell-ECM adhesion are also frequently associated with human diseases such as metastatic tumors. Transformed cell relies heavily on the properties of cell adhesion and migration for tumor invasion and metastasis.

Fibronectin

ECM exists as an interlocked mesh composed of various proteins and glycosaminoglycans. Fibronectin (FN) is one of the primary components of ECM and has major contribution in maintenance of cell adhesion, migration, growth and differentiation (Yamada and Clark, 1996). FN is ubiquitously expressed by a majority of cell types and is crucial for survival, given the fact that FN gene depletion inactivation leads to embryonically lethal mouse (Pankov and Yamada, 2002).

In nature FN exists as a dimer consisting of two identical subunits of 250kDa and both the subunits are connected to each other at their C-termini by two disulphide bonds. Majorly three types of repeating units constitute a monomer of FN (Patel et al., 1987).

Based on solubility, FN can exist either as soluble or insoluble FN. Soluble form of FN is the major constituent of plasma (300µg/ml) and other body fluids. However, it is the insoluble form of FN which constitutes the major component of ECM.

Liver is the major site for FN biosynthesis with hepatocytes being actively involved in the process. As a result of alternative splicing, FN exists in many variants and each variant has different roles for cell adhesion and ligand-binding. This variation in FN isoforms presents the cell a mechanism for alteration in ECM composition based on special needs.

FN type III repeat is responsible for FN binding to integrins. This repeat is 90 amino acids long and is known to occur at least 15 times in each monomer of FN (Pankov and Yamada, 2002).

Integrins recognize FN at the specific tripeptide (Arg-Gly-Asp, or RGD) sequence present on FN. The RGD sequence is present in the type III repeat of FN. The importance of this sequence can be evaluated by the fact that very short peptides containing this RGD sequence are able to compete with FN for the binding site on cell. This competition is strong enough to inhibit overall cell adhesion to FN matrix coated surfaces *in vitro* in a dose dependent fashion (Craig et al., 1995).

1.5 Integrins

Integrins are transmembrane receptors present on the plasma membrane. They exist as heterodimers and interact with extracellular ECM to facilitate cell-ECM adhesion. An integrin molecule is composed of two non-covalently associated glycoprotein subunits called α and β . Both subunits span the cell membrane, with short intracellular C-terminal tails and large N-terminal extracellular domains (Fig. 2). The extracellular portion of the integrin dimer recognizes specific amino acid sequences in ECM proteins such as the RGD tripeptide present in fibronectin. At least 24 distinct combination of integrin heterodimers are known to exist which are formed by the combination of 18 α -subunits and 8 β -subunits. Specific integrin heterodimers preferentially bind to distinct ECM proteins. The repertoire of integrins present on a given cell dictates the choice of ECM component to which the cell will adhere to and migrate (Pytela et al. 1985). This renders integrins as sensors of ECM composition. Integrins have divalent cation binding domains located on the extracellular part of α and β subunits. The binding of integrin to their ligands is heavily influenced by the availability of extracellular divalent cations. Cations like Mg^{2+} and Ca^{2+} , depending on the integrin type, regulate binding of integrin to the ECM. These cations influence the affinity as well as

specificity of integrin binding to its ligand. For example, *in vitro* studies have shown that FN binds to $\alpha 5\beta 1$ integrin only in the presence of 1mM Ca^{2+} and Mg^{2+} (Bazzoni et al., 1995). On the contrary, Fibrinogen (Fg), a glycoprotein important for platelet aggregation that can form heteropolymers with FN is unable to bind $\alpha 5\beta 1$ integrin in the presence of Ca^{2+} and Mg^{2+} (Suehiro et al., 1997).

Integrin activation

Structural studies have shown that integrins exist in 2 conformational states. As per established models integrins show a bent conformation which is considered inactive as integrins in this state have low affinity for ligands. The other conformational state of integrin is the extended conformation. Here the integrins are able to bind their ligands with high affinity and are capable of signaling (Xiong et al., 2001; Takagi et al., 2002; Zhu et al., 2008). Integrins are able to demonstrate two conformational states as a result of bending of extracellular domains between the thigh and calf-1 domain of the α subunit. The β subunit is also able to achieve an inactive or bent conformation due to flexible movement between I-EGF domain 1 and 2. In order to obtain the active conformation, the ectoplasmic domains need to switch to an extended conformation. The extension is believed to be initiated by separation of the cytoplasmic and transmembrane domains upon binding of integrin binding proteins to β integrin cytoplasmic domains. This model of long range conformational changes is referred to as "switchblade" model (Fig 2). However, it is still disputed if integrins can adopt different bent conformations without losing the capability to bind ligands with varying affinities (Carman and Springer 2003; Arnaout et al., 2005).

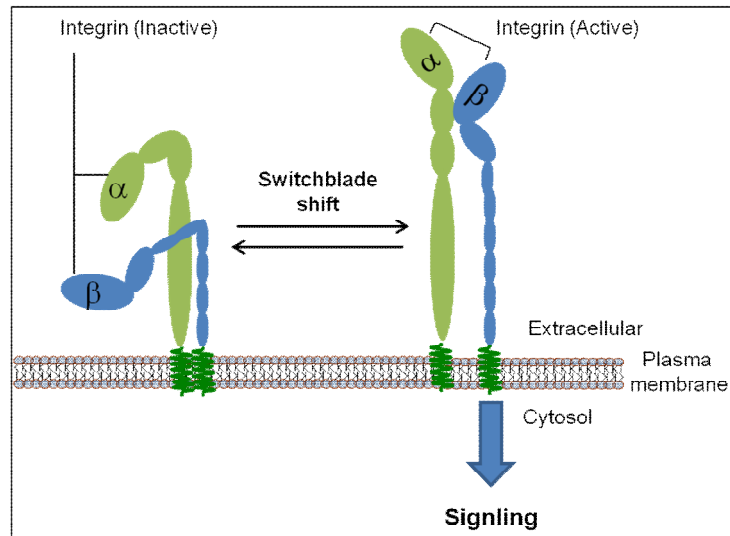


Figure 2: The “switchblade” model of integrin activation.

Inactive integrin is in the bent conformation with low affinity for the ligand. Binding of ligand or cytoplasmic proteins like talin or kindlin to the β subunit leads to separation of the cytoplasmic tails (opening) and extension of the ectodomains (switchblade shift) which renders ligand binding pocket in the head domain accessible for the ligand. Ligand-bound integrin is present in the extended, active conformation capable of downstream signaling (Xiong et al., 2003).

Although most antibodies raised against integrins recognize them irrespective of their conformational states, some monoclonal antibodies are capable of differentiating distinct integrin conformations. Such conformation specific antibodies have greatly enhanced our understanding of integrin activation in response to various stimuli like divalent cation and ligand binding. Also the role of focal adhesion constituents in integrin activation has been deeply studied with the help of such antibodies (Bazzoni et al., 1998). Interestingly, some antibodies are also able to stimulate adhesive function of integrins. Although the exact mechanism by which this is made possible remains debatable, still it is believed that these antibodies are able to aid integrin mediated adhesion by stabilizing the active integrin conformation (Bazzoni et al., 1995). Monoclonal mouse antibody 9EG7 is one such antibody directed against activated conformation of $\beta 1$ integrin and is able to detect reliably ligand binding to integrin (Bazzoni et al., 1995).

Bidirectional signaling through integrins

Integrin activation is regulated by intracellular signals. On the other hand, extracellular ligand binding also renders integrin in active conformation. Both ways of integrin activation result in different biological consequences. This dynamic bidirectional mode of integrin regulation provides the cell with an opportunity to carefully sense the extracellular environment and react to various stimuli.

When intracellular integrin activators like talin or kindlin (Anthis and Campbell, 2011) interact with β integrin tail on the cytoplasmic side, integrins undergo conformational changes resulting in enhanced affinity for extracellular ligands (integrin activation). This mode of signaling is termed 'inside-out' signaling. It has been shown beyond doubt that binding of head domain of talin to β integrin cytoplasmic tail results in dissociation of α and β tails thereby inducing a conformational change in the extracellular region (Fig. 3). This conformational change is responsible for increased affinity of integrins for its ligands (Ginsberg et al. 2005). This inside-out signaling is majorly involved in regulation of adhesion strength thereby enabling strong binding between integrins and the ECM. This interaction allows integrins to transmit signals for cell migration and ECM remodeling and assembly (Shattil et al., 2010).

On the other hand, integrins are capable of behaving like traditional signaling receptors where they transmit information inside cell by 'outside-in' signaling. Upon ligand binding integrins cluster at the plasma membrane and subsequently transduce signals to the cell interior. Like talin, extracellular ligand binding also induces conformational change leading to separation of α and β cytoplasmic domains subsequently leading to interaction of cytoplasmic tails with intracellular signaling molecules (Arnaout et al., 2005).

Signaling molecules that interact with integrins in an event of 'outside-in' signaling include kinases like FAK and Src, small GTPases like Rho, Rac and Cdc42 and scaffolding proteins (acting as adaptor molecules) like cas and paxillin. Post-ligand binding association of integrin heterodimers with the above mentioned proteins result in a complex formation at the integrin cytoplasmic tail collectively referred to as focal adhesion complex. Outside-in signaling is believed to control cell polarity, cytoskeleton structure, gene expression, cell survival and proliferation (Shattil et. al., 2010, Fig. 3).

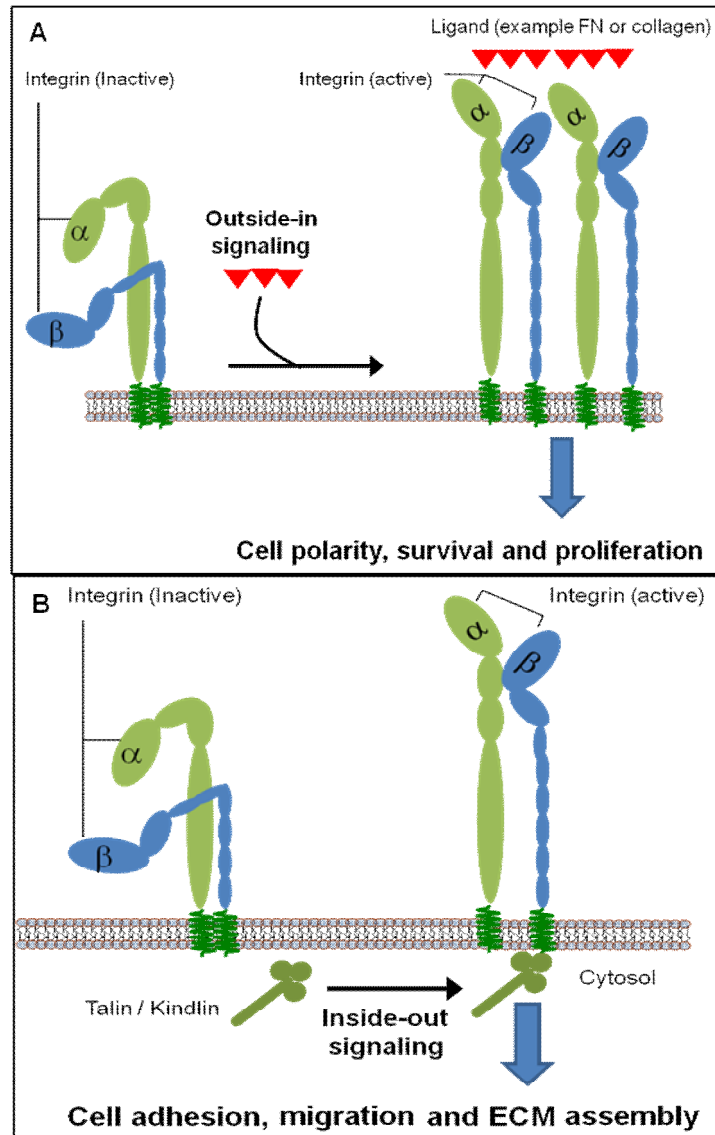


Figure 3: Biological consequences of bi-directional integrin signaling

- (A) Integrins behave like traditional signaling receptors. Integrins are activated upon ligand binding. Ligand binding to integrins causes changes in their conformation and leads to integrin clustering. Both these events together exert effects such as modulating cell polarity, survival and proliferation. This pattern of integrin signaling is termed 'outside-in' signaling.
- (B) In this model integrins are activated as a result of interaction of their cytoplasmic tails with integrin activating proteins like talin or kindlin. This binding leads to conformational changes that result in increased affinity for extracellular ligands (integrin 'activation'). This 'inside-out' signaling controls adhesion strength. The force generated by strong integrin–ECM interaction governs cell migration and ECM remodeling. (Taken from Shattil et. al., 2010).

Above discussed two modes of signaling, although conceptually different, are often closely linked together and in most cases occur in tandem.

Integrin binding proteins

To date, more than 20 different proteins have been shown to directly interact with integrin cytoplasmic tails, with most of them binding to the β subunit. These include actin-binding proteins (e.g. talin, α -actinin), kinases (FAK), adaptor proteins (i.e. kindlin, paxillin, ILK), transcriptional co-activators (JAB1), transmembrane proteins (CD98) and guanine nucleotide exchange factors (Cytohesin-1, -3) (Calderwood et al., 2000). Some of these proteins are depicted in Fig. 4.

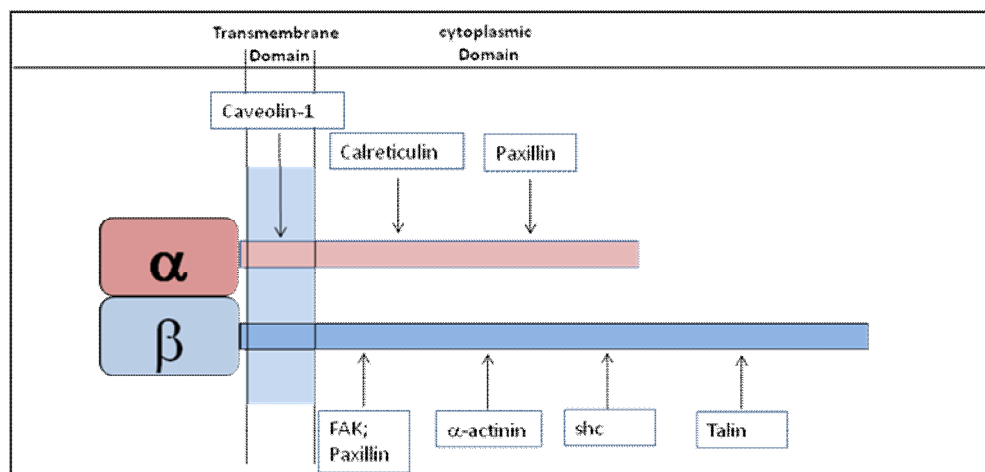


Figure 4: Integrin binding and activating proteins

Diagram showing various integrin binding adaptor/signaling proteins. Focal adhesion kinase (FAK), paxillin, actinin, Shc and Talin bind to β -integrin cytoplasmic tail. α -integrin has a relatively short cytoplasmic tail and is known to interact with paxillin and calreticulin. (Taken from Liu et al., 2000)

Integrins not only act as receptors for extracellular stimuli but also provide mechanical support to the adhering cell. In order to do so, integrins are able to establish direct connection with the cytoskeleton, as actin is the major apparatus inside a cell to facilitate cell spreading, migration and matrix assembly. Integrin-actin link is established by direct or indirect interaction of actin binding proteins with cytoplasmic integrin tails. Talin was the first actin binding protein shown to bind directly to integrin. Talin co-localizes with integrin at specific sites and this interaction mediates connection between integrin and actin cytoskeleton (Horwitz et al., 1986). Talin-integrin interaction is critical for cell survival as talin depleted cells show membrane blebbing and fail to adhere to ECM (Priddle et al., 1998). Talin consists of a large C-terminal rod domain that harbours an N-terminal FERM domain. This domain has further 3 subdomains F1, F2 and F3. It is the F3 subdomain that imparts talin a high affinity for binding to integrin (Calderwood et al., 2002). Apart from talin other proteins like α -actinin, shc, paxillin and calreticulin are known to bind to integrins. All these proteins are involved in FA assembly.

1.6 Focal adhesions

As mentioned before ligand (FN) binding to integrins promotes integrin clustering and subsequent recruitment of actin filaments to the integrin cytoplasmic domains. This process is facilitated by a family of integrin binding proteins including talin, vinculin, α -actinin and filamin. Based on morphological and molecular criteria most cell-ECM adhesion structures can be classified as nascent adhesions, focal complexes focal adhesions and fibrillar adhesions (Fig. 5).

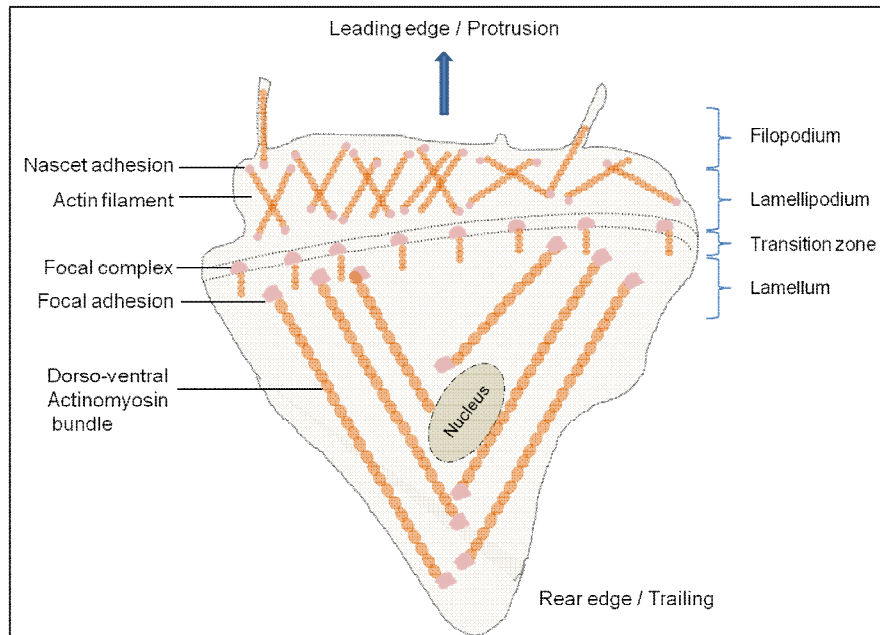


Figure 5: Scheme of migrating cell with focal adhesion initiation and maturation.

Cell adhesion is closely linked to repeated events of cell protrusion at the leading edge. As cell protrudes it displays distinct structures like filopodia and lamellipodia. These structures are supported by actin reorganization within the cell. Early nascent adhesions initially form at the lamellipodium and mature into focal complexes at the 'transition zone' between lamellipodium and lamellum. Focal adhesions further enlarge and orient themselves centripetally. This is accompanied by the bundling and cross-bridging of actin filaments (not shown in above figure) resulting in large focal adhesions located at the ends of thick actinomyosin bundles (Taken from Parsons et al., 2010).

Dynamic process of adhesion structures formation, maturation and disassembly (focal adhesion turnover) is governed by actin polymerization and actomyosin contraction. Cells spreading on FN-coated surfaces show small, short-lived 'nascent adhesions' formed immediately behind the leading edge. These structures rapidly mature and assume larger, dot like shape called 'focal complexes'. Focal complexes lie slightly behind the leading edge of the cell. These are larger in size and persist for several minutes. As cells continue to spread focal complexes further mature into even longer 'focal adhesions'. These are present at the ends of large actin bundles or stress fibers from near the front of the cell along the sides to the cell centre.

To date, more than 60 focal adhesion proteins have been identified in vertebrates. The assembly of these proteins occurs concomitantly with the maturation of adhesion structures (Vicente-Manzanares et al., 2009). This assembly of adhesion proteins enhances mechanical coupling between the F-actin and extracellular matrix and regulates the cycle of adhesion assembly/disassembly.

As soon as cell encounters ECM, connections between cytosolic actin and transmembrane integrin are formed by talin (Jiang et al., 2009). Talin binding in turn induces conformational changes in integrin to enhance binding to the ECM (Calderwood et al., 1999). As a result of integrin clustering and subsequent activation, focal adhesion kinase (FAK) is recruited to the focal adhesion assembly (Roca-Cusachs et al., 2009). Auto-phosphorylation of FAK at 397-Tyr residue activates FAK (Friedland et al., 2009). Active FAK initiates integrin-mediated signaling and phosphorylation of other focal adhesion proteins like paxillin and p130cas (Zaidel-Bar et al., 2007). Subsequently, vinculin is recruited to the focal adhesion and this reinforces mechanical connection between F-actin and transmembrane integrin (Vicente-Manzanares et al., 2009). These signaling and compositional changes promote focal adhesion growth from nascent adhesion structures to an elongated and mature focal adhesion and are accompanied by the recruitment of α -actinin and zyxin, finally leading to association with F-actin (Vicente-Manzanares et al., 2009). Therefore in cell-ECM adhesion orderly assembly of scaffolding and signaling protein is involved in regulation of mechanical interaction between F-actin and ECM (Fig. 6).

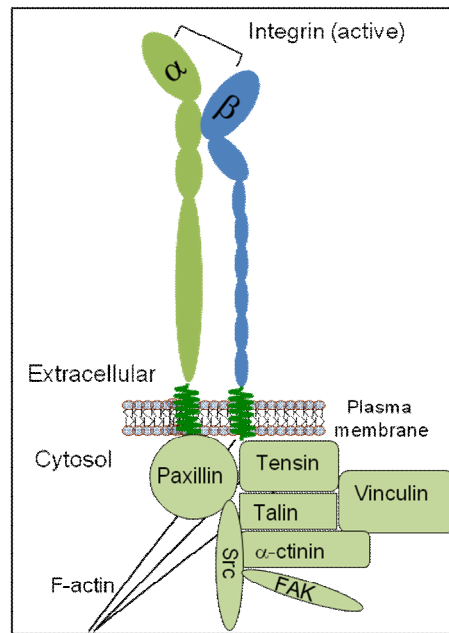


Figure 6: Focal adhesion components and assembly.

Within the cell, the intracellular domain of integrin binds to the cytoskeleton (actin) through adapter proteins such as talin, α -actinin, tensin, vinculin and paxillin. Many other intracellular signaling proteins, such as focal adhesion kinase (FAK) and Src also bind to and associate with these integrin-adapter protein-cytoskeleton complex. This interaction forms the basis of a focal adhesion (Huvneers et. al., 2009)

1.7 Role of actin dynamics for cell adhesion on extracellular matrix

As soon as cells in suspension encounter FN or other ECM molecules they undergo actin reorganization following distinct sequential events. In early phases of adhesion, cells attach and begin to spread on the FN. During this process actin reorganizes near the plasma membrane thus giving rise to cortical actin. Shortly after, cells are maximally enlarged; actin is organized in thin stress fibers. Towards the completion of adhesion process cells are stretched by tensile forces of actin stress fibers. At this point, stress fibers are anchored to the plasma membrane at mature focal adhesion structures (Fig. 7).

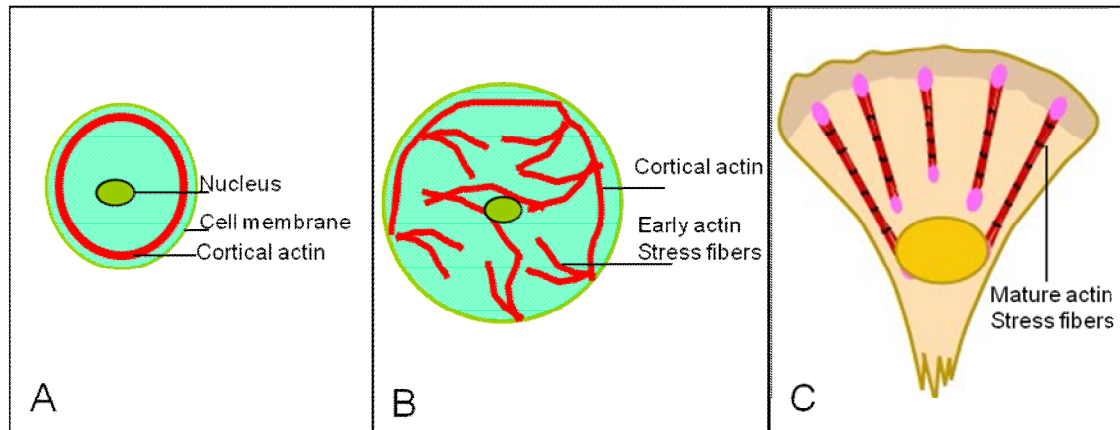


Figure 7: Schematic diagram showing actin dynamics during cell spreading.

Actin reorganization is coupled with cell spreading. When cells encounter an ECM protein like FN their actin is organized towards the cell periphery in bundles called 'cortical actin' (A). As the cell continues to spread it becomes larger in size and its cortical actin begins to diminish and fine early actin 'stress fibers become visible at the lamella (B). Finally, most of the cortical actin is reorganized into thick actin stress fibers and as a result of actinomyosin contractility cells appear to be contracted along the plasma membrane (C) (Loosli et al., 2010).

1.8 Regulation of adhesion dynamics by Rho GTPases

Communication between integrin receptors and the actin cytoskeleton is critical for integrity and stability of cell-ECM adhesions. Integrin involvement in focal complex formation and focal adhesion assembly is regulated by Rho GTPases (Humphries et al., 2005). RhoGTPase belong to the Ras superfamily of proteins which consists of at least 20 members. RhoA, Rac1 and Cdc42 are the most prominent and well characterized members of this superfamily. A hallmark feature of proteins belonging to this family is their ability to switch between an active GTP-bound form that can interact with downstream effectors, and an inactive form that is bound to GDP (Wennerberg et al., 2005).

RhoA, Rac1 and Cdc42 cooperate with each other to regulate cytoskeletal assembly as well as actin and myosin disassembly dynamics. The effect of these proteins on cytoskeleton was first revealed by landmark experiments from the laboratory of Alan Hall, where cells were microinjected with constitutively active members of Rho GTPases and their effect on actin organization was studied (Ridley and Hall, 2004; Nobes and Hall, 1995). Membrane-proximal, activated Cdc42 initiates actin polymerization and bundling. This leads to the formation of filopodia or microspikes on cell surface. In contrast, constitutively active Rac 1 initiates actin polymerization at the cell periphery thereby giving rise to sheet-like lamellopodial extensions and membrane ruffling. Furthermore, active RhoA triggers integrin clustering with integrin-associated proteins like FAK, p130cas and Src to form focal adhesions (Schoenwaelder and Burridge, 1999). RhoA activation also promotes bundling of actin filaments with myosin II filaments to form stress fibers (Hall, 1998) (Fig.8).

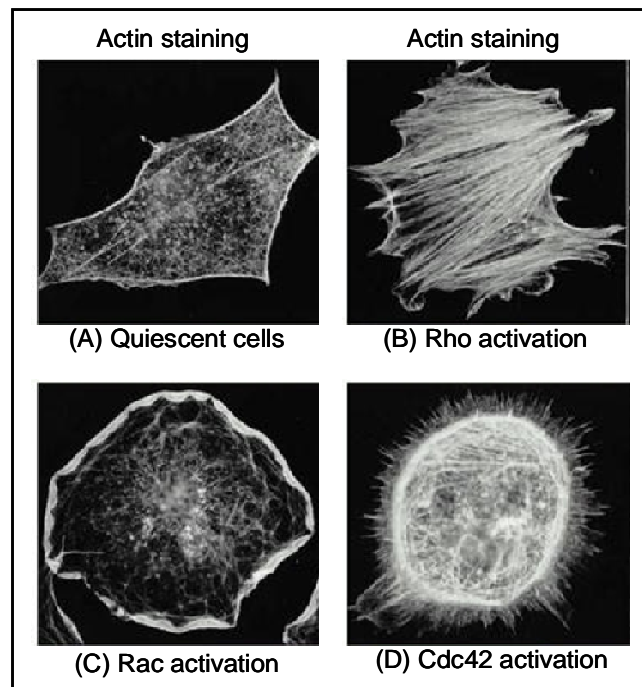


Figure 8: Role of RhoA, Rac1 and Cdc42 in actin dynamics.

The actin filaments have been labeled with fluorescent phalloidin. (A) Serum-starved fibroblasts showing very few actin stress fibers. (B) Microinjection of a constitutively activated form of RhoA causes the rapid assembly of many prominent stress fibers and the cell appears to be heavily contracted (C) Microinjection of activated Rac1 results in the formation of membrane ruffles with strong cortical actin accumulation and relatively very few actin stress fibers (D) Constitutively activated Cdc42 causes the protrusion of many long filopodia at the cell periphery and cell has a circular appearance with dense actin staining (Taken from A. Hall, 1998)

Traditionally, both Rac1 and Cdc42 are considered to be active at the leading edge of migrating and spreading cells (Nobes and Hall, 1995). On the contrary RhoA has been assumed to act at the rear of migrating cells to induce tail retraction (Xu et al., 2003). However, recently this notion is changing as FRET-based ratiometric image analysis of live cells has revealed that the activities of RhoA, Rac1 and Cdc42 are spatio-temporally regulated at the leading edge of spontaneously migrating fibroblasts. Here it was shown that RhoA activation precedes membrane protrusion, whereas Rac1 and cdc42 have a role in reinforcement and stabilization of newly expanded protrusions (Machacek et. al., 2009).

Downstream effectors of RhoA

Apart from its role in actin polymerization, RhoA also acts as a signal transducer. RhoA transduces signal information to downstream effectors, such as the Rho-associated coiled-coil forming kinase (ROCK) (Leung et al., 1995; Ishizaki et al. 1996; Matsui et al., 1996; Nakagawa et al., 1996) and mDia (Watanabe et al., 1997) to elicit its effect on cytoskeletal

reorganization. RhoA directly binds the Rho-binding domain (RBD) of ROCK and stimulates its kinase activity. ROCK1 is a serine/threonine kinase that phosphorylates and activates LIM-kinase 1, which in turn phosphorylates and de-activates cofilin (Fig. 9).

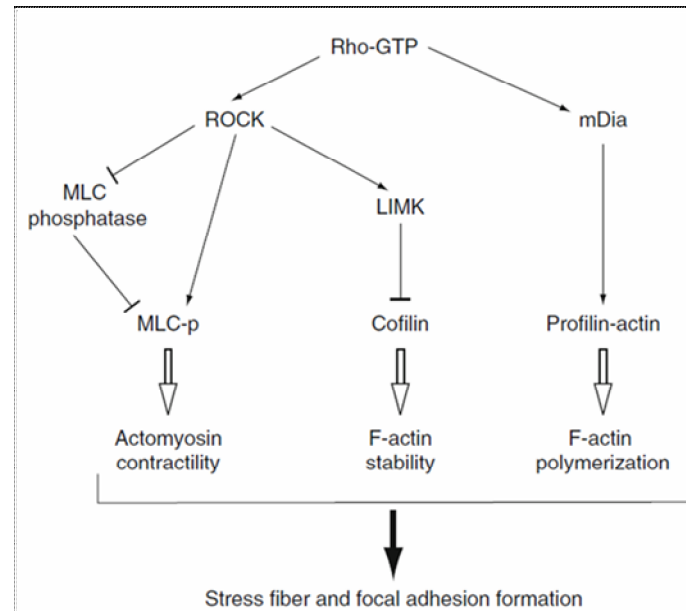


Figure 9: Signaling pathways of RhoA and its effectors.

Hierarchical role of RhoA and its downstream effectors in mediating the effects of RhoA on stress fiber and focal adhesion formation (Pellegrin and Mellor, 2007, Narumiya et al., 2009).

Inactive cofilin results in inhibition filamentous actin de-polymerization in lamellipodia thereby giving rise to rho mediated stress fiber formation (Maekawa et al. 1999).

Downstream of RhoA, ROCK can activate myosin in two ways. Primarily, ROCK increases myosin light chain (MLC) phosphorylation by inhibiting the MLC phosphatase (Kimura et al. 1996). ROCK is also able to directly phosphorylate the regulatory myosin light chain (Amano et al. 1996). On the contrary, mDia triggers actin nucleation and extension of non-branched actin filaments. Although ROCK and mDia act independently of each other, their concerted action is essential for Rho-induced actin reorganization (Narumiya et al. 2009) (Fig.9). Depending on the balance of their activities, they promote actin fibers of various thicknesses and densities (Watanabe et al. 1999).

Regulation of RhoA

As mentioned before regulation of RhoA activity is governed by the GDP/GTP activation cycle. Guanine nucleotide exchange factors (GEFs) are signaling proteins involved in exchange of GDP for GTP and in this process activate their downstream targets such as RhoA. RhoA is active and capable of signaling when bound to GTP. Opposite to GEFs in

action, GTPase activated proteins (GAPs) function to switch-off RhoA signaling by exchanging GTP-bound RhoA with GDP-bound RhoA (inactive). Members of Dbl family of proteins are known to act on RhoA as GEFs. Around 70 members of this family have so far been identified in mammals (Rossman et al., 2005). The sub-cellular localization of Dbl protein governs the spatio-temporal activation of RhoA in response to different stimuli (Schmidt and Hall, 2002). Activation dependence of RhoA due to the changes in sub-cellular localization of a prominent member of this family p190RhoGEF serves as a mechanistic link between cytoskeletal dynamics and RhoA signaling (van Horck et al., 2001; Zhai et al., 2003).

Similar to GEFs, GAPs are also a multifunctional protein family consisting of over 80 family members (Moon and Zheng, 2003). One of the best studied members of this family, p190RhoGAP, when stimulated is shown to suppress integrin signaling transiently. Expression of dominant negative p190RhoGAP results in impaired cell spreading on FN, reduced cell protrusion, and premature assembly of stress fibers. Conversely, over expression of p190RhoGAP augments cell spreading. Also dominant negative p190RhoGAP elevates RhoA activity in cells on fibronectin and inhibits migration. On the contrary, over expression of the wild-type p190RhoGAP decreases RhoA activity, promotes the formation of membrane protrusions, and enhances cell motility (Arthur and Burridge, 2001).

Role of Integrins in RhoA activation

Activation of RhoA post cell adhesion to FN could potentially be regulated via different integrin receptors ($\alpha v\beta 3$ and/or $\alpha 5\beta 1$). $\beta 1$ integrin deficient cells when transfected with either $\beta 1$ or $\beta 3$ subunit and spread on FN show a biphasic regulation of RhoA. However the same was not observed with $\beta 3$ -expressing cells. Interestingly, $\beta 1$ and $\beta 3$ expressing cells show different patterns of focal adhesion formation (Danen et al., 2002). A later report by the same group investigated the effects of different integrins on the ability of cells to migrate on FN. Adhesion to FN through $\beta 1$ integrins (causing high RhoA activity) promoted random migration, whereas adhesion through $\beta 3$ integrins (causing lower RhoA activity) promoted migration in a persistent and polarized manner. Inhibition of RhoA activity in the $\beta 1$ -expressing cells promotes persistent migration similar to cells expressing $\beta 3$ integrin subunit. Interestingly, the type of integrin involved significantly affects the dynamics of the focal adhesions. Cells adhering through $\alpha 5\beta 1$ integrin heterodimers show dynamic focal adhesions with rapid turnover, while those formed by $\alpha v\beta 3$ were more stable and promoted migration in a directed manner (Danen et al., 2005). Interestingly, the expression of the integrin co-receptor tissue transglutaminase (tTG) can also cause clustering of integrins and a concomitant increase in RhoA activity levels (Janiak et al., 2006)

2 Aim of the study

Cell adhesion and migration are essential for development and homeostasis. Whereas altered cell adhesion and migration are known to be important in cardiovascular disease and malignant tumors, the target proteins and molecular interactions that regulate these complex processes, especially at the earlier time points remain incompletely understood.

Recently, we have discovered a novel phosphatase, AUM (aspartate based, ubiquitous, magnesium-dependent phosphatase). By database mining and phylogenetic analysis we have found that this phosphatase belongs to a new emerging class of phosphatases, the HAD-phosphatase family. Western blotting has shown that AUM is abundantly expressed in all investigated mouse tissues including testis. Previous work in the lab has indicated that AUM might be involved in cell-matrix adhesion. However, the underlying mechanisms and AUM-dependent signaling pathways remain unknown.

The aim of this study was to analyze the role of AUM in cell-matrix adhesion and to investigate the involved signaling mechanisms.

Three main questions were addressed:

- 1) How does AUM affect cell adhesion and spreading on fibronectin?
- 2) Which components of cell-ECM adhesion machinery are regulated by AUM?
- 3) Which downstream signaling pathways are regulated by AUM during cell-ECM adhesion?

Answering these questions is expected to provide a better understanding of the biological functions of the novel tyrosine phosphatase AUM.

3 Materials

3.1 List of manufacturers and distributors

1. Abgent, San Diego, CA, USA
2. Abnova, Taipei, Taiwan
3. Addgene Inc. Cambridge, MA, USA
4. Amersham Biosciences, Little Chalfont, UK
5. AppliChem, Darmstadt, Germany
6. Applied Biosystems, Foster City, CA
7. ATCC, Manassas, VA, USA
8. BD Becton Dickinson GmbH, Heidelberg, Germany
9. Beckman Coulter, Krefeld, Germany
10. Biomol Research Lab, Plymouth Meeting, PA, USA
11. Bio-Rad, Munich, Germany
12. Bio-Legend, San Diego, USA
13. BMG Labtech, Offenburg, Germany
14. Calbiochem, Darmstadt, Germany
15. Carl Zeiss AG, Jena, Germany
16. Cell Signaling Technologies, Danvers, CO, USA
17. Clontech, Palo Alto, CA, USA
18. Cytoskeleton Inc., Denver, CO, USA
19. Dharmacon RNAi Technologies, Schwerte, Germany
20. Fujifilm, Düsseldorf, Germany
21. GE Healthcare, Munich, Germany
22. Hartmann Analytic GmbH, Braunschweig, Germany
23. Ibidi, Martinsried, Germany
24. Invitrogen, Karlsruhe, Germany
25. Leica micosystems, Wetzlar, Germany
26. Merck, Darmstadt, Germany
27. Millipore, Billerica, MA, USA
28. NEB, New England, USA
29. PAN Biotech GmbH, Aidenbach, Germany
30. Pierce, Rockford, USA
31. Promega, Heidelberg, Germany
32. Qiagen, Hilden, Germany
33. Roche Applied Science, Mannheim, Germany

34. Roth, Karlsruhe, Germany
35. Serva, Heidelberg, Germany
36. Sigma Aldrich, Munich, Germany
37. Stratagene, La Jolla, CA, USA
38. Thermo Scientific, Rockford, IL, USA
39. Upstate, Lake Placid, NY, USA
40. MWG biotech, Ebersberg, Germany
41. Corning Life Sciences, NY, USA

3.2 Chemicals

β-Mercaptoethanol	5
Acetic acid	36
Acrylamide/bisacrylamide	34
Ammonium persulfate	36
Aprotinin	36
Bovine serum albumin	35
Bromophenol Blue	36
Calcium chloride (CaCl ₂ · 6 H ₂ O)	36
DMSO	5
DTT	36
EDTA	36
EGTA	36
Ethanol	34
Ethidium bromide	36
Glycerol	5
Glycine	34
Hepes	34
Hydrochloric acid (HCl)	36
Isopropanol	5
LB agar	5
LB powder	5
Leupeptin	36
Magnesium chloride (MgCl ₂)	36
Methanol	5
Paraformaldehyde	36
Phosphatase Inhibitor Cocktail I	36

Phosphatase Inhibitor Cocktail II	36
Pepstatin	36
PMSF	36
Ponceau S	24
Protease Inhibitor Cocktail Tablets (complete, EDTA-free)	33
Puromycin	14
SDS	34
Sodium azide (NaN ₃)	26
Sodium chloride (NaCl)	36
Sodium deoxycholate	36
Sodium hydroxide (NaOH)	34
TEMED	36
Tris base / Tris-HCl	34
Triton X-100	36
Tween 20	34
Water (PCR quality)	26

3.3 Nucleotides, nucleic acids and primers

Custom primers	40
DNA ladder	28
dNTPs	28
On-Target Plus, set of individual siRNA oligonucleotides (targeting human or mouse AUM)	19

3.4 Plasmids

pcDNA4-myc/His ₆	
pcDNA4-myc/His ₆ -mAUM ^{D34N}	
pcDNA4-myc/His ₆ -mAUM ^{wt}	
pdEYFP-C1-hAUM ^{wt}	
pdEYFP-C1-hAUM ^{D34N}	

3.5 Antibodies

AlexaFlour-488-conjugated goat anti-mouse, highly cross absorbed	24
---	----

AlexaFlour-488-conjugated goat anti-rabbit, highly cross absorbed	24
AlexaFlour-546-conjugated goat anti-mouse, highly cross absorbed	24
AlexaFlour-546-conjugated goat anti-rabbit, highly cross absorbed	24
AlexaFlour-633-conjugated goat anti-mouse, highly cross absorbed	24
AlexaFlour-633-conjugated goat anti-rabbit, highly cross absorbed	24
Anti-phosphotyrosine, clone 4G10, mouse monoclonal	27
AUM, rabbit polyclonal	Custom made
FAK, rabbit polyclonal	16
GAPDH, mouse monoclonal	16
Goat anti-mouse IgG (Fc), peroxidase conjugated	38
Goat Anti-Rat Ig (Polyclonal/ FITC)	8
Goat Anti-rabbit IgG (Fc), peroxidase conjugated	38
Hamster Isotype control (HTK888/ Alexa 488)	12
Integrin Alpha 5 (PE)	12
Integrin Beta 1 (CD29) (HM β 1-1/ Alexa 488)	12
Integrin Alpha V (CD51) (RMV-7/ PE)	12
Integrin Beta 3 (CD61) (HM β 3-1/ Alexa 488)	12
Integrin Active beta 1 (CD29) (9EG7)	8
Rat IgG _{2a} Isotype control (R35-95)	8
Rat IgG _{2b} Isotype control (PE)	12
Paxillin, rabbit polyclonal	16
Phospho-FAK, mouse monoclonal (Tyr 397)	16
Src (clone 36D10), rabbit monoclonal	16
Tubulin (clone DM1A), mouse monoclonal	36
Vinculin (clone hVIN-1), mouse monoclonal	36
β -Actin (clone C4) mouse monoclonal	27

3.6 Bacterial strain and cell lines

E. coli DH5 α	24
GC1 (CRL-2053)	7

3.7 Tissue culture reagents and materials

Culture dishes/flasks	38
DMEM	29
Fetal bovine serum	29
L-Glutamine	29
Lipofectamine 2000	24
Opti-MEM	24
Penicillin G, sodium salt	29
Phosphate buffered saline 10X (with/without MgCl ₂ /CaCl ₂)	29
Streptomycin sulphate	29
Trypsin/EDTA	29
Corning 96 well plate, clear bottom, black	41

3.8 Other materials

Alexa Fluor -488 phalloidin	24
Alexa Fluor -546 phalloidin	24
Calcein-AM	24
Collagen I	36
Collagen IV	36
Exoenzyme C3 transferase	18
Ethidium bromide	36
Fibronectin from bovine plasma	14
Hybond C nitrocellulose membrane	21
Kanamycin	36
PageRuler prestained protein ladder	24
Poly-L-Lysine	36
Prolong gold, antifade medium	24
Restriction enzymes	28
Soybean trypsin inhibitor	36
Y-27639	14

3.9 Commercial kits

Micro BCA kit	38
Qiagen miniprep kit	32
Rho activation assay kit (Biochemical)	18
Rac activation assay kit (Biochemical)	18
G-LISA RhoA activation assay Kit	18
G-LISA Rac1 activation assay Kit	18
Plasmid purification kit	32

3.10 Software and Databases

BLAST	NCBI;NLM, Bethesda, MD
ExpASY Server	Swiss Institute of Bioinformatics
GraphPad Prism version 4.00	GraphPad software, San Diego, CA, USA
Image Pro version 7.0	Media Cybernetics, MD, USA

3.11 RNA interference tools

All siRNA oligoribonucleotides were purchased from Dharmacon. Four different synthetic siRNA oligoribonucleotides for mouse and human AUM were ordered as ON-TARGET plus set of four (catalog # LQ-041844-01-0002 or # LQ-022877-00-0002, respectively). ON-TARGET plus siCONTROL non-targeting siRNA (catalog # D-001810-01-05) was used as a control in all siRNA experiments. Sequence of siRNA used is shown in table below.

Lentiviral vectors used for establishing stable cell lines expressing shRNA for stable AUM depletion were purchased from Sigma-Aldrich as bacterial glycerol stocks from the MISSION shRNA Program (catalog # SHCLND-NM_025954). The corresponding control shRNA plasmid (catalog # SHC002) was obtained as a DNA stock. Sequence of shRNA used is shown in table below.

Table1: Sequences of shRNA and siRNA used to downregulate AUM

RNA	Construct	Insert sequence (5'- 3')
shRNA	TRCN0000081473	CCGGCGTGGGCACCAACATGGACAACCTCGAGTTGTCCATGTTGGTGCCACGTTTTTG
shRNA	TRCN0000081477	CCGGCTGTAGCCTGAAGACTATCCTCTCGAGAGGATAGTCTTCAGGCTACAGTTTTTG
siRNA	J-041844-11	PUUCCGAUGAUGUCCGCCUUU
siRNA	J-041844-12	PAGCGCCUUAGCUUCUCCGCUU

3.12 Solutions & Buffers

(in alphabetical order)

Antibody diluent

10 mM	Hepes, pH 7.4
0.5 M	NaCl
1%	BSA
0.2%	Tween-20
0.2%	NaN ₃

Blocking buffer

50 mM	Tris-HCl , pH 8.0
2 mM	CaCl ₂
80 mM	NaCl
5% (w/v)	nonfat milk powder
0.2%	NP-40

dNTP stock solutions (PCR)

25 mM	of dATP, dCTP, dGTP, dTTP (each)
-------	-------------------------------------

Laemmli buffer

(SDS-PAGE sample buffer)

62.5 mM	Tris-HCl, pH 6.8
---------	------------------

	10% (v/v)	glycerol
	5% (v/v)	β -mercaptoethanol
	2% (w/v)	SDS
	0.02% (w/v)	Bromophenol Blue
Lysis buffer (for immunoprecipitation)	20 mM	Tris-HCl, pH 7.5
	150 mM	NaCl
	1% (v/v)	Triton X-100
	1 mM	β -glycerophosphate
	2.5 mM	sodium pyrophosphate
	1 mM	sodium orthovanadate
	100-fold	diluted phosphatase inhibitor cocktail 1
	100-fold	diluted phosphatase inhibitor cocktail 2
	1 μ g/ml	Pepstatin
	1 μ g/ml	Leupeptin
	10 μ g/ml	Aprotinin
	1mM	PMSF
RIPA buffer (for cell lysis)	50 mM	Tris-HCl, pH 8.0
	150 mM	NaCl
	1 % (v/v)	NP-40
	0.1% (w/v)	SDS
	0.5% (w/v)	sodium deoxycholate

	1 µg/ml	Pepstatin
	1 µg/ml	Leupeptin
	10 µg/ml	Aprotinin
	1mM	PMSF
	100-fold	diluted phosphatase inhibitor cocktail 1
	100-fold	diluted phosphatase inhibitor cocktail 2
Running buffer (10x), pH 8.7 (SDS-PAGE)		
	250 mM	Tris base
	2 M	Glycine
	10%	SDS
Stripping buffer (for immunoblotting)		
	62.5 mM	Tris-HCl, pH 6.7
	2%	SDS
	100 mM	β-mercaptoethanol, added immediately before use
TAE (50x) (for DNA gels)		
	2 M	Tris-Acetate, pH 8.0
	100 mM	EDTA
TBS (10x)		
	0.5 M	Tris-HCl, pH 7.5
	1.5 M	NaCl

TBS-T

50 mM	Tris-HCl, pH 7.5
150 mM	NaCl
0.1%	Tween 20

Transfer buffers
(for semi-dry blotting)

Anode buffer I	0.3 M	Tris base
	40%	methanol

Anode buffer II	25 mM	Tris base
	40%	methanol

Cathode buffer	25 mM	Tris base
	40 mM	Glycine
	10%	methanol

Tyrode's Buffer (pH 7.4)

137 mM	NaCl
2.7 mM	KCl
12 mM	NaHCO ₃
5 mM	HEPES
1 mM	MgCl ₂
0.5 mM	CaCl ₂
0.1%	Glucose

Confocal images were taken on Leica TCS SP5 confocal microscope (Leica, Germany). Epifluorescence images were taken on a Nikon TE 2000 Eclipse microscope (Nikon, Japan). All oligonucleotides/primers used in this work were synthesized by Europhins MWG Operon.

Western blots were imaged using Fluor Chem Q imaging system from Alpha Innotech. For the quantitative analysis of Western blot signals, membranes were analyzed using Alpha Innotech software (Alpha Innotech, USA).

DNA bands were visualised using UV-transilluminator, UVT28-ME (HEROLAB, Germany). Spectrophotometrical analysis for DNA concentration estimation was performed on a BioPhotometer (Eppendorf, Germany).

Fluorescence measurements were performed on a Perkin Elmer Envision 2104 multilabel reader (Perkin Elmer, USA).

Flow cytometry experiments were performed using BD FACScalibur flow cytometer (BD Biosciences, Heidelberg, Germany).

4 Methods

4.1 Cell biology methods

Cell lines

Cell lines used in this work (HeLa, GC1-spg) were purchased from ATCC (VA, USA), cultured in Dulbecco's modified Eagle's medium (DMEM) containing 4.5 g/l glucose, supplemented with 10% FCS, 2 mM L-glutamine, 100 U/ml penicillin and 100 µg/ml streptomycin at 7% CO₂ and 37°C in a standard cell culture incubator. All cell lines were grown on standard cell culture dishes and passaged for further cultivation every 3-4 days at a ratio of 1:10 to 1:20. To passage cells, the culture medium was removed, cells were briefly washed with Ca²⁺- and Mg²⁺-free D-PBS (Dulbecco's phosphate buffered saline) and incubated with trypsin-EDTA (0.05% trypsin/EDTA) for 5 min at 37°C. Trypsin was neutralized by the addition of FCS-containing culture medium and detached cells were then brought into a single cell suspension by repeated pipetting. Cells were counted under the phase-contrast microscope using a Neubauer chamber. The average cell numbers per square were multiplied with 10⁴ in order to determine the number of cells per milliliter of cell suspension.

Transient transfection

The day preceding the transfection, cells were seeded at the appropriate density in different types of cell culture dishes as per requirement according to the table below (Table 1).

Table 1: Seeding density of GC-1 cells prior to transfection

Tissue culture dish/plate	Number of cells seeded	Growth area, cm²
6- well plate	3 X 10 ⁴	9.6
6-cm petri dish	9 X 10 ⁴	20.8
10-cm petri dish	18 X 10 ⁴	56.7

Next day, plasmids or siRNA oligoribonucleotides and the Lipofectamine™ 2000 reagent were mixed separately with OptiMEM in sterile polystyrene tubes (Table 2).

Table 2: Transfection conditions for transfection of CC-1 cells in different cell culture vessels

Culture vessel	Plating medium	Dilution medium	DNA	siRNA (from 20μM stock)	Lipofectamine 2000
6- well plate	1.0 ml	250 μ l	-	12.5, 25 and 50nM	3 μ l
6-cm dish	3.0 ml	500 μ l	-	25nM	6 μ l
10-cm dish	10 ml	1500 μ l	0.5 μ g	25nM	18 μ l

In case of 6-well plates, 3 μ l of Lipofectamine™ 2000 reagent and 0.1 – 0.5 μ g of the respective plasmids or 12.5 to 50 nM of siRNA oligoribonucleotides were each mixed with 250 μ l of OptiMEM medium and were incubated for 5 min at room temperature. Afterwards, DNA (or siRNA) and Lipofectamine™ 2000 solutions were combined (according to the table above) and incubated for another 20 min at room temperature to form transfection complexes. In the meanwhile, cells were washed once with OptiMEM and the medium was then replaced with indicated amount of OptiMEM (plating medium) as mentioned in the table above. The transfection mix (e.g. for 500 μ l in case of 6-well plates) was added while rocking the plate, and the cells were incubated in a cell culture incubator for 4 hours. After that, the transfection medium was replaced with standard growth medium containing FBS and antibiotics. 24 hours (for overexpression experiments) or 72 h (for RNAi experiments) after transfection, cells were either used for further experiments, fixed for immunofluorescence or lysed with RIPA buffer for immunoblotting.

Immunocytochemistry

To study actin dynamics and focal adhesion formation in cells spreading on fibronectin, immunocytochemistry was performed. Cells were fixed for 20 min at RT in 4% paraformaldehyde, followed by permeabilization with 0.5% Triton X-100 for 10 min. The permeabilized cells were blocked for 1 hour in $\text{Ca}^{2+}/\text{Mg}^{2+}$ -free PBS containing 3% BSA, and were subsequently incubated for 1 hour with appropriate primary antibodies (diluted 1:100-1:400 in $\text{Ca}^{2+}/\text{Mg}^{2+}$ -free PBS containing 1% BSA). The cells were washed twice in 1% BSA, and were incubated for 1 h at RT with appropriate secondary, Alexa Fluor-labeled anti-rabbit or anti-mouse antibodies (1:400, diluted in PBS/1% BSA). To stain filamentous actin, samples were incubated with Alexa Fluor-labeled phalloidin (1:400). After washing the samples three times with $\text{Ca}^{2+}/\text{Mg}^{2+}$ -free PBS, cell nuclei were counterstained with DAPI (1 μ g/ml in PBS) for 5 min and the specimen were embedded in ProLong Gold Antifade reagent (Invitrogen, USA). Cells were analyzed using confocal microscopy (see below).

Confocal Laser-Scanning Microscopy

Compared to epifluorescence microscopy where the entire specimen is illuminated evenly, confocal microscopy uses point illumination and a pinhole in an optically conjugate plane before the detector to minimize out-of-focus signals. Since fluorescence extremely close to the focal plane is detected the resultant image's optical resolution is much better than that of conventional wide field fluorescence microscope. Briefly, a laser beam is focused by an objective lens into a small focal volume at optimum depth of the specimen. Next, a beam splitter separates off fluorescent wavelengths from original excitation wavelength. After passing a pinhole, the light intensity is detected by a photo-detection device which converts the light signal into an electrical signal that is then recorded by a computer (Taylor and Wang 1980). The live or fixed and antibody-labeled cells were analyzed under the confocal laser scanning microscope TCS SP5 (Leica, Germany) with a Plan-Apochromat 40x/NA1.3 or 63x/NA1.4 objectives. The acquired images were analyzed and processed using the Leica AF software.

RNA interference

Gene knockdown through RNA interference (RNAi) has developed into a widely used tool for the analysis of protein function (Elbashir et al., 2001). RNA interference in eukaryotes can be triggered by double stranded RNA (dsRNA), which is also the genetic material of certain viruses (Belvins et al., 2006). As the name implies, dsRNA has two complementary strands. When dsRNA with antisense strand complementary to the transcript of a targeted gene is introduced into cells, it results in the degradation of the targeted mRNA and the consequential silencing of the target gene. Broadly, two distinct steps are involved in this process. In the first step, the cellular enzyme Dicer recognizes and cleaves long dsRNA into short interfering (si)RNA molecules/oligoribonucleotides of 21 to 23 nucleotides in length. In the second step, these oligoribonucleotides are incorporated in a multi-component RNA-induced silencing complex (RISC), leading to the sequence-specific cleavage of RNA transcripts of the target gene (Dykxhoorn et al., 2003). As a result, the synthesis of the encoded protein is either completely or partially suppressed, without the gene being affected (Tuschl and Borkhardt, 2002).

To initiate RNA interference-mediated gene silencing, synthetic shRNA oligoribonucleotides (or their cellular products, the siRNAs) can be directly transfected into cells (Fig. 10).

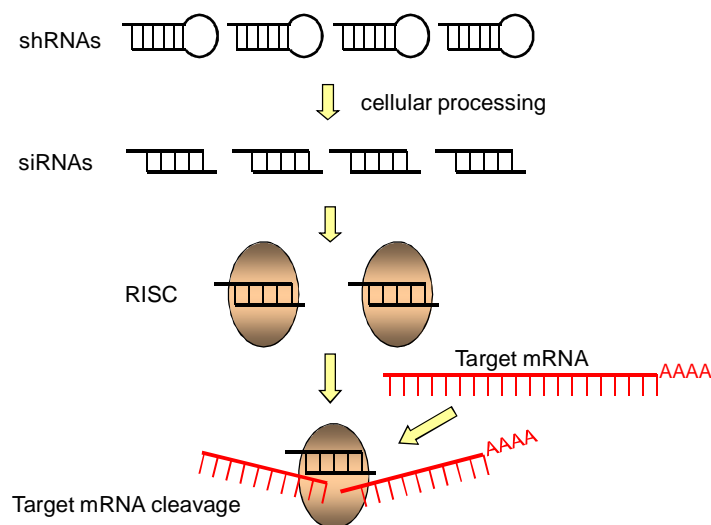


Figure 10: A model for gene inactivation via RNA interference.

Short hairpin (sh) RNA oligoribonucleotides are processed to 21-23-nt long short interfering (si)RNA duplexes by intracellular enzymes. The siRNA duplexes are incorporated into a siRNA containing ribonucleoprotein complex, forming the RNA-induced silencing complex (RISC). The RISC mediates sequence-specific target RNA degradation by targeting homologous mRNAs for degradation due to its endonuclease activity (modified from Tuschl and Borkhardt, 2002).

Validation of the RNAi tools

Cellular AUM expression was downregulated using two different methods. The first approach was the stable depletion of AUM in GC-1 cells using lentiviral-mediated shRNA delivery. (Duraphe, 2009). Several shRNAs targeting different regions of AUM were used. For experimental purposes in this work, GC-1 cells expressing two different shRNA sequences were used, as shown in Table 3

Table 3: Sequences of shRNA used to specifically down-regulate mAUM expression

Construct	Insert sequence (5' - 3')
TRCN0000081473	CCGGCGTGGGCACCAACATGGACAACCTCGAGTTGTCCATGTTGGTGCCACGTTTTTG
TRCN0000081477	CCGGCTGTAGCCTGAAGACTATCCTCTCGAGAGGATAGTCTTCAGGCTACAGTTTTTG

Other approach was transient transfection of synthetic siRNA oligoribonucleotides in the host cells. Two different oligoribonucleotides targeting two different regions of AUM sequence were used. The corresponding sequences of the employed oligoribonucleotides are presented below. GC-1 cells were seeded at low density on the day before transfection. Next day, the cells were transfected with two different individual siRNA oligoribonucleotides (Table 4). Forty-eight – 72 hours post-transfection, cells were lysed in RIPA buffer and lysates were tested for AUM downregulation by immunoblotting with AUM-specific antibodies (see 3.5).

Table 4: siRNA sequences used to downregulate mAUM expression

Construct	Antisense Sequence (5'- 3')
J-041844-11	PUUCCCGAUGAUGUCCGCCUUU
J-041844-12	PAGCGCCUUAGCUUCUCCGCUU

Following diagram gives an overview of the si/shRNA target regions in the ORF of mAUM.

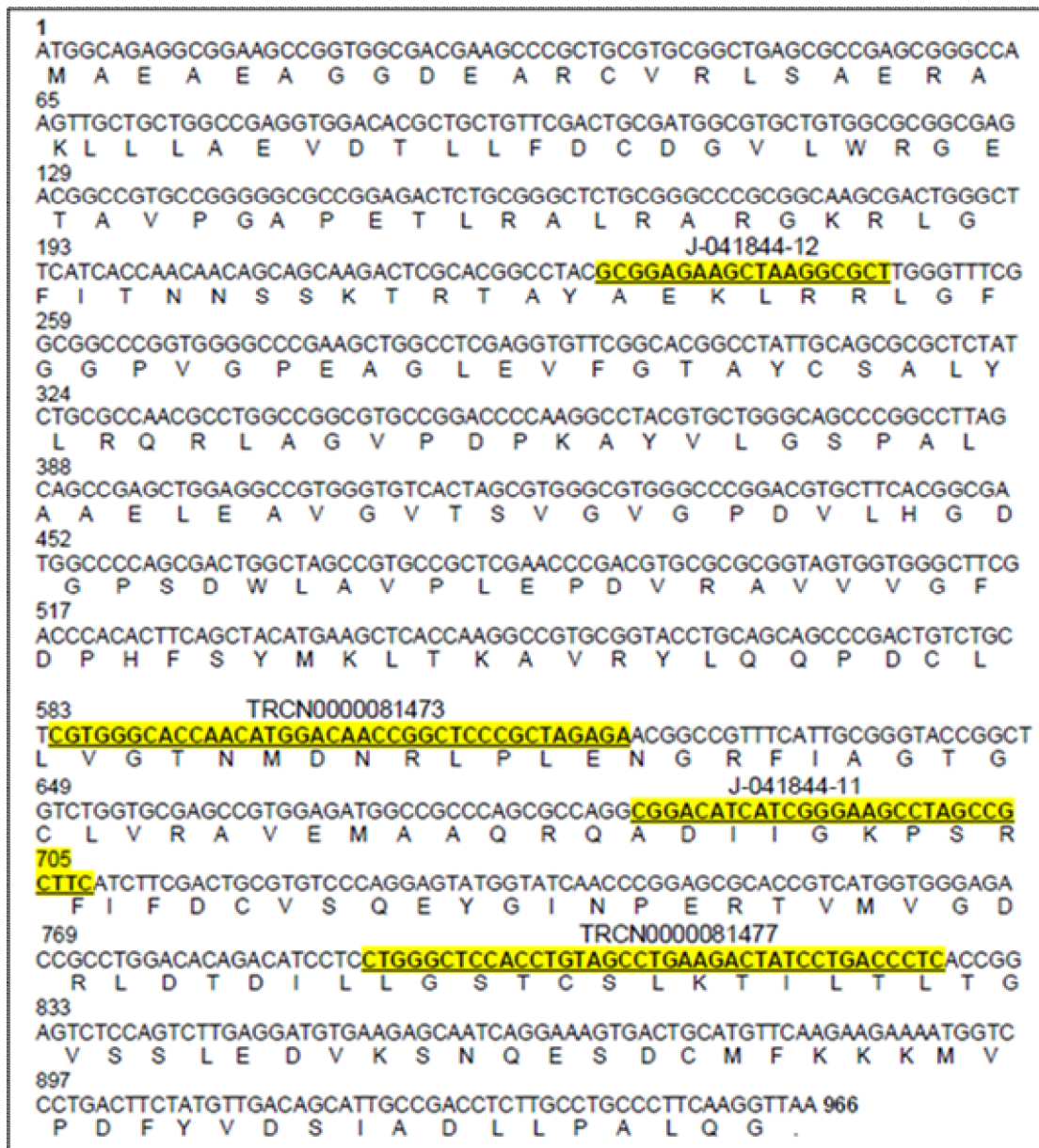


Figure 11: Localization of the mAUM siRNA/shRNA in open reading frame of mouse AUM.
Refer to tables 3 and 4 for the designations used in the figure

4.2 Cell biological assays

Cell spreading on fibronectin

Cell adhesion to extracellular matrix (ECM) proteins such as fibronectin (FN), collagen, or laminin triggers signaling cascades involving rapid tyrosine phosphorylation and dephosphorylation events (Sieg et al., 1998). To initiate FN mediated signaling cascades, cells growing in petri-dishes were starved overnight with DMEM supplemented with containing 4.5 g/l glucose, 2 mM L-glutamine, 100 U/ml penicillin and 100 µg/ml streptomycin at 7% CO₂ and 37°C in a standard cell culture incubator. Next day, 10-cm culture dishes, sticky slides or glass coverslips were coated with 10 µg/ml of fibronectin for 1.5 hours. In the meantime, the starved cells were washed once with PBS and trypsinised for 2 minutes (limited trypsinisation). Trypsinization was stopped using 0.5 mg/ml soybean trypsin inhibitor, and cells were counted using a Neubauer chamber and resuspended in DMEM supplemented with 0.1% BSA.

For Rho/Rac activity assays, 5×10^6 cells were suspended in 1 ml DMEM supplemented with 0.1% BSA. For all the other purposes, 1×10^6 cells/ml were used. FN coated dishes were washed with PBS, the cell suspension was spread on the plates, and cells were incubated for the indicated time points at 37°C. For Rho/Rac activity assays, cells were then lysed by the addition of 500 µl of 3x lysis buffer on ice to achieve a final concentration of 1x lysis buffer in the whole cell lysates.

Cell area determination of fixed cells

To analyze effect of AUM depletion on cell spreading, the area of cells spreading on fibronectin was analyzed. GC-1 cells expressing control or AUM shRNA were seeded on FN-coated slides (sticky slide, ibidi, Martinsried) for 5, 10, 20 or 40 min at 37°C, fixed and stained for F-actin with phalloidin; nuclei were labeled with DAPI. Cells were imaged under an epifluorescence microscope using a 60x objective. For an unbiased analysis, the slides were scanned systematically in a predetermined fashion using a motorized stage, and the individual images were subsequently tiled together into one large image. Outlines of individual cells were drawn and the cell areas were calculated from the circumference using Image Pro software. The cell area of at least 300 cells per condition was measured in two independent experiments, and the effect of AUM knock down on cell area was plotted as fold increase with respect to control shRNA transduced cells.

Cell- ECM adhesion assay

Cell-ECM adhesion assays were performed using the fluorogenic dye calcein acetoxymethyl ester (calcein-AM). This method provides a fast and sensitive method for estimating cell adhesion. Calcein-AM is as such non-fluorescent but once loaded into cells, is cleaved by

endogenous esterases and as a result is converted into the highly fluorescent calcein (Akeson and Woods, 1993; see Fig. 12). Calcein has been shown not to interfere with the cell adhesion process (Akeson and Woods, 1993). Also the fluorescent calcein is well-retained in the cytoplasm of living cells.

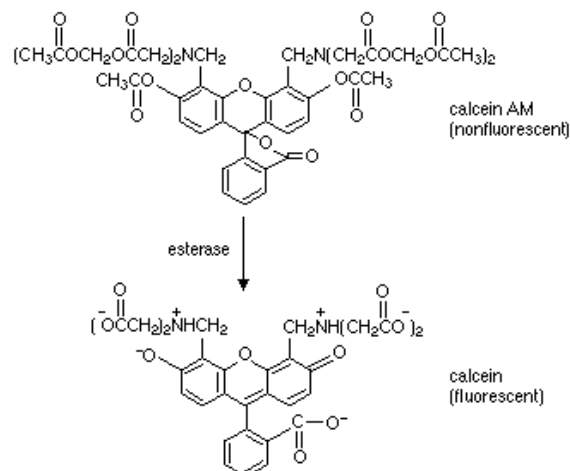


Figure 12: Schematic diagram showing conversion of Calcein AM to Calcein by intracellular esterases (Iain D. Johnson, Current Protocols in Cytometry, May 2001)

Overnight serum starved cells were labeled with 1 μM Calcein-AM diluted in PBS containing Ca^{2+} and Mg^{2+} for 15 minutes in a cell culture incubator. Stained cells were washed once with PBS and trypsinized for 2 minutes (limited trypsinization), and trypsinization was stopped by adding 0.5 mg/ml soybean trypsin inhibitor to the cell suspension. Cells were counted using a Neubauer chamber and resuspended at a concentration of 6×10^5 cells/ml in DMEM supplemented with 0.1% BSA. 50 μL of the cell suspension (corresponding to 30,000 cells) were seeded into 96-well micro titer plates precoated with FN as follows: 96-well blackwalled transparent plates were coated with 10 $\mu\text{g/ml}$ FN by diluting FN at the above concentration in Ca^{2+} and Mg^{2+} free PBS, pH 7.2. 100 μl of this solution was added to each well for coating and incubated at 37°C for 1.5 hours. After incubation the wells were washed twice with 100 μl of PBS. Coated wells were blocked by adding 100 μl of 0.1% BSA in DMEM in each well and incubated for approximately 30 minutes at room temperature. Afterwards, the wells were washed with BSA-free DMEM, cells were seeded in the wells, and the plates were incubated for various time points at 37°C in the cell culture incubator.

After the incubation, unbound cells were removed by washing thrice with PBS. To this end, 200 μl of PBS were carefully added to each well, and after a light swirling, the plate was flipped and patted on a paper towel. Afterwards, 100 μl of PBS was added to each well, followed by the addition of 100 μl of lysis buffer containing 1% Triton X-100 in 50 mM Tris, pH 7.5. Cells were incubated at room temperature for 15-20 minutes and after a gentle

mixing, the resulting fluorescence was read using a multiwell fluorescence reader. Calcein was excited at 485nm and the light emitted at 520 nm was recorded. The resulting fluorescence intensity was plotted and is proportional to the number of cells adhered to the surface of the coated well.

4.3 Flow cytometry

Fluorescence activated cell sorting (FACS) or flow cytometry is a technique used for fluorescence based cell sorting and/or the quantification of fluorescently labeled (cell surface) molecules. Suspended single cells are passed through an electronic fluorescent detection apparatus in a laminar stream of fluid. Typically, an antibody is chosen that specifically binds to the protein(s) of interest on the cell surface. The bound antibody is either directly conjugated with a fluorophore or is detected using a fluorescently labeled secondary antibody. Since multiple antigens can be labeled simultaneously, this technique allows the multiparametric analysis of the cell surface characteristics of up to thousands of cells per second.

To analyze the surface expression of integrins using flow cytometry, cells (either overnight serum starved or left unstarved) were briefly trypsinised and treated with soybean trypsin inhibitor as described before. 2×10^5 cells were suspended in DMEM or in modified Tyrode's buffer. The cell population to be analyzed was either left untreated or was treated with fibronectin. Next, cells were fixed by the addition of 1 volume of 4% paraformaldehyde in calcium-free PBS supplemented with 1mM $MgCl_2$ at 4°C for 15-20 minutes. The fixing solution was removed by centrifuging the cells at 1000 rpm for 3 minutes and by removing the supernatant. The cells were again resuspended in modified Tyrode's buffer and primary antibodies were added according to the table below (table 5).

The cells were incubated with the integrin-specific or with the appropriate isotype control antibody (negative control) for 60 minutes at 4°C. Post incubation, cells were washed once with 1 ml of Tyrode's buffer (Brandt et al., 2009) and labeled with a secondary antibody as indicated in table 5 for 1 hour at 4°C in Tyrode's buffer. Finally, cells were washed again in 1 ml of Tyrode's buffer and analysed with a BD FACS Calibur Bioanalyzer. When fluorescently labelled primary antibodies were available, cells were analysed directly without further secondary antibody staining.

Table 5: Antibodies used for FACS analysis

Antibody	Amount antibody/10 ⁵ cells	Clone / Fluorophore	Isotype
α 5-integrin	10 μ L (0.25 μ g)	238307 / PE	Rat IgG 2 _b
β 1-integrin (CD29)	1 μ L (0.5 μ g)	HMB1-1 / Alexa 488	Hamster IgG
α v-integrin (CD51)	1 μ L (0.2 μ g)	RMV-7 / PE	Rat IgG ₁
β 3-integrin (CD61)	1 μ L (0.5 μ g)	HMB3-1 / Alexa 488	Hamster IgG
β 1-integrin (CD29), active conformation	4 μ L (2.0 μ g)	9EG7 / not conjugated	Rat IgG 2 _a
Rat IgG2 _a Isotype control	2 μ L (1.0 μ g)	R35-95 /not conjugated	Rat IgG 2 _a
Goat Anti-Rat Ig	2 μ L (1.0 μ g)	polyclonal / FITC	Goat Ig
Rat IgG2 _b Isotype control	1 μ L (0.025 μ g)	141945 / PE	Rat IgG 2 _b
Hamster Isotype control	1 μ L (0.5 μ g)	HTK888 / Alexa 488	Hamster IgG

4.4 Molecular biology methods

Plasmid preparation

Small scale plasmid isolation

For preparation of small amounts of plasmid DNA, a Mini-prep DNA extraction kit was used. Plasmids were isolated according to the manufacturer's instructions. Briefly, 3 ml LB medium containing the appropriate antibiotic was inoculated with a single bacterial colony and was incubated overnight at 37°C with constant shaking. Cultures were transferred into 2 ml Eppendorf tubes and bacterial cells were pelleted by centrifugation (Centrifuge 5415 D, Eppendorf, Hamburg; 12,000 rpm, 1 min, RT). The pellets were lysed and DNA was eluted from the columns by the addition of 50 μ l of elution buffer (10 mM Tris-HCl, pH 8.0) and subsequent centrifugation (12,000 rpm, 2 min, RT).

Large scale plasmid isolation

To isolate large quantities of plasmid DNA for transfection in eukaryotic cells, a Maxi-prep DNA extraction kit was used according to the instructions of the manufacturer. A single bacterial colony was inoculated in 2 ml LB medium containing appropriate antibiotics, and

cells were grown at 37°C for 6-8 h with constant agitation. Afterwards, this culture was used as inoculum for 100ml of LB medium with appropriate antibiotics and this culture was incubated at 37°C with constant agitation overnight. Cells were pelleted by centrifugation (Avanti J-20 XP Centrifuge, Beckman Coulter; 6,000 x g, 15 min, 4°C), and DNA was isolated as described in the manufacturer's protocol. Finally, the DNA pellet was resuspended in 500µl of Tris-HCl (10mM Tris-HCl, pH 8.0), and the DNA concentration was determined photometrically. DNA samples were adjusted to a concentration of 0.5 – 1 µg/µl, aliquoted and stored at –20°C.

Quantification of nucleic acids by photometric measurement

The photometric determination of nucleic acid concentrations was carried out using a BioPhotometer (Eppendorf, Germany). The absorbance was measured in quartz cuvettes (d = 1 cm) at 260 and 280 nm (A260 and A280). Absorbance of Tris-HCl (10mM pH 8.0) was used as blank. The nucleic acid concentration was calculated based on the fact that an absorbance of 1 at 260 nm corresponds to an average DNA concentration of 50µg/ml. The purity of isolated DNA was determined using the ratio A260/A280. Ratio of 1.8 to 1.9 was considered to be of optimum purity for most of the downstream applications.

Restriction digests of plasmid DNA

The enzymatic digestion of DNA with restriction endonucleases was carried out using the manufacturer's recommended buffers (NEB, USA). 10U of enzyme was used to digest 1µg of DNA at 37°C in a ThermoMixer (ThermoMixer compact, Eppendorf, Germany) for one hour. The efficiency of digestion was checked by agarose gel electrophoresis.

DNA gel electrophoresis

Agarose gels were prepared by boiling 1% (w/v) agarose in 1xTAE buffer in a microwave oven, followed by the addition of ethidium bromide (0.5µg/ml). DNA sample buffer containing Orange G DNA loading dye was added to the DNA samples, and the gel was run at constant voltage. The separation of DNA was evaluated on a UV table and documented using the UVT28-ME (HEROLAB, Germany).

Site-directed mutagenesis

The catalytic aspartate in hAUM was point mutated to asparagine (hAUM^{D34N}) using site-directed mutagenesis according to the Quickchange XL site directed mutagenesis kit purchased from Stratagene. Briefly, 100 ng of hAUM plasmid was employed as a template in the mutagenesis reaction with the primer 5'-GTGGACACGCTGCTGTTCAACTGCGATGGCGTGCTGTGG-3' and its reverse complement. The PCR reaction was performed with Platinum Pfx Polymerase (5 min at

94°C, 12 cycles at 94°C for 30 sec, 58°C for 1 min, and at 68°C for 5 min, followed by 1 min at 68°C). One μl of DpnI enzyme was added to the PCR mix for digestion of the methylated template. The PCR product was transformed into competent DH5 α cells, and the obtained colonies were screened for the desired mutation by sequencing.

4.5 Protein biochemical methods

Sample preparation for immunoblot analysis

GC-1 spg cells growing in culture dishes were washed with $\text{Ca}^{2+}/\text{Mg}^{2+}$ -free PBS, and lysed by addition of ice-cold RIPA lysis buffer directly into the dish. The cells were scraped from the plate on ice and lysate was collected in pre-cooled 1.5 ml Eppendorf tubes. These lysates were further incubated on ice for 20 minutes and centrifuged at 15,000 rpm for 10 min at 4°C. The supernatants containing the soluble whole cell lysates were collected and the pellets containing insoluble components were discarded. The lysates were stored in aliquots at -20°C .

Estimation of protein concentration

The protein concentration of cell lysates was determined using the Micro BCA Protein Assay Kit. This is a colorimetric assay that allows detection and quantification of the total protein content in a sample. The assay is based on the principle that peptide bonds present in the protein sample are able to reduce Cu^{2+} to Cu^{1+} under alkaline conditions (the Biuret reaction). The amount of Cu^{2+} reduced is proportional to the amount of protein present in the solution. In principle, two molecules of bicinchoninic acid chelate with one Cu^{1+} ion thereby resulting in the formation of a purple-colored product that strongly absorbs light at a wavelength of 562 nm (Smith et al., 1985).

To measure the protein concentration, the BCA solution was prepared by mixing the components of the Micro BCA Protein Assay Kit according to manufacturer's instructions. Cell lysate (5 μl) was diluted in a microtitre plate with water to make a volume of 150 μl of protein solution. Then, 150 μl of BCA solution was added to each probe, and samples were incubated for 1 hour at 37°C. A BSA standard curve ranging from 2 to 10 μg of BSA per well supplemented with 5 μl of lysis buffer was used for the purpose of quantification of total protein amount in the test samples. The extinction of the samples was determined at 560 nm in a Perkin Elmer Envision 2104 multi label reader.

SDS-Polyacrylamide Gel Electrophoresis (SDS-PAGE)

SDS-PAGE is a commonly used method for separating proteins based on their molecular masses using polyacrylamide gels and sodium dodecyl sulfate (SDS). SDS is used as a protein denaturing agent and also imparts uniform negative charge to the proteins (Laemmli,

1970). The technique of SDS-PAGE followed by immunoblotting is a commonly used method for protein expression analysis.

Protein samples were adjusted to equal protein concentrations, mixed with Laemmli buffer, denatured by boiling at 95°C for 5 min and loaded onto SDS-PAGE gels. The electrophoresis was carried out in running buffer at a constant current (25 – 30 mA). Proteins were first concentrated in the stacking gel [4.5% (v/v) acrylamide solution (29:1 v/v acrylamide / bis-acrylamide), 0.1% SDS, 0.1% APS and 0.1% TEMED, 125 mM Tris-HCl pH 6.8], and then separated in the running gel [12% (v/v) acrylamide solution (29:1 v/v acrylamide / bis-acrylamide), 0.1% SDS, 0.1% APS and 0.1% TEMED, 375 mM Tris-HCl pH 8.8]. To separate low molecular weight proteins, running gels with 8% (v/v) acrylamide solution were used. SDS-PAGE was performed on the Bio-Rad mini gel apparatus (Bio-Rad, Munich).

Immunoblot analysis

Immunoblotting is commonly used technique for semi-quantitative detection of specific proteins in a given sample of cell lysates. After proteins are separated on polyacrylamide gels based on their molecular weight the proteins are electrophoretically blotted on highly charged nitrocellulose membrane. This membrane is further probed with specific primary antibodies to detect a particular protein. Bound primary antibodies can then be detected by using secondary antibodies coupled with horseradish peroxidase (HRP) (Towbin et al., 1979).

Proteins were transferred from the SDS-PAGE gels onto nitrocellulose membranes using a TRANSBLOT semidry blotting apparatus (Bio-Rad, Munich). After equilibration of the SDS-PAGE gel in cathode buffer for 5 min, the blotting sandwich was assembled. For that, two lower sheets of Whatman paper were equilibrated in anode buffer I, one sheet of Whatman paper together with the nitrocellulose membrane in anode buffer II and three other sheets of Whatman paper in cathode buffer. Proteins were transferred electrophoretically at constant current (70 mA for 1 mini-gel) for variable times depending on the molecular mass of the proteins of interest. A pre-stained protein marker was used as a molecular weight marker and to monitor electrophoretic transfer. Western blot membranes were stained for equal protein loading with Ponceau S (0.2% in 5% acetic acid) and were scanned for documentation. Afterwards, membranes were blocked in blocking buffer for 30 min at room temperature under constant agitation. Primary antibodies were applied at dilutions of 1:500-1:1,000 (or 1:10,000 for α -tubulin- and β -actin-directed antibodies) in antibody diluent, and membranes were incubated overnight at 4°C under constant agitation in primary antibody solution. Afterwards, membranes were washed (3 x 5 min) with TBS-T or rinsed in water and probed for 1 – 2 h with horseradish peroxidase (HRP)-labeled secondary antibodies, diluted 1:5,000 in blocking buffer. After washing (3 x 5 min) with TBS-T or rinsing in water, Western

blot membranes were treated with the enhanced chemiluminescent (ECL) Western Blotting Detection System and exposed to X-ray films or digital images of membranes were taken on an Alpha Innotech imaging system (San Leandro, CA, USA) and bands were quantified using the software from the same company.

Reprobing of nitrocellulose membranes

In some cases, the same membranes were probed for several different antigens. For this purpose, nitrocellulose membranes were placed in stripping buffer and incubated at 55°C for 30 min under constant agitation to remove primary and secondary antibodies. After that, membranes were washed three times in a large excess of TBS-T, blocked again with blocking buffer for 30 min at room temperature under constant agitation and then re probed with other primary antibodies to detect the other antigen.

4.6 RhoA/Rac1 activity assay

Rho family proteins act as molecular switches that transmit cellular signals through an array of effector proteins. Both RhoA and Rac1 are well established mediators of cell-ECM adhesion by their ability to influence actin dynamics (Ridley, 2006). Rho and Rac switch between an active, GTP bound state and an inactive, GDP-bound state (Hall, 1998). Many Rho/Rac family effector proteins specifically recognize the GTP-bound (active) form of Rho/Rac. This feature is employed in affinity capture assays to semi-quantitatively analyze the Rho/Rac protein activation status in cells (Ren et al., 1999).

Traditionally, this assay has been performed using a pull-down method, wherein the Rho-GTP-binding domain (RBD) of a RhoA effector or p21 binding domain (PBD) of the Rac1 effector protein, p21 activated kinase 1 (PAK) is coupled to agarose beads, allowing affinity based detection of the active Rho and Rac in cells by immunoblotting.

Another effective method requiring less time and sample is the ELISA based method. Here, RBD or PBD protein is immobilized to the wells of a 96-well plate. Active Rho/Rac proteins contained in the cell lysates bind to the wells while inactive Rho/Rac is removed during washing steps. The bound active Rho/Rac is then detected with a Rho- or Rac-specific antibody.

Both pull down and ELISA based methods were used to detect active Rho and Rac levels in cells.

Active Rho/Rac Pull-down assay

Cells were grown to 70-80% confluence in 10-cm dishes and starved overnight. Next day 5×10^6 cells resuspended in 1 ml DMEM supplemented with 0.1% BSA were spread on fibronectin coated dishes for the indicated time points and lysed with addition of 500 μ l of 3x lysis buffer on ice to achieve the final concentration of 1x lysis buffer in the whole cell lysates (described above). Levels of active RhoA / Rac1 were measured using the RhoA/Rac1 Activation Assay Kit purchased from Cytoskeleton, Inc (CA, USA) according to manufacturer's instructions. Briefly, cells were lysed in 3x lysis buffer containing (150 mM Tris, pH7.5; 30 mM $MgCl_2$; 1.5 M NaCl and 6% Igepal) and the insoluble material was removed by centrifugation at 10,000 rpm for 2 minutes at 4°C. Clarified lysates were incubated for 1 h at 4 °C with 50 μ g of Rhotekin-RBD beads for active Rho pull-down and 20 μ g of PAK-PBD beads for active Rac pull-down. Beads were then washed once with washing buffer (25 mM Tris, pH 7.5; 30 mM $MgCl_2$; 40 mM NaCl) and resuspended in 20 μ l of Laemmli buffer, and boiled for 5 min. Western blots were then performed for RhoA or Rac1 to quantify Rho/Rac precipitation for each condition.

Active RhoA/Rac1 G-LISA assay

Enzyme-linked immunosorbent assay (ELISA)-based Rho GTPase activity assays (G-LISA; Cytoskeleton, USA) were used to measure the relative RhoA/Rac1 activity of serum-starved cells after spreading on fibronectin for the indicated time points. Whole cell lysates were processed as per the RhoA/Rac1 G-LISA activation assay kit protocol. Briefly, 60 μ l of whole cell lysate was mixed with an equal volume of ice cold binding buffer (as supplied in the kit possibly containing ficoll, dextran, or polyethylene glycol, or any combination). From this mixture, 50 μ l was added to the microwells containing immobilized RBD or -PBD proteins, and incubated on an orbital shaker at 200 rpm at 4°C for 30 minutes. Post incubation, the wells were emptied by inverting them and by washing twice with wash buffer (50 mM Tris pH 7.5, 100 mM NaCl, and 30 mM $MgCl_2$ as supplied in the kit). Bound, active RhoA/Rac1/2/3 was detected by incubation with specific primary antibody recognizing either RhoA or Rac1/2/3 isoforms for 45 minutes at room temperature. Unbound antibody was washed out and bound antibody was detected by incubating the wells with a HRP-conjugated secondary antibody at room temperature for 45 minutes. This was followed by a colorimetric reaction using the chromogenic substrate (BCIP/NBT as supplied in the kit), and absorbance was read at 490 nm.

5 Results

5.1 AUM knockdown by RNA interference

AUM is ubiquitously expressed in all mouse organs and tissues tested (Fig. 13), with maximum expression observed in the testis (Duraphe, 2009).

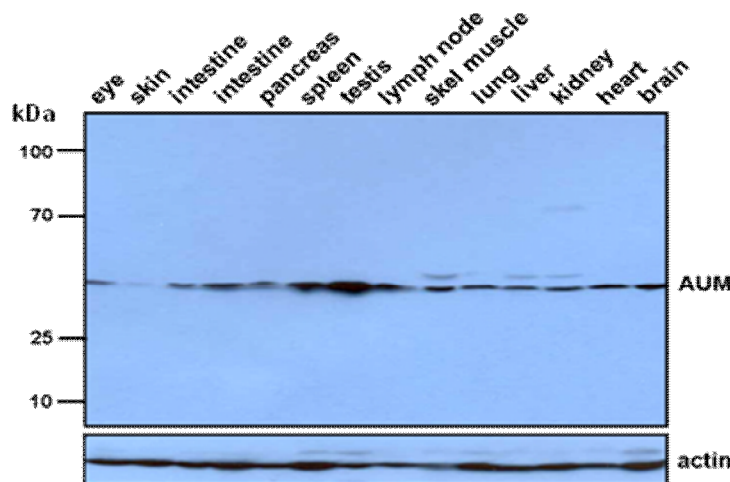


Figure 13: Analysis of AUM expression in mouse tissues.

Mouse tissue lysates were separated by SDS-PAGE, transferred onto nitrocellulose membrane and then analyzed by immunoblotting for AUM expression. AUM is ubiquitously expressed in mouse tissues with highest expression found in testis (taken from Duraphe, 2009).

Stable AUM depletion

Given the high expression of AUM in testis, we used a mouse testis derived cell line (GC-1) to investigate the cellular functions of AUM. These cells are adherent mouse spermatogonial cells of epithelial morphology (Hofmann et al., 1992).

For a long-term and uniform depletion of AUM, we stably expressed shRNAs in GC-1 cells (Duraphe, 2009). Briefly, lentiviruses harboring different AUM-specific shRNAs and one established control shRNA were generated and used for transduction of GC-1 cells. Cells stably expressing the respective shRNAs were selected using puromycin. Two out of five tested shRNA constructs (#77 and #73), yielded an effective AUM depletion in cells (Fig. 14). Both cell clones showed a considerable depletion of AUM, with clone #77 (referred herewith as m77) having the lowest amount of AUM.

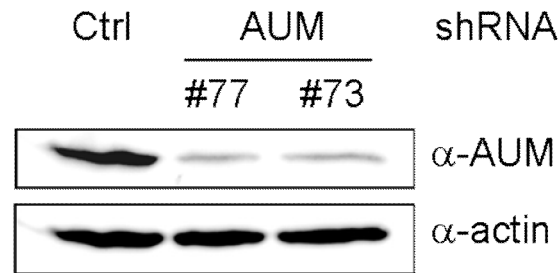


Figure 14: Stable AUM depletion by shRNA

GC1 cells were transduced with lentiviruses encoding for control shRNA (Ctrl) or AUM-targeted shRNA constructs (#73 and #77). Equal amounts of cell lysates were separated by SDS-PAGE and immunoblotted with an AUM-specific antibody. Equal loading of total protein was confirmed by immunoblotting for actin.

Transient AUM depletion

Protein downregulation mediated by shRNA is a stable way of protein depletion from the cells. However, this might activate some compensatory mechanism in the cells. In order to avoid these potential effects acute depletion of AUM was achieved by transfecting GC-1 cells with AUM-targeted siRNA. Two different siRNAs targeting different regions of AUM were transfected in GC-1 cells. A non-targeting siRNA was also transfected separately and this served as control. Most siRNAs elicit protein downregulation in a dose dependent manner and excess amount of siRNA in cells might lead to off-target effects. Therefore it is important to transfect siRNA in minimal possible amount that is able to elicit significant target protein downregulation. Different concentrations (12.5, 25 and 50 nM) of each siRNA oligoribonucleotide were transiently transfected to determine the minimum amount of siRNA required for successful AUM depletion (Fig. 15). Here we observed that both the transfected AUM targeting siRNAs efficiently depleted AUM levels in transfected GC-1 cells. Moreover, 25nm of siRNA was sufficient to achieve a significant reduction in AUM protein expression in these cells.

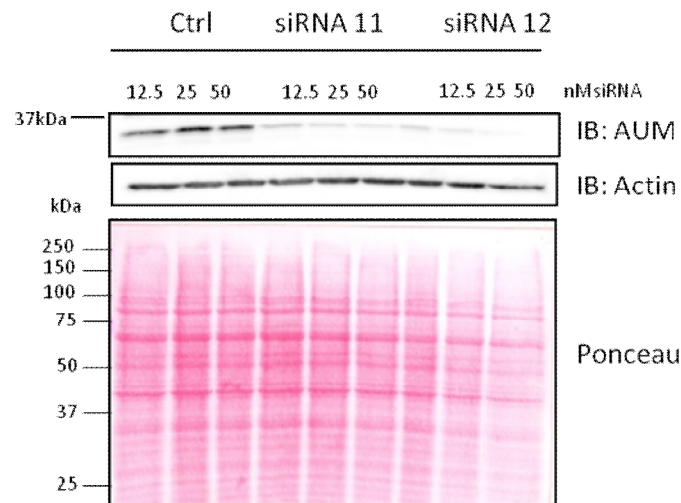


Figure 15: Transient AUM depletion by siRNA.

GC-1 cells were transfected with 12.5-50 nM of a non-targeting control siRNA (Ctrl) or AUM-directed siRNAs (#11 and #12). Cells were lysed 72 hours post transfection and immunoblotting was performed to check for levels of AUM depletion. 25 nm of both AUM-targeted siRNAs showed a strong silencing of AUM. The membrane was probed with an anti-actin antibody to test for equal protein loading. Shown below is the Ponceau S-staining of the whole blot.

5.2 AUM is involved in early cell spreading

Previous studies in the laboratory have indicated that AUM is involved in the regulation of actin dynamics (Duraphe, 2009). When cells in culture adhere to fibronectin (FN), they reorganize their actin (Fig. 7). In the early phases of cell adhesion, cells attach and begin to spread on the substrate, organizing actin in peripheral filopodia and lamellipodia (Defilippi et al., 1999). To analyse the potential role of AUM in cell spreading, control shRNA and AUM depleted cells (clone m77) were allowed to spread on fibronectin (FN) coated (10 μ g/ml) dishes for different time points (5, 10 and 20 minutes). Spreading cells were fixed with 4% PFA and stained with phalloidin to visualise F-actin. Stained cells were imaged with an epifluorescence microscope (Fig. 16A) and total cell area of individual cells was measured as detailed under Materials and Methods.

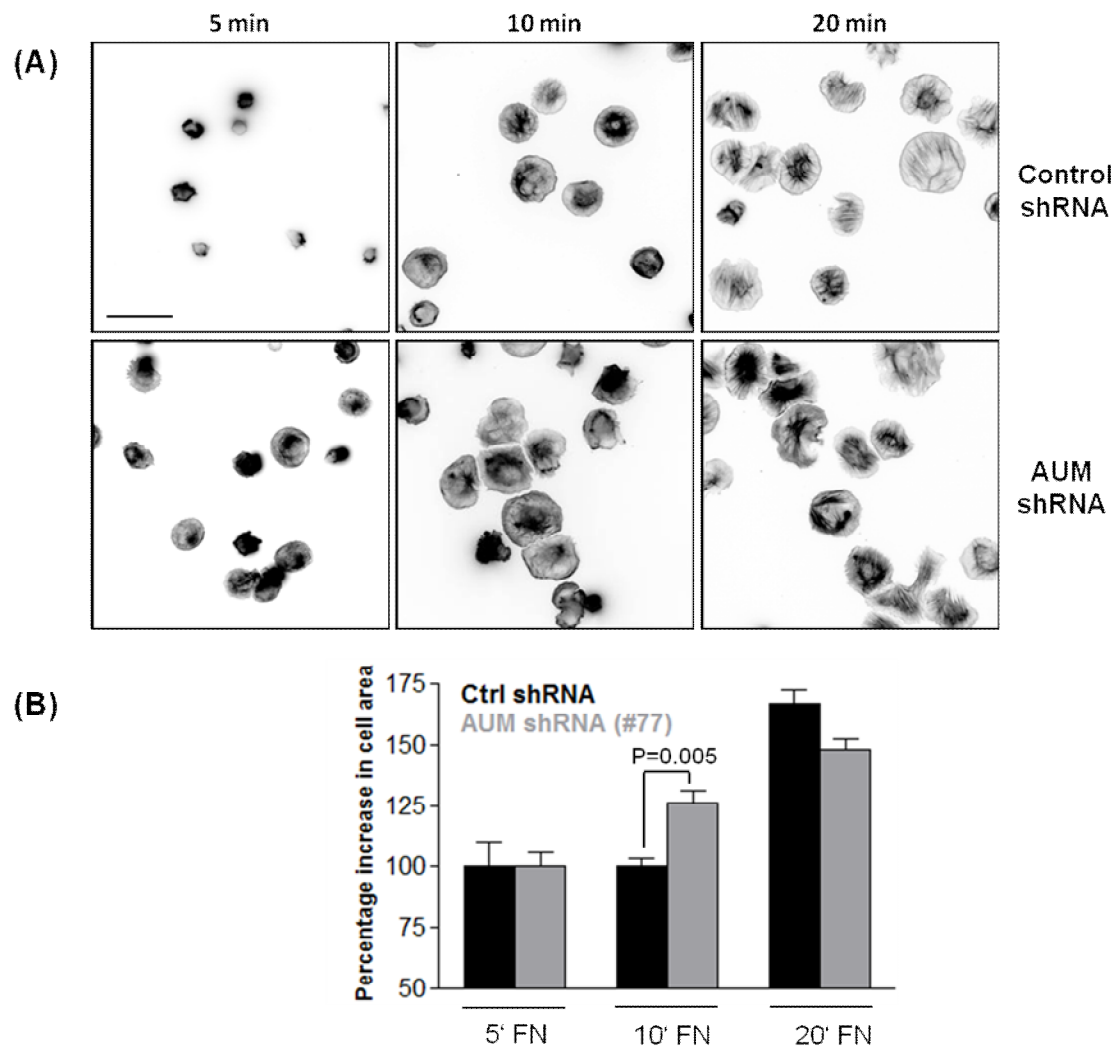


Figure 16: AUM depletion accelerates cell spreading on FN.

(A) Cells expressing control shRNA or AUM shRNA were allowed to spread on FN coated surfaces for the indicated time points and fixed with 4% PFA. To visualise F-actin cells were stained with Phalloidin. Micrographs of stained cells were acquired using an epifluorescence microscope with 63x magnification. Scale bar represents 10 μ m.

(B) Quantification of cell area of spreading cells. Multiple images from different fields were tiled into one. The cell areas were measured after thresholding the images. Values obtained were normalized against control shRNA expressing cells after 5 min of spreading and plotted as percentage increase in size with respect to the same for all other conditions. At least 300 cells per condition were analyzed (values indicate means \pm SEM, P values were calculated using paired Student's t-test). The average cell area of AUM depleted cells is approximately 25% larger than of control cells after 10 min of spreading on FN.

At least 300 cells per condition were scored for cell area. After 10 minutes of spreading on FN, AUM depleted GC1 cells on an average had 25% more surface area when compared to control shRNA expressing cells (Fig. 16B). However, we did not observe any significant change in cell area between control and AUM depleted cells at later (20 minutes) or earlier (5 minutes) time points. This transient increase in cell area after AUM depletion suggests a possible role of AUM in regulation of early events in cell spreading.

5.3 AUM regulates early cell-ECM adhesion

Regulation of focal adhesion turnover by actin re-organisation heavily influences adhesion of cells to ECM (Parsons et al., 2010). Increased spreading of AUM depleted cells on fibronectin points towards a possible role of AUM in cell-ECM adhesion. This prompted an investigation of the role of AUM in cell adhesion.

GC-1 cells preferentially adhere to FN

Cellular ECM is composed primarily of fibrous polymers like fibronectin, collagen and laminin along with other proteoglycans. Cells exhibit high degree of specificity in their adhesion to different ECM components. To study the role of AUM in cell adhesion we performed cell adhesion assay. Here, equal number of calcein stained fluorescent cells were allowed to adhere to microwell plate coated with different ECM-components for defined time points. After incubation, unbound cells were washed and resultant fluorescence from the adhering cells was measured. Given the wide variety of ECM polymers we first tested the specificity of GC-1 cells towards different ECM fibers. For this 96-well microtiter plates were coated with collagen I, collagen IV or FN. Poly-L-lysine (PLL) is a widely used neutral tissue adhesive and was used here as a control for cell adhesion. GC-1 cells showed maximum affinity for fibronectin followed by PLL. Collagen I and collagen IV coated wells minimally supported GC-1 cell adhesion (Fig. 17). Based on these results all further experiments were conducted on fibronectin coated surfaces.

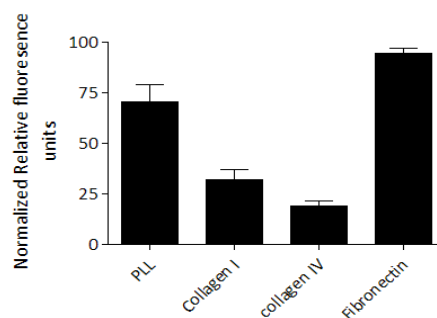


Figure 17: GC-1 cells preferentially adhere to Fibronectin

GC-1 cells were serum starved, detached by limited trypsinization, loaded with calcein-AM, and seeded onto coated (Poly-L-lysine (PLL), Collagen I, Collagen IV or FN) 96-well microplates for 40 minutes. Afterwards, unbound cells were washed away, and cell adhesion was measured fluorimetrically using a microplate reader. Values obtained were normalized to the fibronectin coated wells and expressed as percentages. Cells preferentially adhere to FN as compared to both types of collagen tested.

Effect of AUM on Cell-FN adhesion

To study the role of AUM in cell-fibronectin adhesion, cell adhesion assays were performed with control and AUM depleted cells. Serum starved cells were used to minimize the effect of

proteins like vitronectin and fibronectin (normally present in the serum) on cells adhering to fibronectin coated surface. Overnight starved, calcein stained cells were detached by limited trypsinisation and subsequently treated with soybean trypsin inhibitor to inactivate trypsin. Cells were counted and 30,000 cells in 50 μ l volume were seeded in each well of FN (10 μ g/ml) coated 96-well microtiter plate. Each condition in every experiment was performed in triplicates. After cell seeding, plates were incubated for different time points (5, 10, 20 and 40 minutes) in a cell culture incubator. Post-incubation unbound cells were washed away and the resultant fluorescence from fibronectin-bound calcein stained cells in each well was recorded using a fluorescence reader.

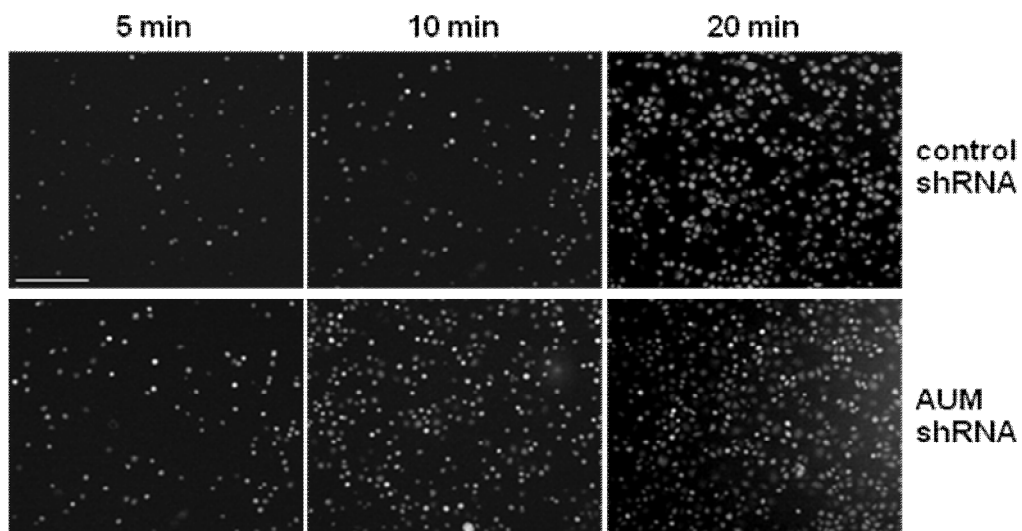


Figure 18: Adhesion of AUM depleted cells to fibronectin.

Representative images of time-based cell adhesion assay. Seen here are calcein labeled cells (white dots in images above) adhering to fibronectin coated surface. Control and AUM shRNA expressing GC-1 cells were serum starved, detached by limited trypsinization, loaded with calcein-AM, and seeded onto FN-coated 96-well microplates for indicated time points. Unbound cells were washed away, and adhering cells were imaged using an epifluorescent microscope. Scale bar represents 100 μ m.

Representative fluorescent images of calcein labeled cells adhering to fibronectin coated wells of microtiter plate are shown above (Fig. 18).

Visual observations clearly suggests that AUM depleted cells adhere faster on fibronectin after 10 minutes incubation and this difference appears to be lost after 20 minutes. To quantify cell adhesion, fluorescence intensity from the adhering cells was measured using fluorescence reader and the values obtained were represented graphically (Fig. 19).

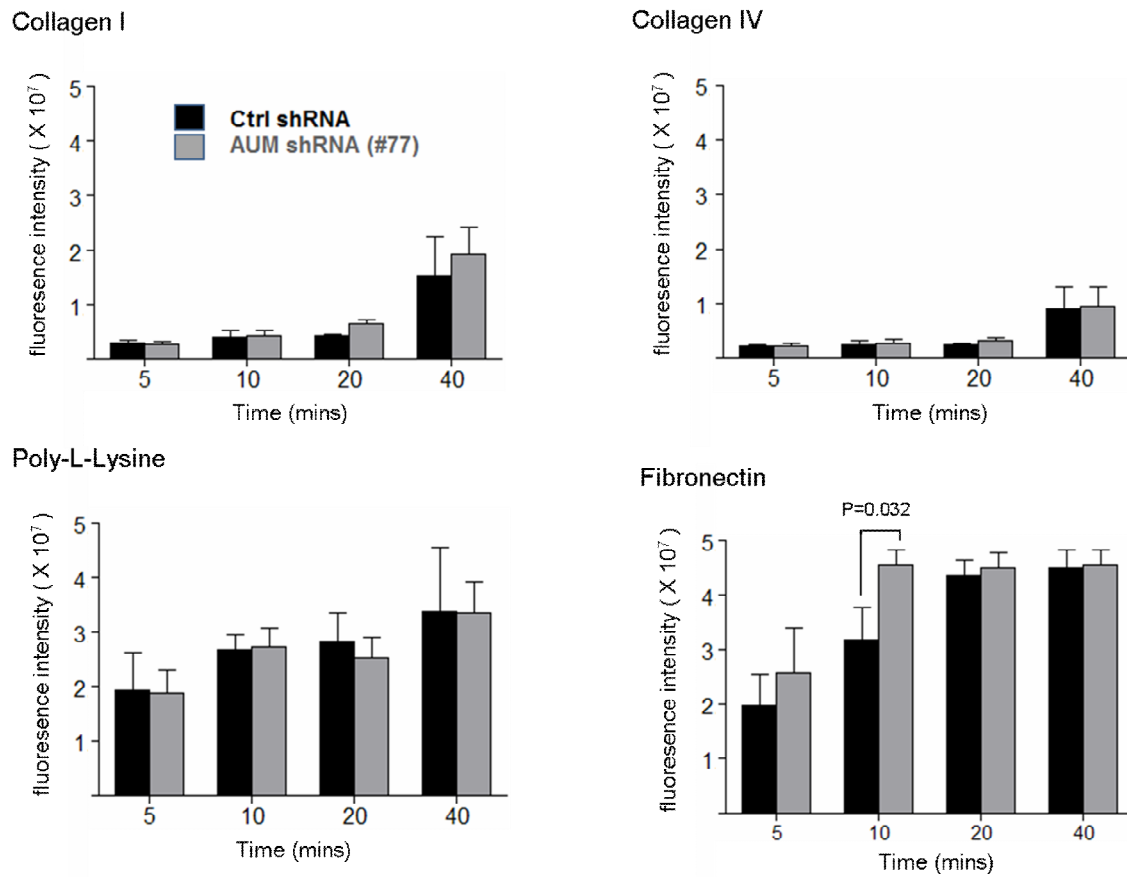


Figure 19: AUM depletion accelerates cell adhesion on FN.

GC-1 cells expressing control (black bars) or AUM shRNAs (grey bars) were serum starved, detached by limited trypsinization, loaded with calcein-AM and seeded onto Collagen I, Collagen IV, PLL or FN-coated 96-well microplates and incubated for the indicated time points. Unbound cells were washed away, and fluorescence intensity from adhering cells was measured fluorimetrically on a microplate reader. Results are means of three independent experiments performed in triplicates. Error bars represent ± S.D. P value was calculated using Student's t-test.

As described before, apart from FN, cell adhesion on collagen I and collagen IV was also tested. As a positive control for cell adhesion PLL was used as a neutral adhesive. However under similar conditions, no difference in cell adhesion was observed between control and AUM depleted cells adhering on collagen I, IV and PLL coated surfaces at all the time points tested. Interestingly, after 10 minutes of adhesion on FN, AUM depleted cells show increased adhesion (1.5 fold) when compared to control cells (Fig. 19). After 5 minutes of incubation, AUM depleted cells showed a non significant tendency for preferred adhesion to FN. Later time points tested (20 and 40 minutes) failed to show any difference on adhesion to FN between control and AUM depleted cells. This observation was in concordance with the cell spreading assays shown before (Fig. 16) suggesting that AUM mediated effect on cell adhesion and spreading are robust but transient in nature. More importantly this suggests that AUM is involved in early events of cell adhesion to substratum. To rule out the possibility that the observed effects of AUM depletion on cell adhesion are due to a specific

clone of shRNA another AUM depleted cell line expressing a different shRNA clone (m73) (Fig. 14) was used in similar assay along with m77 (used previously). Here also we observed a similar transient effect and both the AUM depleted clones adhered preferentially on FN after 10 minutes of incubation. However, fewer m73 AUM shRNA expressing cells adhered to fibronectin as compared to cells expressing clone m77 (Fig. 20) possibly due to less efficient knockdown of AUM in m73 cells than m77 cells (Fig. 16). No difference was observed at later time points tested (Fig. 20).

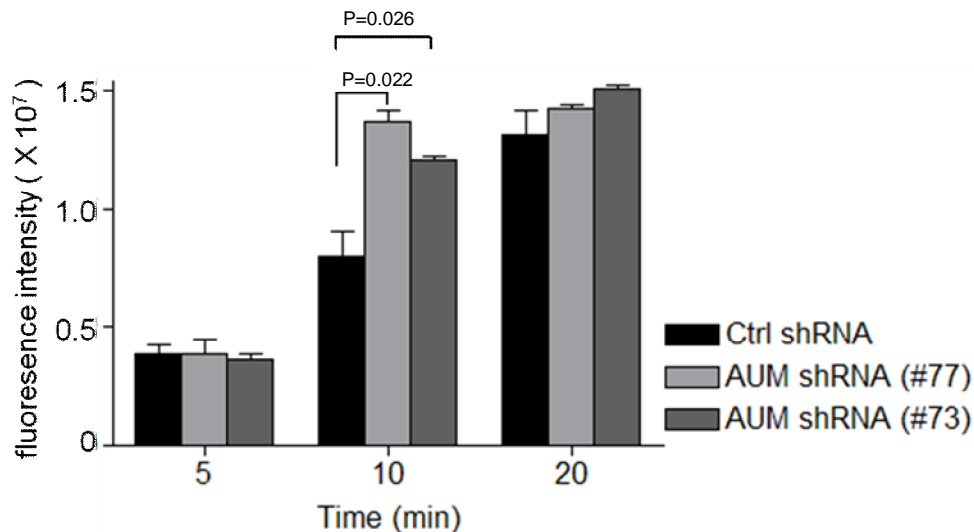


Figure 20: AUM depletion accelerates cell adhesion on FN.

GC-1 cells expressing control (black bars) or AUM shRNAs (#77; light grey bars) or AUM shRNA (#73; dark grey bars) were serum starved, detached by limited trypsinization, loaded with calcein-AM, and seeded onto FN-coated 96-well microplates for the indicated times. Unbound cells were washed away, and cell adhesion was measured fluorimetrically on a microplate reader. Results are means of three independent experiments performed in triplicates. Error bars represent \pm S.D. P value was calculated using Student's t-test.

5.4 Acute AUM depletion also leads to increased cell adhesion on FN

shRNA mediated down regulation of protein expression results in stable loss of protein expression. Such a condition might result in cells switching to compensatory mechanisms to overcome a particular protein deficiency. In order to rule out the possibility that compensatory mechanisms are the cause of the observed difference in the control-shRNA versus AUM-depleted cell adhesion to FN, GC-1 cells were transfected with AUM-targeting siRNA. This approach results in an acute and transient depletion of AUM in cells.

After verifying successful siRNA mediated AUM depletion by immunoblotting, adhesion assay were performed with same cells in conditions similar to those used for adhesion assay with AUM shRNA expressing cells.

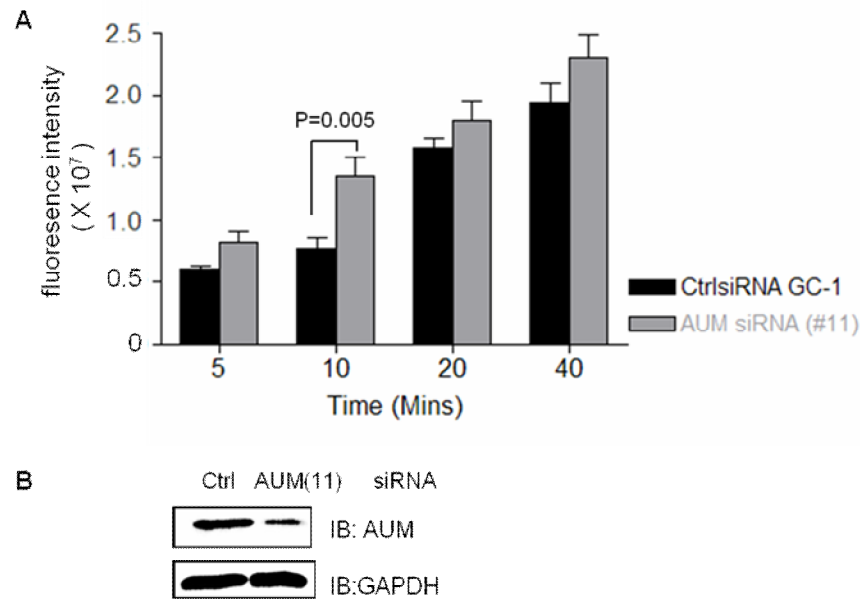


Figure 21: Acute AUM depletion also leads to increased cell adhesion on FN.

(A) GC-1 cells expressing control (black bars) or AUM siRNA (grey bars) were serum starved, detached by limited trypsinization, loaded with calcein-AM, and seeded onto FN-coated 96-well microplates for the indicated times. Unbound cells were washed, and cell adhesion was measured fluorimetrically on a microplate reader. Results are means of three independent experiments performed in triplicates. Error bars represent \pm S.D. P value was calculated using Student's t-test.

(B) Western blot probed with AUM antibody showing successful silencing of AUM after siRNA treatment. Equal loading of total protein lysate was ensured by reprobing the same blot with GAPDH antibody (shown below).

Similar to cells expressing AUM shRNA, acute depletion of AUM with siRNA in GC-1 cells also resulted in increased adhesion to fibronectin at earlier time points of 5 and 10 minutes (Fig. 21). Almost two fold increase in cell adhesion to FN was observed with cells acutely depleted of AUM when compared to their control counterparts. Similar to previously observed results a transient increase in cell adhesion to FN was observed as at later time points of 20 and 40 minutes there was no difference in adhesion between control and AUM siRNA treated cells. Taken together, AUM depletion leads to preferential adhesion of cells to FN coated surfaces irrespective of the method used to downregulate AUM. This observation strongly indicates a role for AUM in early cell adhesion.

5.5 Re-expression of AUM normalizes cell adhesion

So far we observed increase in cell adhesion to FN after AUM depletion. To confirm if the observed increase in cell adhesion is AUM specific, rescue experiments for the mutant phenotype were performed by transiently re-transfecting AUM in AUM-depleted cells. One of the primary concern in this was to choose a species variant of AUM that is not targeted by the shRNA already expressed in the cells. Sequence analysis revealed that AUM shRNA present in GC-1 cells can not target human AUM (hAUM). Therefore, hAUM was transiently

transfected in AUM shRNA expressing cells and adhesion assay was performed. Another aspect of AUM mediated cell adhesion is if AUM is required for the above observed effects in its capacity as a phosphatase or it's simply required as a protein scaffold. To study this AUM depleted cells were also transfected with mutated hAUM (hAUM-^{D34N}) where aspartate at the active site was mutated thus resulting in enzymatically inactive AUM. It has been previously shown that mutating aspartate at 34th position (active site) in AUM sequence renders AUM enzymatically inactive (Duraphe, 2009).

In order to rescue AUM depleted cells, it was essential to transfect the correct amount of hAUM construct in order to yield AUMshRNA expressing cells with a total amount of exogenous (human) AUM that is similar to the endogenous AUM levels found in controlshRNA expressing cells. To achieve this, AUMshRNA expressing cells were transfected with different concentrations of hAUM^{wt} or hAUM^{D34N} constructs. 48 hours post-transfection cells were lysed and probed for AUM expression by immunoblotting. Densitometric analysis of the immunoblots revealed that 30ng of the hAUM^{wt} or hAUM^{D34N} construct were sufficient to achieve similar levels of total AUM in depleted and control cells (Fig. 22).

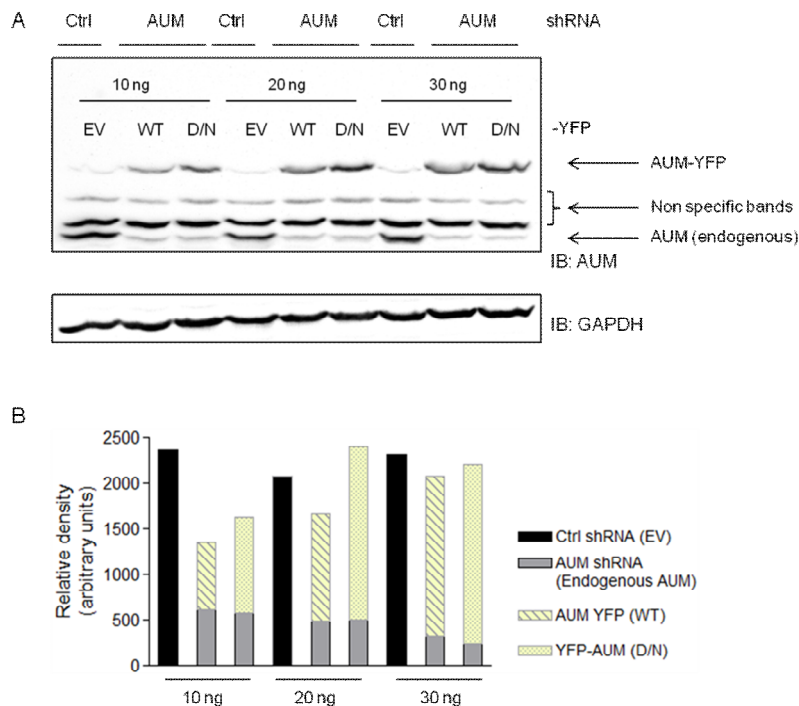


Figure 22: Re-expression of AUM to rescue AUM depletion.

(A) AUM shRNA expressing cells were transfected with 10, 20 and 30 ng of YFP-hAUM^{wt} [AUM YFP (WT)] or hAUM^{D34N} [AUM YFP (DN)] plasmid using lipofectamine as described (methods section). Cells were lysed 48 hours post transfection and immunoblotting was performed as above to check for AUM expression. Since hAUM is tagged with YFP it migrates slower than endogenous AUM and is recognized as a separate band. Control cells were transfected with the empty vector (EV) alone. Equal loading of total protein lysate was ensured by reprobing the same blot with GAPDH antibody (shown below). YFP-hAUM^{D34N} shown as YFP-hAUM (D/N) in the figure.

(B) Densitometric quantification of the above blot. Black bars indicate control shRNA cells transfected with empty vector and grey bar indicates levels of endogenous AUM in AUM depleted cells. Expression of YFP-hAUM^{wt} is shown as yellow bars with angled stripes and YFP-hAUM^{D34N} is shown as yellow bars with dots. YFP-hAUM^{wt} and YFP-hAUM^{D34N} values are stacked with endogenous AUM values to allow comparison with the EV transfected control shRNA cells. YFP-hAUM^{D34N} shown as YFP-hAUM (D/N) in the figure.

Densitometric quantification of the above blot showed that 30ng of hAUM plasmid when transfected in AUM depleted cells was sufficient to rescue AUM deficiency. Based on the above results, control shRNA cells were transfected with 30ng of vector alone. AUM shRNA cells were transfected with 30ng each of either empty vector or hAUM or the mutated hAUM (hAUM^{D34N}). All the transfected cells were serum starved overnight and cell adhesion assay was performed as before. After 10 minutes of adhesion on fibronectin, AUM-depleted cells re-expressing AUM failed to show increased adhesion on fibronectin. Rather the extent of adhesion was similar to that of control shRNA treated cells (Fig. 23A). AUM transfection was controlled by western blot (Fig. 23B). These results clearly demonstrate that the observed increase in AUM depleted cell adhesion to fibronectin is indeed AUM mediated.

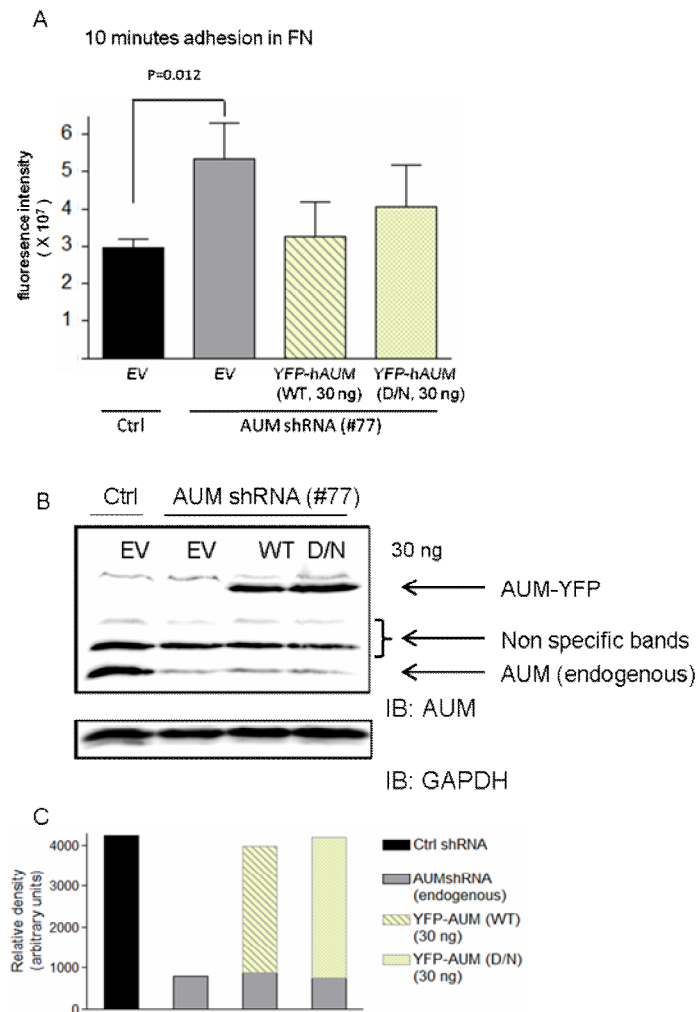


Figure 23: Re-expression of AUM normalizes increase in cell adhesion due to AUM depletion.

(A) Control (black bars) and AUM shRNA (grey bars) expressing cells were transfected with 30ng of indicated vector using lipofectamine as described (methods section). Cells were serum starved, detached by limited trypsinization, loaded with calcein-AM, and 30,000 cells were seeded in each well of FN-coated 96-well microplates for 10 minutes. Post incubation, unbound cells were washed away, and cell adhesion was measured fluorimetrically on a microplate reader. Results are means of three independent experiments performed in triplicates. Error bars represent \pm S.D. P value was calculated using Student's t-test. YFP-hAUM^{D34N} shown as YFP-hAUM (D/N) in the figure.

(B) Cells were lysed 48 hours post transfection and immunoblotting was performed as above to check for levels of AUM. Since hAUM is tagged with YFP it is recognized as a separate band than the endogenous AUM. Control cells were transfected with the empty vector alone. Equal loading of total protein lysate was ensured by reprobing the same blot with GAPDH antibody (shown below).

(C) Densitometric quantification of the above blot. Black bar indicates control shRNA cells transfected with empty vector and grey bar indicates levels of endogenous AUM in AUM depleted cells. Expression of YFP-hAUM^{wt} is shown as yellow bars with angled stripes and YFP-hAUM^{D34N} (shown as YFP-hAUM (D/N) in the figure) is shown as yellow bars with dots. YFP-hAUM WT and YFP-hAUM^{D34N} values are stacked with endogenous AUM values to allow comparison with the EV transfected control shRNA cells.

5.6 Accelerated adhesion due to AUM-depletion is integrin dependent

Cell adhesion to the extracellular matrix (ECM) is mediated by a variety of matrix molecules and integrin proteins (Schwartz et.al. 1995). Integrins act as transmembrane linkers between ECM molecules and cytoplasmic proteins that anchor the actin cytoskeleton to the membrane. Many members of the integrin family recognize an Arg-Gly-Asp (RGD) motif present in their ligands (Hynes and Yamada, 1982). In fact, peptides containing this motif can efficiently block these integrin–ligand interactions. It is the residues outside the RGD motif, however, that provide specificity as well as high affinity for each integrin–ligand pair (Pierschbacher and Ruoslahti, 1984). To analyze the role of integrins in accelerated adhesion of AUM-depleted cells to FN, adhesion assay was performed in the presence of RGD peptides. Two different hexamer variants of RGD peptides were used. One with the sequence H-Gly-Arg-Gly-Asp-Thr-Pro-OH (GRGDTP) has been shown to inhibit binding of fibrinogen, fibronectin, vitronectin, and von Willebrand factor to platelets apart from inhibiting cell attachment to collagen, fibronectin, and vitronectin. Other hexamer with sequence H-Gly-Arg-Gly-Asp-Ser-Pro-OH (GRGDSP) was more specific in the sense that it inhibits FN binding to platelet-binding sites. Both the peptides have been shown earlier to effectively block fibronectin mediated cell-ECM adhesion (Gehlsen et al., 1988). Peptide with the sequence H-Gly-Arg-Ala-Asp-Ser-Pro-OH (GRADSP) was used as a control peptide since it has been shown to be inactive in blocking cell-FN interactions. In comparison to the RGD peptide the control peptide has alanine substituted for glycine residue, present in the middle of the RGD sequence. Prior to cell adhesion both control and AUM-depleted cells were trypsinised and treated with 200µM of either control or RGD peptides (both variants separately) for 30 minutes. Post incubation cell adhesion on fibronectin coated microtiter wells was performed as before. Since AUM-depleted cells display accelerated adhesion on FN after 10 minutes, RGD or control peptide treated cells were also incubated for similar time on fibronectin. It is known that RGD mediated blocking of cell-fibronectin adhesion is reversible. To rule out any such possibility cells were seeded on FN coated microtiter plate in the presence of 200µM of RGD peptide (Fig. 24).

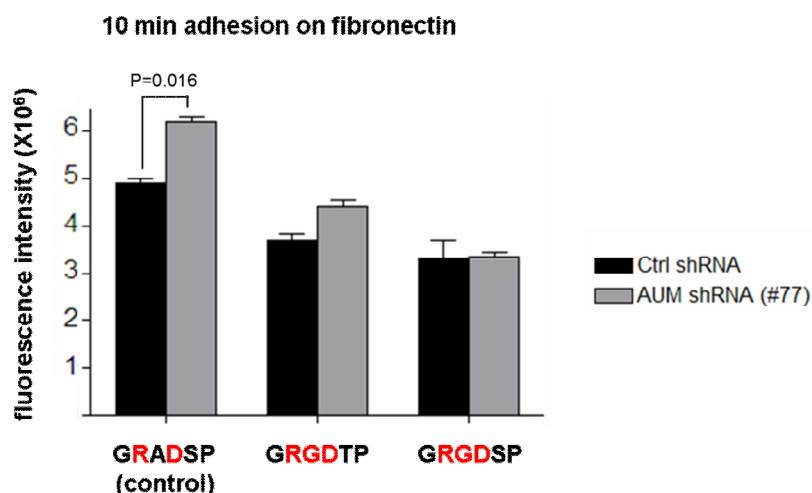


Figure 24: Accelerated adhesion due to AUM-depletion is integrin-dependent.

Control (black bars) and AUM shRNA (grey bars) expressing cells were serum starved overnight, trypsinised and treated with 200 μ M of indicated peptides (RGD sequence is shown in red) for 30 minutes. Post incubation cells were, loaded with calcein-AM, and 30,000 cells were seeded in the presence of the indicated peptides to each well of FN-coated 96-well microplates for 10 minutes. After 10 minutes unbound cells were washed away, and cell adhesion was measured fluorimetrically on a microplate reader. Results are means of three independent experiments performed in triplicates. Error bars represent \pm S.D. P value was calculated using Student's t-test.

AUM-depleted cells treated with control peptide showed increase adhesion to FN after 10 minutes when compared to the control shRNA cells. This was in concordance with previous observation that AUM depletion leads to increased cell adhesion on FN. Interestingly, both control shRNA and AUM shRNA expressing cells when treated with 200 μ M of either variant of RGD peptide showed attenuated adhesion to fibronectin. Moreover, accelerated adhesion of AUM-depleted cells after 10 minutes of adhesion on fibronectin was lost and rather was similar to the control shRNA expressing cells. Both the variants of RGD peptides exhibited similar effect on cell adhesion (Fig. 24). These results strongly indicate towards the possible role of integrins in increased cell adhesion of AUM-depleted cells to FN.

5.7 Cell surface expression of integrins

Integrins are a large family of heterodimeric transmembrane glycoproteins that connect cells to the extracellular matrix proteins of the basement membrane or to ligands on other cells. Integrins contain large (α) and small (β) subunits of sizes 120-170 kDa or 90-100 kDa, respectively, and mediate direct cell-ECM recognition and interaction. Integrins contain binding sites for divalent cations Mg^{2+} and Ca^{2+} , which are often necessary for integrin function. Driven by the above result that AUM-depletion induced accelerated cell adhesion probably by involving integrins, the surface expression of various integrin molecules on control and AUM depleted GC-1 cells was analyzed. We have shown before that AUM depleted GC-1 cells preferentially adhere to FN. The major fibronectin receptor in cells is the

$\alpha 5 \beta 1$ integrin, a heterodimer of noncovalently associated $\alpha 5$ and $\beta 1$ subunits. Another integrin heterodimer, $\alpha v \beta 3$, is also known to recognize fibronectin. Both these heterodimers are ubiquitously expressed. In order to estimate the cell surface expression of these heterodimers, control and AUM-depleted cells growing in DMEM supplemented with 10% FCS were trypsinized, fixed with 4% PFA and stained with the antibodies recognizing the different integrin subunits. Stained cells were analyzed by flow cytometry. This method is a reliable way to estimate cell surface expression of integrins as it analyses thousands of cells at the same time. As a negative control for staining, cells were also stained with the corresponding isotype antibodies. The data acquired with FACS are represented as histograms. These are graphs that display a single measurement parameter (relative fluorescence or light scatter intensity) on the x-axis and the number of events (cell count) on the y-axis. In order to quantify these histograms, the geometric means (geo means) of different peaks were plotted (Fig. 25).

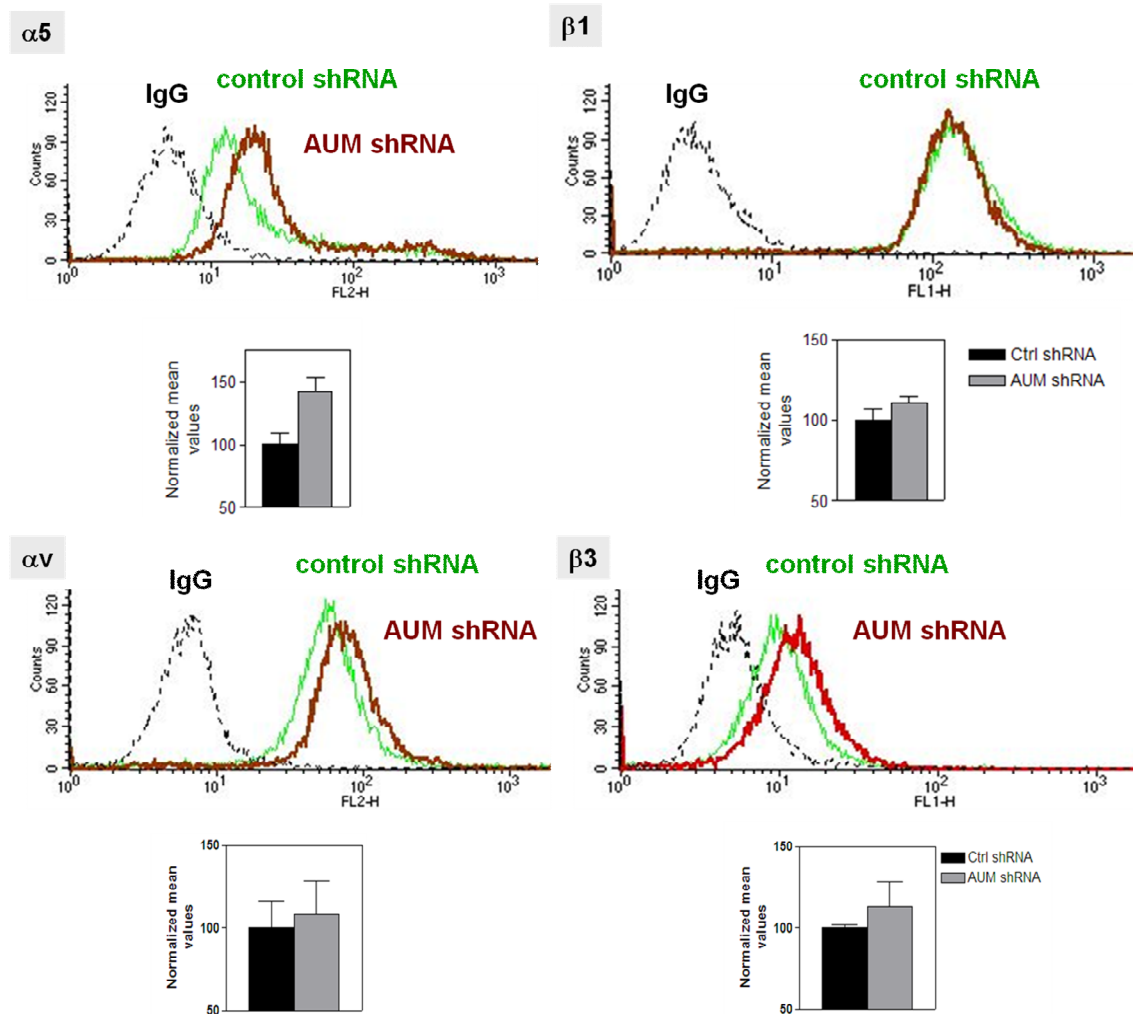


Figure 25: Cell surface expression of various fibronectin binding integrin subunits.

Control and AUM-depleted cells growing on culture dishes in DMEM supplemented with 10% FCS were trypsinised and equal number of cells were incubated with the indicated integrin subunit specific monoclonal antibody conjugated with fluorophores. Antibodies recognizing both the alpha integrin subunits were conjugated with PE and beta 1 and 3 antibodies were conjugated with FITC. Post incubation cells were analysed with FACS and values obtained were expressed as histograms. Separate histograms obtained from control and AUM depleted cells were overlaid for comparison. Geo means from these histograms was plotted as bar graph for quantification. Above are the overlays of representative histogram profile. Preceding each histogram overlay the integrin subunit tested is indicated. Dashed black line shows the isotype control staining. Green and red lines indicate control or AUM shRNA cells, respectively. Below each histogram overlay is the quantification data expressed as bar graph obtained from geo means of individual experiments. Values were normalized to control shRNA and expressed as percentage. Results are means of three independent experiments. Error bars represent \pm S.D.

Of the selected integrins profiled here for their cell surface expression, only $\alpha 5$ integrin subunit showed a significant 1.5 fold increase in the surface of AUM depleted cells when compared to the control cells. However, the other 3 integrin subunits tested ($\beta 1$, $\beta 2$ and αV) showed similar levels of cell surface expression between control and AUM depleted cells (data not shown).

5.8 AUM-depleted cells have more active $\beta 1$ -integrin on cell surface

Adhesive events mediated by transmembrane $\alpha\beta$ heterodimers in the integrin family are dynamically regulated. Studies with the platelet specific integrin heterodimer $\alpha IIb\beta 3$ have indicated that both integrin activation (Charo et. al., 1991) and ligand binding are followed by conformational changes of integrin receptor (Kouns et. al., 1990). Integrin is considered “active” when bound to ligand (Du et. al., 1991). The study of variable integrin activation states has been facilitated by the use of monoclonal antibodies that selectively recognize distinct “active” integrin conformation.

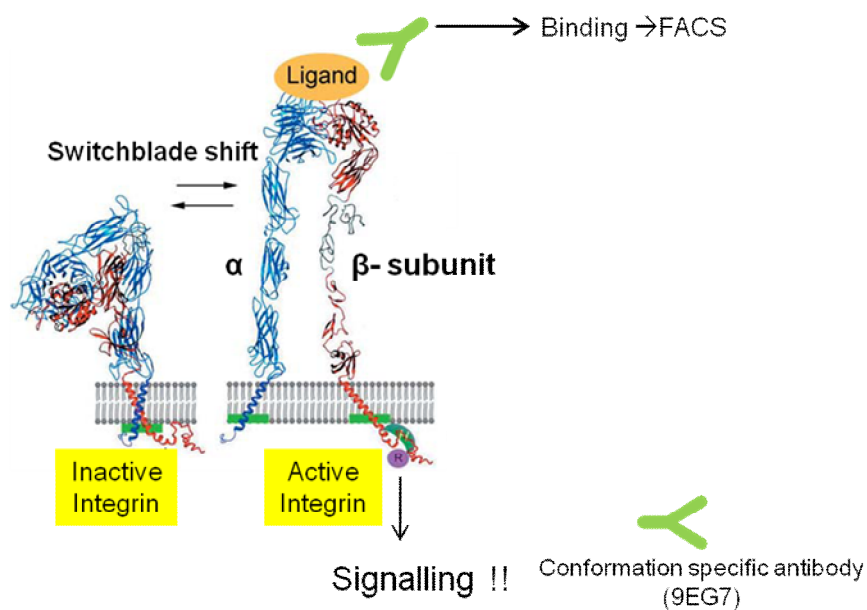


Figure 26: Monoclonal antibody 9EG7 recognizes active conformation of $\beta 1$ integrin. (Bazzoni et al., 1998).

Previous results (Fig. 25) showed that $\beta 1$ integrin is expressed on the cell surface of both control and AUM-depleted cells. The antibody used here recognizes total $\beta 1$ integrin present on the cell surface irrespective of its activation state. However, as shown above (Fig. 26) activation state specific monoclonal antibody 9EG7 is able to recognize active conformation of $\beta 1$ integrin. To check if there exists a difference between control and AUM-depleted cells with respect to presence of active integrin on the cell surface, both the cell types were stained with 9EG7 antibody and analysed by FACS

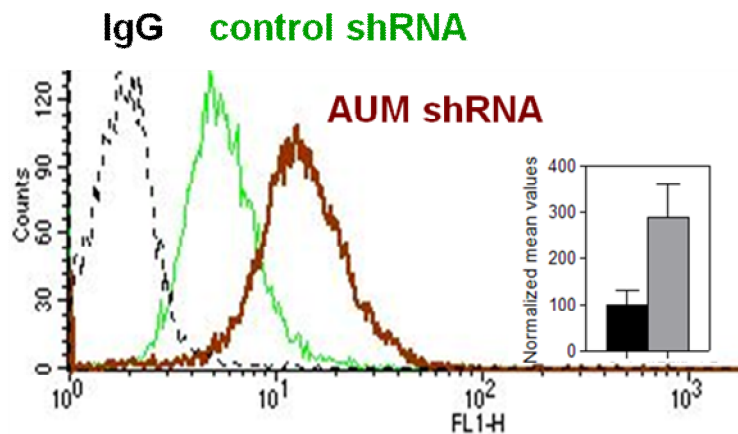


Figure 27: AUM depleted cells have more active $\beta 1$ integrin receptors.

Cell surface expression of conformationally active $\beta 1$ integrin recognized by 9EG7 antibody. Cells growing in DMEM and 10% FCS were trypsinised and equal number of cells was incubated with 9EG7 monoclonal antibody and FITC-labeled secondary antibody sequentially. Stained cells were analyzed with FACS and the Geo means obtained from the histograms was plotted for quantification. Above are the overlays of representative histogram profile. Dashed black line shows the isotype control staining. Green and red lines indicate control and AUM shRNA cells respectively. Next to the histogram overlay (inset) is the quantified data obtained from geo means of individual experiments. Values were normalized to control shRNA and expressed as percentage. Black and grey bars represent control or AUMshRNA expressing cells respectively Results are means of three independent experiments. Error bars indicate \pm S.D.

AUM-depleted and control cells growing in the presence of 10% FCS failed to show any difference in cell surface expression of total $\beta 1$ integrin (Fig 25). However, when probed with 9EG7 antibody that recognizes 'active' $\beta 1$ integrin conformation, AUM depleted cells displayed almost a 3-fold increase in cell surface expression when compared to the control cells (Fig. 27). This observation clearly shows increased presence of conformationally active $\beta 1$ integrin in the absence of AUM.

$\beta 1$ -integrin activation is FN-dependent

$\beta 1$ integrin activation is ligand dependent. Upon binding an extracellular ligand such as FN, activated integrins generate an intracellular signal and their function can also be regulated from within the cell, thereby rendering them capable of signaling bidirectionally (Takada et. al., 2007). Also integrins are transmembrane links between extracellular contacts and the actin microfilaments of the cytoskeleton. Since AUM-depleted cells show accelerated adhesion on FN at early time points (10 minutes), it is important to study if $\beta 1$ integrin activation is dependent on FN. To mimic the conditions of cell adhesion on fibronectin both control and AUM-depleted cells were serum starved overnight. Starved cells were trypsinized and treated with or without $2\mu\text{g}$ fibronectin per 100,000 cells. Fibronectin treated and untreated cells were incubated at 37°C for 10 minutes in suspension. By this experiment we

attempted to mimic condition in the cell adhesion assay performed earlier. Since the whole experiment was performed using cells in suspension they are unable to spread and adhere. Still, integrin receptors present on the cell surface encounter FN leading eventually to conformationally 'active' integrin. Also, this experiment can answer the question whether FN alone is sufficient for $\beta 1$ integrin activation in the absence of AUM, or whether additional signaling proteins are also required in the process.

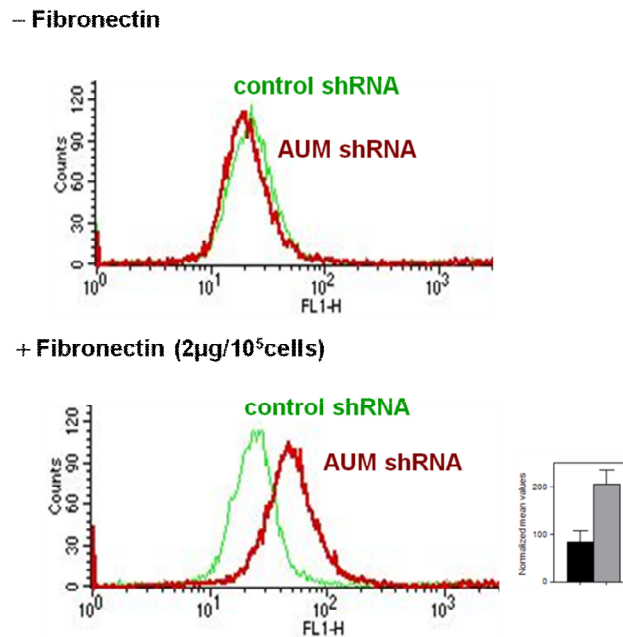


Figure 28: $\beta 1$ integrin receptor activation is AUM dependent.

Surface expression of active $\beta 1$ integrin recognized by 9EG7 antibody. Cells growing in DMEM and 10% FCS were serum starved overnight, trypsinised and equal number of cells were incubated with or without (as indicated) with fibronectin. Post-incubation, cells were sequentially stained with 9EG7 monoclonal antibody and FITC-labeled secondary antibody. Stained cells were analyzed with FACS and the Geo means obtained from the histograms were plotted for quantification. Above are the overlays of representative histogram profile. Green and red lines indicate control or AUM shRNA cells, respectively. Next to the histogram overlay is the quantified data obtained from geo means of individual experiments. Values were normalized to control shRNA and expressed as percentage. Black and grey bars represent control or AUMshRNA expressing cells, respectively. Results are representative of three independent experiments. Error bars indicate \pm S.D.

Here, serum starved cells failed to show any difference in the levels of active $\beta 1$ integrin on the cell surface. Intriguingly, fibronectin simulation of suspended, serum-starved cells elicited a strong increase (two-fold) in active $\beta 1$ integrins on the cell surface in AUM-depleted cells (Fig. 28). These results strongly indicate that fibronectin or serum-stimulation itself is sufficient to reveal AUM-dependent regulation of $\beta 1$ integrins, and that no additional signaling inputs are required.

5.9 AUM influences actin dynamics during adhesion and spreading

As soon as cells encounter fibronectin, they begin to reorganize their actin following distinct sequential events. In the early phases of cell adhesion, cells attach and begin to spread on the ECM, organizing actin in peripheral filopodia and lamellipodia. At this time early focal contacts are occasionally present at the edges of the cells. Soon after adhesion, cells are maximally enlarged and organize actin in thin stress fibers resulting in cell stretching due to the tensile forces of the actin cables. At this time, stress fibers are anchored to the plasma membrane at mature focal adhesion structures. To see differences in actin stress fiber formation between control and AUM depleted cells, starved cells were spread on fibronectin coated dishes for 10 minutes, fixed and stained with phalloidin (Fig. 29).

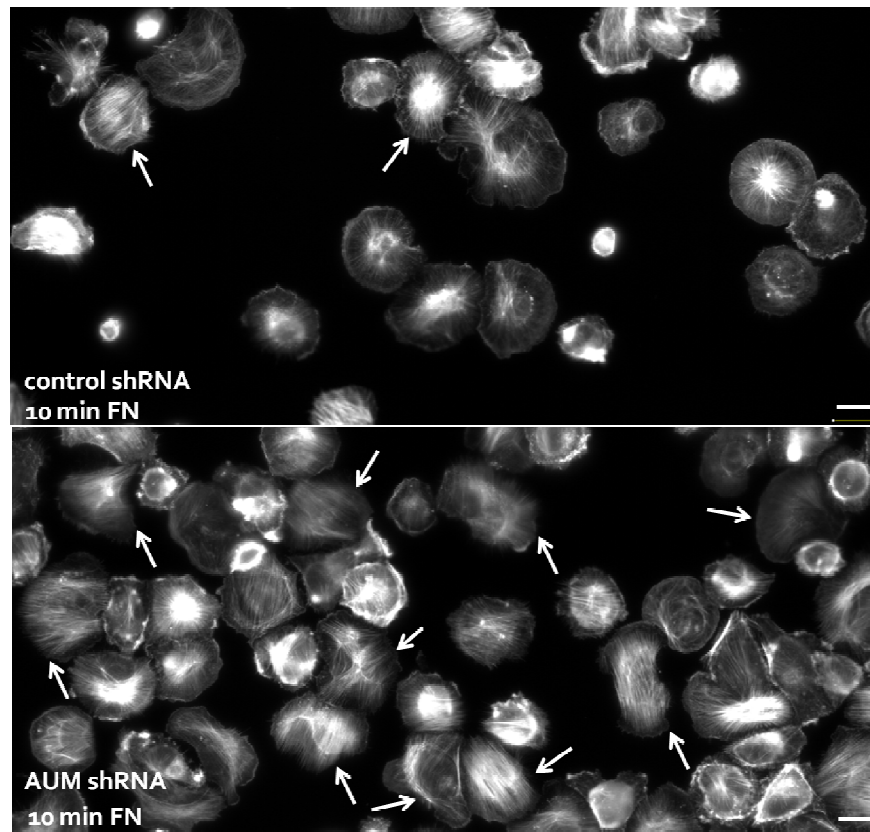


Figure 29: AUM depleted cells have more actin stress fibers.

After 10 min of adhesion, AUM depleted cells show more actin stress fibres than control cells when spread on FN coated wells. The images were acquired with 63X magnification and multiple images were tiled together. Scale bar, 10 μ M

Stained cells were imaged using an epifluorescence microscope. Post 10 minutes incubation on fibronectin, AUM-depleted cells showed more stress fiber formation when compared to control cells that showed more cortical actin formation with little stress fibers (Fig. 29). This remains only a visual observation based on the phalloidin staining pattern observed for

hundreds of cells adhering to FN under an epifluorescence microscope and was not quantified in this study.

5.10 AUM is a negative regulator of RhoA

Cytoskeleton assembly, as well as actin dynamics, is regulated by the balance of members of small GTP binding proteins like RhoA, Rac1 and Cdc42 (Nobes and Hall 1995). Active RhoA has been found to localize to membrane ruffles and lamellipodia, and is involved in regulation of actin assembly (Goode and Eck, 2007). RhoA also contributes towards actin polymerization at integrin-based focal adhesions and membrane protrusions. Visual observation that AUM-depleted cells have possibly more actin stress fibers (Fig. 29) hinted towards the involvement of these small GTP binding proteins in AUM regulated early cell adhesion. Also, active RhoA has been implicated in increased cell adhesion. To test the possible involvement of the Rho family of proteins in AUM-mediated regulation of cell adhesion to FN, G-LISA assays were employed. These assays estimate levels of active RhoA or Rac1 (GTP bound RhoA or Rac1 is considered functionally active). Serum starved control and AUM-depleted cells were allowed to spread on fibronectin coated dishes for defined time points. Spread cells were lysed and the lysates were incubated with immobilized Rho/Rac-GTP-binding proteins. Post-incubation, inactive, GDP-bound Rho/Rac was washed away, and bound; active GTP-bound proteins were detected with a RhoA/Rac1 specific antibody.

After 10 minutes of spreading on fibronectin, active RhoA levels doubled in AUM-depleted cells. Cells lacking AUM also showed a significant increase in active RhoA levels after 15 minutes although the difference to the control shRNA cells was attenuated at this time point. However, at earlier and later time points tested no significant difference was observed in levels of active RhoA (Fig. 30). On the other hand, Rac1 G-LISA failed to show any difference between control and AUM-depleted cells at all the time points tested (Fig. 30). To further confirm these observations by another method RhoA and Rac1 pull down assays were performed. Here, active RhoA and Rac1 was bound to beads coated with RBD-Rhotekin for RhoA and PAK-PBD for Rac1. Both RBD region of rhotekin and PBD region of Pak have been shown to effectively bind to active RhoA or Rac1, respectively. As before, cells spreading on fibronectin for 10 and 20 minutes were lysed and incubated with above mentioned beads. Unbound RhoA and Rac1 was washed away, and bead-bound proteins were resolved using SDS-PAGE and Western blotting using RhoA and Rac1 specific antibodies (Fig. 31).

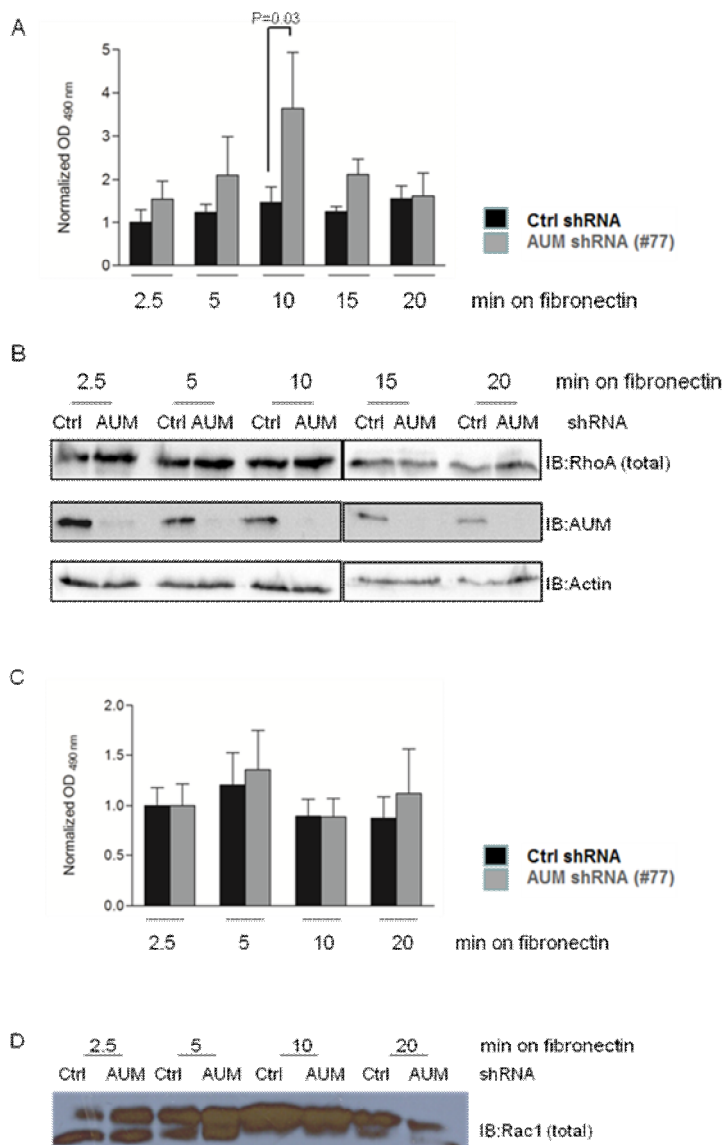


Figure 30: AUM depleted cells have more active RhoA.

(A) RhoA activation in cells spreading on fibronectin. Control and AUM-depleted cells were serum starved overnight and spread on fibronectin coated dishes for indicated time points and lysed. Cell lysates were subjected to RhoA G-LISA assay. Absorbance was read at 490nm. The above results are normalized pooled means of three independent experiments performed in triplicates. Error bars indicate \pm S.D.

(B) Immunoblotting was performed as above to check for levels of total RhoA in the cell lysates used for above mentioned G-LISA assay. Same membrane was reprobbed for AUM and actin to check for efficient knockdown and equal loading respectively. Shown immunoblot is representative of 3 independent experiments.

(C) Rac1 activation in cells spreading on fibronectin. Control and AUM-depleted cells were serum starved overnight and spread on fibronectin coated dishes for indicated time points and lysed. Cell lysates were subjected to Rac1 G-LISA assay. Absorbance was read at 490nm. The above results are normalized pooled means of three independent experiments performed in triplicates. Error bars indicate \pm S.D.

(D) Immunoblotting was performed as above to check for levels of total RhoA in the cell lysates used for above mentioned G-LISA assay. Shown immunoblot is representative of 3 independent experiments.

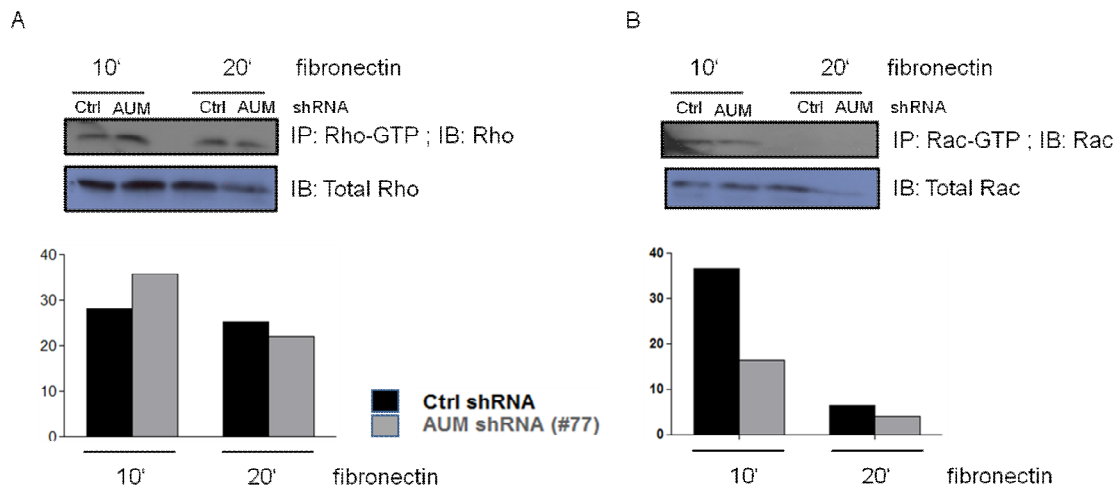


Figure 31: Increased active RhoA in AUM depleted cells.

(A) RhoA activation in cells spreading on fibronectin. Control and AUM-depleted cells were serum starved overnight and spread on fibronectin coated dishes for indicated time points and lysed. Cell lysates were subjected to Rho-pull-down assay. Bound active Rho was detected by immunoblotting. Total Rho levels were estimated by Western blot and probing with antibody recognising inactive and active Rho (total Rho). Below is the densitometric analysis of the above shown blot. Results are representative of 3 independent experiments

(B) Rac1 activation in cells spreading on fibronectin. Control and AUM-depleted cells were serum starved overnight and spread on fibronectin coated dishes for indicated time points and lysed. Cell lysates were subjected to Rac-pull-down assay. Bound active Rac was detected by immunoblotting. Total Rac levels were estimated by Western blot and probing with antibody recognising inactive and active Rac (total Rac). Below is the densitometric analysis of the above shown blot. Results are representative of 3 independent experiments

Similar to the G-LISA results (Fig 30), pull-down assays also showed an increase in active RhoA levels after 10 minutes, whereas after 20 minutes the levels of active RhoA remained unchanged. On the contrary, Rac1 levels appeared to decrease after 10 minutes in AUM-depleted cells (Fig. 31), whereas no changes in active Rac1 levels could be detected in the Rac1 G-LISA (Fig. 30). This observed change in levels of active RhoA level and Rac1 may be due to the fact that RhoA activation precedes Rac1 activation after the onset of cell adhesion to FN. Also, the observation that AUM-depleted cells have higher levels of RhoA activity upon cell adhesion on fibronectin may explain the results from adhesion assay showing that AUM depleted cells tend to adhere and spread faster on fibronectin, since active RhoA is well-known to be important in the process of focal adhesion formation and maturation (Hall, 1998).

Increased adhesion due to AUM-depletion is RhoA/ROCK dependent

To test if elevated levels of active RhoA are required for the accelerated adhesion of AUM-depleted cells to fibronectin, RhoA was inactivated by treatment with C3-transferase before performing the adhesion assay. The C3-transferase exoenzyme from *Clostridium botulinum* is an ADP ribosyl transferase that selectively ribosylates RhoA, RhoB and RhoC proteins on asparagine residue 41, rendering them inactive. C3-transferase has extremely low affinity for

other members of the Rho family such as Cdc42 and Rac1 and therefore does not affect these GTPases. Initially, to see if C3-transferase effectively reduces the levels of active RhoA in AUM-depleted GC-1 cells, cells treated with the indicated amounts of C3-transferase for indicated time points were subjected to G-LISA analysis (Fig. 32).

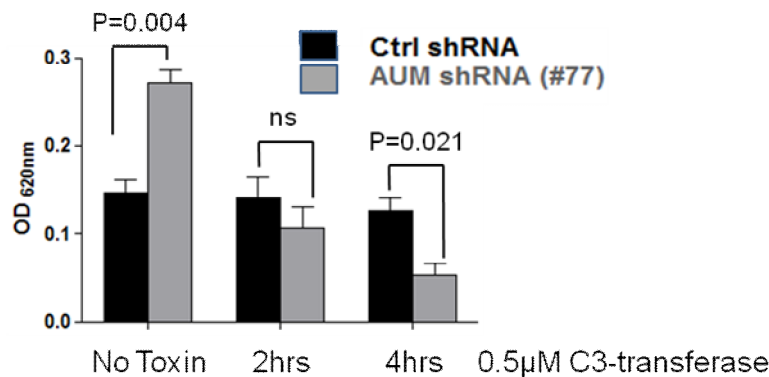


Figure 32: C3-transferase effectively reduces active RhoA levels in AUM depleted cells.

RhoA activation in cells treated with C3-transferase. Control and AUM-depleted cells were serum starved overnight and treated with 0.5 µM C3-transferase for the indicated time points and lysed. Cell lysates were subjected to G-LISA assays. Absorbance was read at 490 nm. Bars indicate mean value of experiment performed in triplicates. Error bars indicate \pm S.D.

Above results show that treatment of cells with 0.5 µM C3-transferase effectively reduces the levels of GTP bound RhoA in AUM-depleted cells. After 2 hours of treatment, the levels of active RhoA were similar in control and AUM-depleted cells. However, after 4 hours of treatment, C3-transferase apparently had a stronger effect on AUM-depleted cells than on control shRNA cells, as the levels of active RhoA were significantly lower than the control cells (Fig. 32).

Similar conditions were used to perform the cell adhesion assays. Cells growing in dishes were starved overnight and treated with 0.5 µM C3-transferase for 1 and 6 hours. Treated cells were used to perform cell adhesion assay on fibronectin as before.

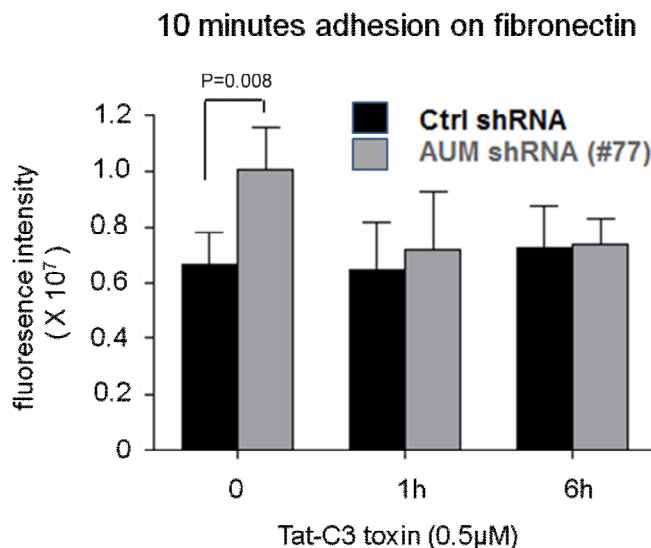


Figure 33: Increased adhesion of AUM-depleted cells on fibronectin is due to increased active RhoA .

Overnight starved control (black bars) and AUM shRNA (grey bars) expressing cells were treated with 0.5μM of C3-transferase for indicated time points. Cells were detached by limited trypsinization, loaded with calcein-AM, and 30,000 cells were seeded in each well of FN-coated 96-well microplates for 10 minutes. Post incubation, unbound cells were washed, and cell adhesion was measured fluorimetrically on a microplate reader. Results are means of three independent experiments performed in triplicates. Error bars represent \pm S.D. P value was calculated using student's t-test.

AUM depleted cells treated with C3-transferase failed to show accelerated adhesion to FN and rather were the same as control cells (Fig. 33). This experiment clearly demonstrates that the increased adhesion of AUM depleted cells on Fibronectin is due to an increased RhoA activity.

The actions of active RhoA on the actin cytoskeleton are elicited by effectors that are activated downstream of RhoA. Two important downstream effectors of RhoA are ROCK (Rho-associated coiled-coil forming kinase) and mDia (mammalian homolog of drosophila diaphanous). ROCK activity results in stabilization of actin filaments and an increase in their formation. The action of ROCK on actin is directly governed by RhoA. To check if active ROCK is involved in accelerated adhesion of AUM-depleted cells to FN, cells were treated with a specific ROCK inhibitor Y-27632. This compound inhibits ROCK by binding to the catalytic site and has a K_i of 140nm for the same (Ishzaki et. al., 2000).

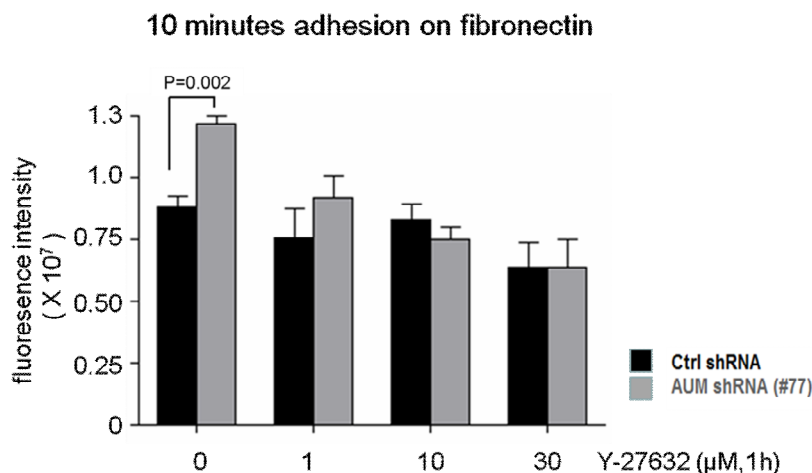


Figure 34: Increased adhesion of AUM-depleted cells on fibronectin is due to increased ROCK activity.

Overnight starved control (black bars) and AUM shRNA (grey bars) expressing cells were treated with indicated amount of Y-27632 for 1 hour (methods section). Cells were detached by limited trypsinization, loaded with calcein-AM, and 30,000 cells were seeded in each well of FN-coated 96-well microplates for 10 minutes. Post incubation, unbound cells were washed, and cell adhesion was measured fluorimetrically on a microplate reader. Results are means of three independent experiments performed in triplicates. Error bars represent \pm S.D. P value was calculated using Student's t-test.

Similar to cells treated with C3-transferase, AUM-depleted cells treated with the specific ROCK inhibitor Y-27632 failed to show accelerated cell adhesion on fibronectin after 10 minutes. Rather, the number of cells adhering to fibronectin was similar for control and AUM-depleted cells post Y-27632 treatment (Fig. 34). Cumulatively, both the results depicted in Fig. 35 and 36 suggest that AUM probably acts as a negative regulator of RhoA and ROCK activation during early events of cell adhesion to FN.

5.11 AUM-depletion induces faster focal adhesion maturation

Cells spreading on FN coated surfaces initially exhibit small, short-lived adhesions (nascent adhesions) which form immediately behind the leading edge in the lamellipodium. Nascent adhesions then mature to larger, dot-like adhesions called focal complexes. Focal complexes reside slightly further back from the leading edge, at the lamellipodium–lamellum interface, are slightly larger in size (approximately 1 μ m in diameter) and persist for several minutes. As the migration cycle continues, focal complexes can continue to mature into larger, elongated focal adhesions, which are typically 2 μ m wide, and 3–10 μ m long and reside at the ends of large actin bundles or stress fibres that extend from near the front of the cell along the sides to the cell centre or the rear (Parsons et al., 2010) (Fig. 7).

Focal adhesions are found at the cell membrane where the cytoskeleton interacts with proteins of the extracellular matrix. The clustering of integrins at these sites attracts a large complex of proteins and initiates intracellular regulatory processes, by which such events as

cell migration and anchorage-dependent differentiation are controlled. Focal adhesion kinase (FAK) is a protein tyrosine kinase which is recruited at an early stage to focal adhesions and which mediates many of the downstream responses. The binding of extracellular matrix ligands to integrins triggers autophosphorylation of FAK at Tyr-397 leading to activation of FAK through phosphorylation of Tyr residues (Tyr-576 and Tyr577) in the kinase domain activation loop.

Control and AUM shRNA expressing cells were allowed to spread on FN for 10, 20 and 40 minutes (Fig. 35), and fixed with 4% PFA. Immunostaining was performed on fixed cells with antibody recognizing phosphorylated (Tyr-392) FAK. Stained cells were imaged using confocal microscopy. Clearly, after 10 minutes of spreading on FN AUM depleted cells show large and centripetally oriented focal adhesions when compared to control cells which show relatively small sized focal adhesions at the peripheral plasma membrane. However after 40 minutes focal adhesion structures appeared similar in size and position in both control and AUM depleted cells (Fig. 35).

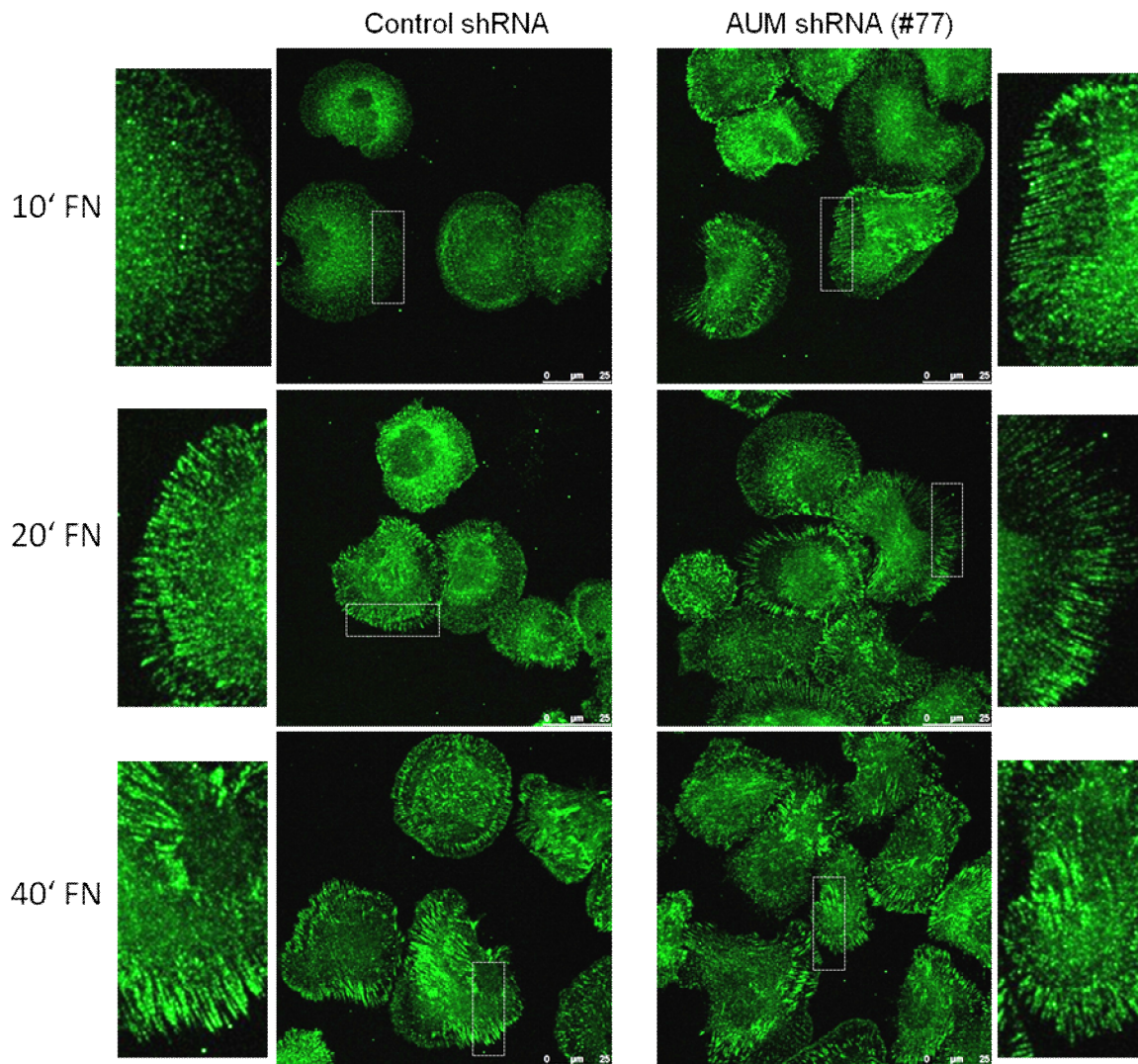


Figure 35: AUM-depletion influences focal adhesion elongation and maturation.

Control and AUM depleted cells stained with phosphor-FAK (397). Confocal images of cells spreading on FN for indicated time points fixed and stained with pFAK -397 antibody. Smaller panels next to each image show an enlargement of area indicated by the white dotted rectangle. Scale bar represents 25 μ M.

5.12 AUM-depleted cells have more phosphor-tyrosine content

Many focal adhesion proteins are known to undergo tyrosine phosphorylation upon recruitment to the focal adhesion complex, which leads to a strong adhesion to the ECM (Bass et al., 2008). Previously shown results clearly show a role of AUM in early cell adhesion and spreading. Also, AUM was previously shown to be a tyrosine phosphatase. All these facts point towards the hypothesis that AUM might influence phosphorylation status of proteins involved in cell adhesion in general and specifically in the focal adhesion assembly in order to regulate cell-FN adhesion. To this end, cells spreading on FN for indicated time points (Fig. 36) were stained with anti phosphotyrosine monoclonal antibody 4G10.

At all the time points tested i.e. after 10, 20 and 40 minutes on FN, AUM depleted cells showed enhanced levels of phosphotyrosine content of focal adhesion structures when compared to control shRNA expressing cells (Fig. 36). Also, in concordance with previous observation (Fig. 35), after 10 minutes of adhesion on FN AUM depleted cells had longer and more centripetally oriented focal adhesions than the control cells. After 20 minutes this difference in focal adhesion organization between control and AUM-depleted cells began to fade out and after 40 minutes both control and AUM –depleted cells appeared similar with respect to focal adhesion structure. This again confirms that AUM is involved in early cell adhesion and effect of AUM on cell adhesion is robust but transient in nature.

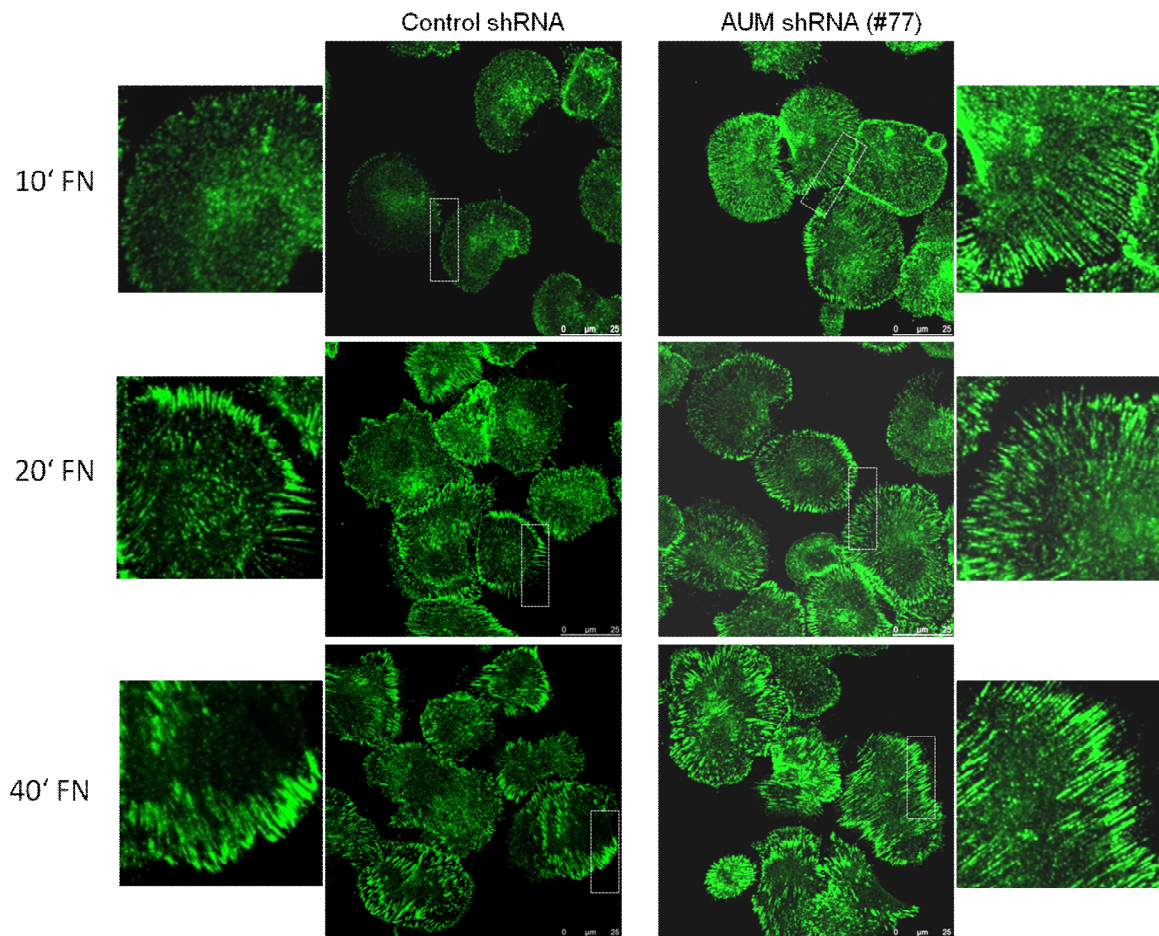


Figure 36: AUM depleted cells have increased phospho-tyrosine content in focal adhesions.

Control and AUM depleted cells were stained for total cellular phosphotyrosine with the monoclonal antibody 4G10. Shown are confocal images of cells spreading on FN for the indicated time points. Smaller panels next to each image show an enlargement of area indicated by the white dotted rectangle. Scale bar represents 25 μM.

6 Discussion

Cell adhesion to ECM is vital for the development and tissue homeostasis. These adhesions play a critical role in regulating tissue formation, tissue architecture and signaling across cell membranes (Yamada and Geiger, 1997). Cell-ECM adhesion occurs at specialized sites called 'focal adhesions' where integrins bridge between the ECM and the actin cytoskeleton, through a network of scaffold and signaling proteins (Barrier and Yamada, 2007). The organization and dynamics of focal adhesions are tightly regulated by associated signaling components. These groups of signaling molecules exert their effect on cell adhesion by the co-ordinated action of kinases and phosphatases. Intracellular signaling heavily relies on the ability of proteins to be reversibly phosphorylated by protein kinases and protein phosphatases. Such phosphorylation alters target proteins by inducing conformational changes, creating docking sites for other proteins and causing intracellular relocation (Stoker, 2005). Several kinases such as Src and FAK (Schaller et al., 1994) and phosphatases such as PTP1B and PTP-PEST (Garton and Tonks, 1999) have been implicated in the regulation of cell adhesion and focal adhesion dynamics.

Intense efforts and development in technology in the past few years have enormously enhanced our understanding of signaling and regulation of cell-ECM adhesion. Nevertheless, the events regulating early cell adhesion and spreading remain poorly understood. While we understand in details the events governing later stages of cell spreading, it is the earlier events that determine if a cell will adhere to a surface in the first place (Cuvelier et al., 2007). More importantly, little is known about the interplay of kinases and phosphatases in the regulation of early cell adhesion and spreading.

By database mining, our laboratory has recently discovered a previously un-described HAD phosphatase (Duraphe, 2009). This enzyme shares homology with chronophin (CIN), a cytoskeletal regulatory HAD phosphatase also identified by our laboratory before. This previously unidentified phosphatase was cloned and named AUM (for aspartate based ubiquitously expressed, magnesium-dependent HAD phosphatase). Screening of phosphopeptide libraries and biochemical studies showed that AUM acts as a tyrosine phosphatase, although its substrate(s) have not been unequivocally identified up to now. Initial data from the lab suggested that AUM might be involved in cell-ECM adhesion (Duraphe, 2009).

The major aim of this thesis was to further analyze the potential role of AUM in cell-ECM adhesion.

6.1 Effect of AUM on cell adhesion and spreading

Since maximum expression of AUM was observed in testis (Fig. 13), we employed GC-1 cells to study the function of AUM. Based on the characteristics observed using phase contrast and electron microscopy, GC-1 cells correspond to a stage between spermatogonia type B and primary spermatocyte. These cells are derived from germ cells of the testis, exhibit an epithelial morphology, and are adherent in nature (Hofmann et al., 1992). To specifically understand the role of AUM in cell adhesion these cells were stably depleted of AUM using shRNA.

The ability to quantitatively measure cell adhesion to an immobilized substrate is fundamental for the investigation of the molecular mechanisms underlying these processes. To this end, we established fluorescence-based cell adhesion assays in microtiter plates. It is important to state here that cell adhesion is an extremely complex process that involves many different molecular interactions, including receptor-ligand binding, changes in the fluxes through intracellular signaling pathways, and modulation of cytoskeletal assembly. Consequently, adhesion assays not only measure the contacts between a cell and extracellular adhesion proteins, but also provide information about other cellular events (Humphries, 2001).

Different cells respond differently to different extracellular matrices. The first major issue was to identify the ECM molecule preferred by GC-1 cells for adhesion. Since information on GC-1-ECM adhesion was not available in the literature, we tested three different ECM molecules i.e. collagen I, IV and FN in our adhesion assays. We observed that GC-1 cells rapidly adhere to FN, whereas GC-1 cell adhesion to collagen I and IV takes much longer (Fig. 17). These results directed this study towards FN mediated adhesions. FN is one of the best studied extracellular matrix glycoproteins that binds to integrins and is known to support cell adhesion (Legate et al., 2009) and wound repair (Grinnel F. 1984).

To identify the role of AUM in cell adhesion, cells stably depleted of AUM were compared with control shRNA treated cells. We allowed the cells to adhere to FN for different time points (5, 10, 20 and 40 minutes) and compared cell-adhesion between control and AUM-depleted cells. We clearly observed that AUM-depleted cells show increased adhesion to FN at earlier time points i.e. after 5 and 10 minutes (Fig. 19). However, no differences in cell adhesion to FN between control and AUM-depleted cells were observed at later time points such as 20 and 40 minutes. To rule out the possibility that the observed effects are non-specific (due to off-target effects of the particular shRNA), another cell line deprived of AUM using a different shRNA that targets another region of AUM was used. These cells also showed a similar effect on cell adhesion to FN. Based on these results we conclude that AUM-depletion induces increased cell adhesion that is robust, but transient in nature. These

results suggest that AUM might function as a negative regulator of early cell adhesion events.

One possibility that arises from these assays is that AUM-depletion leads to faster cell spreading on FN. This issue can be addressed by cell spreading assays. Here, control shRNA and AUM shRNA cells were allowed to spread for similar time points on FN as used in the adhesion assays and were fixed and stained with phalloidin. Post staining, total cell area was measured. As shown in Fig. 16, after 10 minutes of spreading on FN, AUM-depleted cells were at least 25% larger with respect to total cell area when compared to control shRNA expressing cells. However, no significant changes in cell area were observed at earlier or later time points. This indicates that AUM-depletion leads to faster cell spreading on FN and that similar to the effects observed in cell adhesion assays, the effect of AUM on cell spreading is also transient.

Both above discussed experiments were conducted using GC-1 cells stably devoid of AUM by shRNA. However, stable depletion of a specific protein might induce compensatory mechanisms to overcome this particular protein's deficiency. In order to ensure that the observed effects of AUM-depletion are indeed due to AUM, cells were also treated with AUM specific siRNA. Gene silencing mediated by siRNA leads to acute deficiency of targeted proteins in cells. Wild type GC-1 cells were transiently transfected with either non-targeting control siRNA or AUM directed siRNA and their adhesive properties to FN coated wells were compared. Similar to results obtained from adhesion assay with AUM shRNA treated cells, acute depletion of AUM in GC-1 cells resulted in a transient increase in cell adhesion to FN at earlier time point (Fig. 21). Collectively, these results revealed the involvement of AUM in early events of cell adhesion to FN.

6.2 Effect of AUM depletion on cell adhesion can be rescued

Several approaches can be used to minimize false positives results when using siRNA or shRNA. This includes using several shRNAs against the same gene which we have discussed before (Fig. 20). The definitive control, however, remains the rescue of the RNAi effects by the expression of the target gene that is resistant to the shRNA. Sequence analysis revealed that human AUM (hAUM) is not targeted by the shRNA present in AUM-depleted GC-1 cells. However, a caveat is that over-expression of the rescue protein may itself exert an effect on the cell. Hence we performed a titration of the rescue cDNA (hAUM) to express the rescue protein to a level similar to the endogenous protein before knockdown. Densitometric analysis of Western blots performed on cells expressing different amounts of hAUM cDNA showed that 30ng of hAUM cDNA was sufficient to bring the level of AUM to endogenous, pre-silencing levels in AUM-depleted cells (Fig. 22). As mentioned before, cell-ECM adhesion is supported by many proteins by their enzymatic actions or simply by acting as protein scaffolds. To see if AUM is involved in cell-ECM adhesion as a phosphatase or as

a protein scaffold, AUM depleted cells were also transfected with mutated hAUM (hAUM^{D34N}) where aspartate at the active site was mutated thus resulting in enzymatically inactive AUM. Enhanced adhesion of AUM-depleted cells to FN was attenuated when these cells were rescued with hAUM. Moreover, the extent of adhesion to FN for the rescued cells was similar to that of control shRNA treated cells. Interestingly, cells transfected with catalytically dead hAUM did not show statistically significant increase in adhesion to FN (Fig. 23). However, multiple repetitions of similar experiment showed a trend for increased adhesion to FN. There could be two possible reasons for this observation. One, that AUM is simply required as a protein scaffold as far as cell adhesion to FN is concerned. Another explanation might be that AUM is somehow partially required as an enzyme in this process and this is possibly beyond the scope of the technique to detect. More experiments with different approaches will be needed to definitely address this aspect of AUM in cell-ECM adhesion.

6.3 Integrins are involved in AUM mediated cell adhesion

Cell adhesion to ECM is mediated by integrins. The sequence Arg-Gly-Asp (RGD) is the essential structure recognized by cells in FN. When immobilized onto a surface, the RGD-containing peptides promote cell adhesion in a manner similar to that of FN, whereas in solution the same peptides can inhibit the attachment of cells to a surface coated with FN (Pierschbacher and Ruoslahti, 1984). Changes in the peptides as small as the exchange of alanine for the glycine or glutamic acid for the aspartic acid, which constitute the addition of a single methyl or methylene group to the RGD tripeptide, eliminate these activities (Pierschbacher and Ruoslahti, 1984). RGD peptides can be used to assess the involvement of RGD-binding integrins in cell adhesion (Barczyk et al., 2010). To evaluate the involvement of integrins in increased cell adhesion of AUM-depleted cells to FN, cells were treated with RGD peptides and adhesion assays were performed in the presence of these peptides. Here we observed that increased cell adhesion of AUM-depleted cells after 10 minutes on FN was completely abolished and suppressed to the level of control cells. We used two variants of RGD peptide to be sure of the effect. Both the peptides had similar effect on AUM-depleted cell adhesion to FN (Fig. 24). These results implicate towards involvement of integrins in AUM-influenced cell adhesion to FN.

Apart from integrins, other glycosaminoglycan molecules expressing on the cell surface like syndecan-4 is also able to bind to extracellular matrix molecules like collagen and FN (Carey DJ, 1997). Both integrins and syndecan-4 use different modes of ligand binding. Integrins ($\alpha 5 \beta 1$) bind directly to the RGD peptide present on FN (Arnout et al., 2005), whereas syndecan-4 interacts with heparin-binding motif of FN (Bernfield et al., 1999). Several independent groups have shown that simultaneous involvement of integrin and syndecan receptor in focal adhesion formation (Woods et al., 1986; Bloom et al., 1999; Bass et al., 2007). However, fibroblasts isolated from syndecan-4 null mice still develop focal adhesions

and actin stress fibres when plated on FN (Echtermeyer et al., 2001; Ishiguro et al., 2000) showing that syndecan-4 is not an integral part of the adhesive machinery but rather modulates signals downstream of integrins (Bass et al., 2008). These results show that during cell adhesion integrin involvement is dominant over other potentially involved molecules like syndecan-4.

Since only a few integrin heterodimers such as $\alpha 5\beta 1$, $\alpha V\beta 3$, $\alpha 11\beta 3$, $\alpha 8\beta 1$, $\alpha V\beta 5$, $\alpha V\beta 6$ and $\alpha V\beta 8$, are known to recognize the RGD motif within their ligands (Barczyk et al., 2010), we checked the cell surface expression of widely expressed and FN specific integrins like $\alpha 5$, $\beta 1$, αV and $\beta 3$. FACS analysis was performed for control and AUM-depleted cells growing on-dish in presence of FCS and stained with fluorescently labeled, integrin specific antibodies. Flow cytometry is an extremely useful technique for this purpose as it can reliably analyze thousands of cells simultaneously at a given time. A comparison between the control shRNA and AUM shRNA expressing cells showed a strong increase in the cell surface expression of $\alpha 5$ integrin in AUM-depleted cells (Fig. 25). However, the cell surface expression of $\beta 1$, αV and $\beta 3$ integrins was similar in both control and AUM depleted cells. Increase in cell surface expression of $\alpha 5$ integrin in AUM-depleted cells definitely indicates the involvement of integrins in control and AUM-depleted cell adhesion to FN. $\alpha 5\beta 1$ Integrin heterodimer bind FN to induce phosphorylation of pY-397-FAK which further activates downstream signaling components including paxillin and ERK1/2 (Luo et al., 2007; Mitra and Schlaepfer, 2007). Based on confocal image analysis of control and AUM-depleted cells stained with pY397-FAK, AUM depletion possibly leads to increased phosphorylation of pY397-FAK (Fig. 35). This observation may partially explain the observed increase in the abundance of $\alpha 5$ integrin on AUM-depleted cell surface. Other possibility can be that AUM can directly influence $\alpha 5$ integrin transportation to cell surface. However, this possibility is not covered in this study and substantial investigation is required in this regard.

6.4 Effect of AUM on integrin activation

The results of this study so far prompted us to investigate the status of $\beta 1$ -integrin activation in control and AUM-depleted cells. A close interaction of the membrane-proximal extracellular domains is necessary to maintain the integrin receptor in a low affinity state. Once ligated to ligand such as FN and clustered in adhesion complexes, the integrin depicts an extended conformation where the “legs” in the extra-cellular region are separated (i.e., the distance between the α and β subunits increases) (Fig. 2). Integrin in which “leg” movement is constrained cannot mediate efficient cell adhesion and spreading.

The monoclonal antibody 9EG7 has been previously found to recognize an epitope induced by manganese on the integrin beta 1 chain (Lenter et al., 1993). It has been shown that the 9EG7 epitope pinpoints to aspartate 522 located between I-EGF domain 1 and 2 of the β -

subunit and that binding of 9EG7 reports active (extended) conformations of β 1-integrin (Askari et al., 2010). Interestingly, we also found that AUM-depleted cells growing in the presence of FCS showed nearly 3 times more active β 1-integrin on the cell surface when compared to control shRNA expressing cells (Fig. 27). This increase in cell surface expression of α 5 and β 1-integrin possibly explains the observed increase in cell adhesion of AUM-depleted cells to FN.

Integrins are capable of signaling bi-directionally. Ligand binding from cell exterior can activate integrin and also internal signals originating from the cytosol (e.g., binding of talin to the β 1-integrin tail) are also capable of inducing conformational changes in integrins that lead to their activation. To investigate mechanism of integrin activation further, overnight starved cells (deprived of FCS) were challenged with soluble FN and the status of active β 1-integrin was compared between control and AUM-depleted cells. The serum in which cells normally grow contains various proteins such as FN and vitronectin that are capable of integrin activation. Withdrawal of FCS from the culture medium resulted in similar levels of active β 1-integrin in both control and AUM-depleted cells. Interestingly, when challenged with soluble FN, AUM-depleted cells again showed increased cell surface expression of active β 1-integrin similar to the cells growing in FCS (Fig. 28). The above experiments show that AUM is possibly a negative regulator of integrin activation and moreover that integrin activation in AUM-depleted cells is FN dependent. Taken together, these observations indicate that AUM is capable of modulating integrin activation.

6.5 AUM modulates actin dynamics mediated by its effect on RhoA

Integrin engagement regulates the activity of several members of the Rho family of small GTPases, which in turn control the growth or contraction of filamentous actin stress fibers. Rho kinase plays a major role in mediating rearrangement of the actomyosin cytoskeleton downstream of Rho. Early cell adhesion to FN in the absence of AUM indicates the involvement of Rho GTPases. To analyze the effect of AUM depletion on Rho GTPases during early cell adhesion on FN, active RhoA and Rac1 levels were determined. Both RhoA and Rac1 exert effects on cell adhesion and spreading and often act antagonistically. RhoA regulates stress fiber formation and cell contraction, whereas Rac1 and CDC 42 regulate the formation of lamellopodia and filopodia (Hall, 2005). Here we found that RhoA levels were doubled in AUM depleted GC-1 cells when compared to control cells after 10 minutes of cell adhesion on FN (Fig 30 and 31).

This in concordance with the our observations that the effect of AUM depletion in adhesion and spreading assays was also a transient phenomenon, as after 20 mins of adhesion on FN both control and AUM depleted cells showed no difference with respect to active RhoA levels. In contrast to active RhoA levels, Rac1 levels remain unchanged between control and

AUM depleted cells after adhesion on FN at all the time points tested. Since RhoA or Rac1 activation precedes the effects that these GTPases exert on cell adhesion and spreading, we also tested earlier time points such as 2.5 and 5 mins. Increased levels of active RhoA were already seen after 5 mins of adhesion to FN in AUM depleted cells. Maximum RhoA was observed after 10 mins or 15 mins, respectively. AUM appears to be negative regulator as RhoA as in the absence of AUM we observed an increase in active/GTP-bound RhoA levels. Downstream effectors of RhoA include ROCK and mDia. Our studies show that there is an active involvement of ROCK in this process as AUM depleted cells treated with specific ROCK inhibitor Y27639 failed to show accelerated adhesion to FN after 10 mins (Fig. 34). After the initial spreading event, RhoA activity gradually increases, concomitant with the formation of stress fibers and maturation of focal adhesions. Small GTPase guanine nucleotide exchange factors (GEFs) such as p115 RhoGEF and GTPase activating proteins (GAPs) such as p190 RhoGAP have been implicated in this process, but it is not clearly understood what triggers their activity (Dubash et al, 2007; Lim et al, 2008). The above results strongly indicate role of AUM in regulating the activity of the above mentioned GEFs and or GAPs. Current investigations in the lab are focusing on this aspect.

6.6 Role of AUM in focal adhesion formation and maturation

AUM depleted cells spreading on FN show elongated and more centripetally oriented focal adhesions than control shRNA treated cells (Fig 35 and 36). Focal adhesions mature from focal complexes, which are initially dot like structure. As focal complexes or nascent adhesions mature they appear more elongated and centripetally oriented, spanning around the actin stress fibers of the adhering cells (Parsons et al., 2010). Maturation of focal adhesions is a hallmark of cell-ECM adhesion and their formation is majorly governed by integrin interaction with ECM molecules such as FN and internal RhoA signaling. RhoA has been strongly implicated in maturation of focal adhesions (Humphries et al., 2005). We previously observed an increase in active $\beta 1$ integrin on cell surface of AUM deficient cells. Also, increased levels of active RhoA were seen in AUM depleted cells. Both these factors contribute to focal adhesion maturation. So far, we have imaged focal adhesions using conventional confocal microscopy. Recent advances in microscopic techniques have led to the development of total internal reflection fluorescence (TIRF) microscopy. This technique is currently being used by the group to view focal adhesion formation in the presence or absence of AUM. By this we should be able to precisely quantify the effect of AUM on focal adhesion formation and maturation.

6.7 Possible model for role of AUM in cell adhesion and spreading

Taken together, we could show in this initial functional study on the cellular roles of the novel phosphatase AUM that AUM is involved in the regulation of early cell adhesion and spreading. AUM depleted GC-1 cells show more functionally active $\beta 1$ integrin on the cells surface. This effect is dependent on FN as serum starved control and AUM deficient cells show similar amounts of active $\beta 1$ integrin on their surfaces. Our results so far suggest that AUM function is regulated by integrins and possibly AUM is also involved in integrin activation. It is conceivable that AUM and integrins are mutually regulated. This possibility is indicated in the flowchart below by using a double directional arrow (Fig. 37).

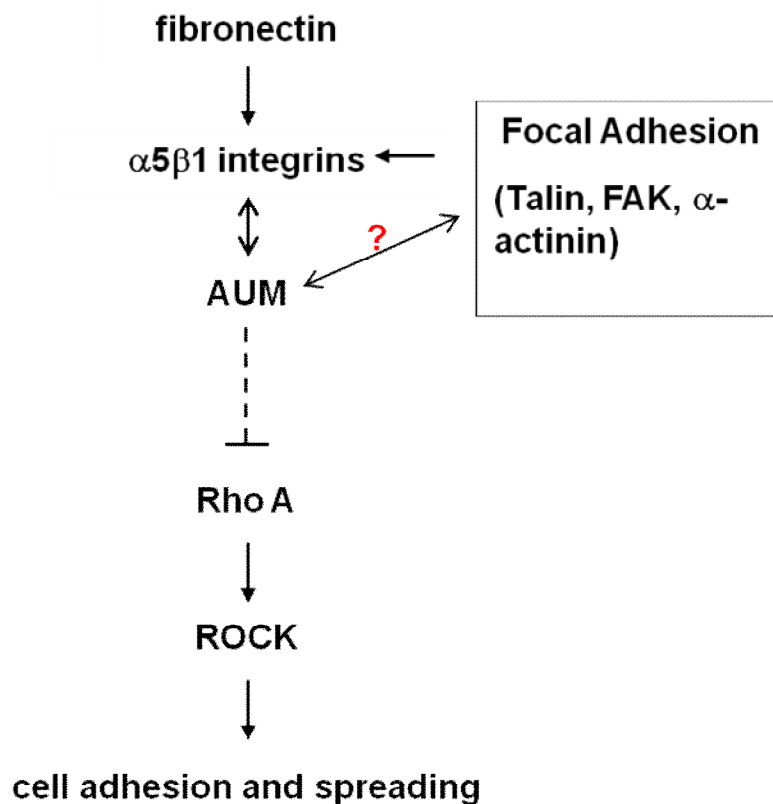


Figure 37: Flow diagram showing possible role of AUM in early cell adhesion to FN.

One point of further investigation not covered in this study is the internalization of integrin receptors that is initiated as soon as cells encounter an ECM molecule (Echarri et al., 2007). Experiments need to be performed using pharmacological agents that block integrin internalization to see if the dynamics of integrin internalization/recycling are different in control shRNA and AUM depleted cells.

Also AUM seems to be involved in focal adhesion maturation. Results shown in this work suggest that AUM might act as a negative regulator and/or modulator of focal adhesion

maturation. Focal adhesions are complex assembly of adhesion signaling proteins. Proteins such as talin and vinculin can be used as marker molecules to study AUM-dependent focal adhesion maturation. Currently, immunoprecipitation studies with various focal adhesion molecules are ongoing in the laboratory to identify interaction partners of AUM. This would enable us to clearly understand the enzymatic and scaffolding role of AUM in focal adhesion formation and maturation during adhesion to the ECM.

Many proteins in focal adhesion complexes are regulated by phosphorylation by Src family kinases. In its capacity as a tyrosine phosphatase, AUM could be very well involved in reversing the action of src family kinases. To this end, biochemicals as well as functional studies are presently being carried out to investigate the enzymatic functions of AUM in cell adhesion to ECM.

Although we still do not fully understand the exact role of the novel phosphatase AUM in cell adhesion to ECM, this study has shown for the first time that AUM is involved in early cell adhesion to the ECM by modulating integrin activation. The fact that $\alpha 5 \beta 1$ integrin are involved in cancer progression (Maschler et al., 2005) and observation in this study that AUM-depleted cells show increased $\alpha 5 \beta 1$ integrin on the cell surface might make it worthwhile to predict that AUM might be involved in carcinogenesis. Given the important role of regulated cell adhesion and de-adhesion for cell motility, future studies should investigate the potential role of AUM for cell migration.

7 Summary

Cell adhesion and migration are essential for development and homeostasis. Adhesion to the extracellular matrix occurs at specialized plasma membrane domains where transmembrane adhesion receptors, signaling proteins such as kinases and phosphatases, and a large number of adaptor proteins interact with the cytoskeleton in a tightly regulated and synchronized fashion. Whereas altered cell adhesion and migration are known to be important in cardiovascular disease and malignant tumors, the target proteins and molecular interactions that regulate these complex processes still remain incompletely understood. Whereas numerous kinases are known to regulate cell adhesion dynamics, information about the involved protein phosphatases is still very limited.

A newly emerging phosphatase family contains the unconventional active site sequence DXDX(T/V) and belongs to the haloacid dehalogenase (HAD) superfamily of hydrolases. Our laboratory has recently discovered AUM, a novel phosphatase that belongs to this poorly characterized enzyme family. Initial findings pointed toward a potential involvement of AUM in the regulation of cell adhesion to the extracellular matrix.

The objective of the present study was to study the potential role of AUM in cell adhesion. We could show that cells stably depleted of AUM are characterized by accelerated adhesion on immobilized fibronectin. To confirm these findings, we used an siRNA-based approach for the acute depletion of AUM and observed a similar phenomenon. Rescue experiments were performed with stably AUM-depleted cells to ensure that the above mentioned effects are indeed AUM specific. We observed that the re-addition of AUM normalizes cellular adhesion kinetics on fibronectin. These results clearly show that AUM exerts important functions in cell-matrix adhesion. To investigate the molecular basis of these effects, we have characterized integrin expression patterns using flow cytometry. Interestingly, fibronectin-stimulated AUM-depleted cells are characterized by an increase in the cell surface expression of conformationally active β 1-integrins. Consistent with the important role of β 1-integrins in the regulation of RhoA activity, we also observed a specific increase in RhoA-GTP, but not Rac1-GTP-levels during cell adhesion to fibronectin. Consistent with these findings and with the important role of RhoA for focal adhesion maturation, AUM depleted cells showed more elongated and more centripetally oriented focal adhesions as compared to control cells when spread on fibronectin.

Taken together, this study has revealed an important role of AUM for cell-matrix adhesion. Our findings strongly suggest that AUM functions as a negative regulator of β 1-integrins and RhoA-dependent cytoskeletal dynamics during cell adhesion.

8 Zusammenfassung

Die Adhäsion und Migration von Zellen auf extrazellulären Matrixmolekülen ist essentiell für die Entwicklung und Homöostase vielzelliger Organismen. Die Adhäsion an extrazellulärer Matrix findet über spezialisierte Plasmamembran-Domänen statt, an denen transmembranäre Adhäsionsrezeptoren, Signalproteine wie Kinasen und Phosphatasen und eine große Anzahl von Adapterproteinen auf eng regulierte und synchronisierte Weise mit dem Zytoskelett interagieren. Während feststeht, dass Veränderungen der Zelladhäsion und Migration eine wichtige Rolle zum Beispiel bei kardiovaskulären Erkrankungen und bei metastasierenden Tumoren spielen, sind die Schlüsselmoleküle und Protein-Protein-Interaktionen, welche diese Prozesse regulieren immer noch unvollständig verstanden. Obwohl von zahlreichen Kinasen bekannt ist, dass sie die Zelladhäsions-Dynamik regulieren, existieren kaum Informationen über an diesen Prozessen beteiligte Phosphatasen.

Seit Kurzem wird einer noch wenig charakterisierten Phosphatase-Familie mit der unkonventionellen Aminosäuresequenz DXDX(T/V) im aktiven Zentrum des Enzyms vermehrt Beachtung geschenkt. Diese Phosphatasen gehören zur Haloazid-Dehalogenase (HAD) Superfamilie von Hydrolasen. Unserem Labor ist es kürzlich gelungen, eine neue Phosphatase aus dieser Enzymfamilie zu identifizieren. Erste Befunde aus unserer Arbeitsgruppe weisen darauf hin, dass AUM möglicherweise an der Regulation der Zelladhäsion an extrazelluläre Matrixmoleküle beteiligt sein könnte.

Das Ziel der vorliegenden Arbeit war es, die mögliche Rolle von AUM bei der Zelladhäsion genauer zu untersuchen. Es gelang uns zu zeigen, dass stabil AUM-shRNA exprimierende Zellen durch eine beschleunigte Adhäsion auf immobilisiertem Fibronectin gekennzeichnet sind. Um diese Befunde zu erhärten, wurde endogenes AUM mittels transienter Expression von siRNAs akut depletiert. Auch unter diesen Bedingungen konnte gezeigt werden, dass eine Reduktion der endogenen AUM-Proteinexpression die Zelladhäsion auf Fibronectin beschleunigt. Weiterhin wurden *rescue*-Experimente mit stabil AUM-depletierten Zellen durchgeführt, um sicherzustellen, dass die oben genannten Effekte spezifisch sind. Dabei wurde beobachtet, dass die Re-Expression von AUM die zelluläre Adhäsionskinetik auf Fibronectin normalisiert. Diese Ergebnisse belegen eindeutig, dass AUM wichtige Funktionen bei der Zell-Matrix-Adhäsion erfüllt. Um die molekulare Grundlage dieser Effekte zu untersuchen, haben wir zunächst das zelluläre Integrin-Expressionsmuster mittels Durchflußzytometrie charakterisiert. Interessanterweise konnte nachgewiesen werden, dass Fibronectin-stimulierte, AUM-depletierte Zellen vermehrt β 1-Integrine in ihrer aktiven Konformation auf der Zelloberfläche exprimieren. Übereinstimmend mit der wichtigen Rolle

von β 1-Integrinen für die Regulation der RhoA-Aktivität konnten wir auch eine spezifische Zunahme der RhoA-GTP, nicht aber der Rac1-GTP-Spiegel während der Zelladhäsion auf Fibronektin beobachten. Konsistent mit diesen Ergebnissen und der bekannten Rolle von RhoA für die Reifung fokaler Adhäsionen, zeigten AUM-depletierte Zellen im Vergleich zu den Kontrollzellen vermehrt elongierte und zentripetal orientierte fokale Adhäsionen.

Zusammengenommen ist es in der vorliegenden Arbeit gelungen, eine wichtige Rolle von AUM bei der Zell-Matrix-Adhäsion aufzudecken. Unsere Befunde legen nahe, dass AUM im Rahmen der Zell-Adhäsion als ein negativer Regulator von β 1-Integrinen und der RhoA-abhängigen Zytoskelett-Dynamik fungiert.

9 References

Abercrombie M, Heaysman JE, Pegrum SM (1971) The locomotion of fibroblasts in culture. IV. Electron microscopy of the leading lamella. *Exp Cell Res* **67**: 359-367

Akeson AL, Woods CW (1993) A fluorometric assay for the quantitation of cell adherence to endothelial cells. *J Immunol Methods* **163**: 181-185

Alonso A, Sasin J, Bottini N, Friedberg I, Osterman A, Godzik A, Hunter T, Dixon J, Mustelin T (2004) Protein tyrosine phosphatases in the human genome. *Cell* **117**: 699-711

Amano M, Ito M, Kimura K, Fukata Y, Chihara K, Nakano T, Matsuura Y, Kaibuchi K (1996) Phosphorylation and activation of myosin by Rho-associated kinase (Rho-kinase). *J Biol Chem* **271**: 20246-20249

Angers-Loustau A, Cote JF, Charest A, Dowbenko D, Spencer S, Lasky LA, Tremblay ML (1999a) Protein tyrosine phosphatase-PEST regulates focal adhesion disassembly, migration, and cytokinesis in fibroblasts. *The Journal of cell biology* **144**: 1019-1031

Angers-Loustau A, Cote JF, Tremblay ML (1999b) Roles of protein tyrosine phosphatases in cell migration and adhesion. *Biochem Cell Biol* **77**: 493-505

Anthis NJ, Campbell ID (2011) The tail of integrin activation. *Trends in biochemical sciences* **36**: 191-198

Arias-Salgado EG, Lizano S, Sarkar S, Brugge JS, Ginsberg MH, Shattil SJ (2003) Src kinase activation by direct interaction with the integrin beta cytoplasmic domain. *Proc Natl Acad Sci U S A* **100**: 13298-13302

Arnaout MA, Mahalingam B, Xiong JP (2005) Integrin structure, allostery, and bidirectional signaling. *Annu Rev Cell Dev Biol* **21**: 381-410

Arthur WT, Burridge K (2001) RhoA inactivation by p190RhoGAP regulates cell spreading and migration by promoting membrane protrusion and polarity. *Mol Biol Cell* **12**: 2711-2720

Arthur WT, Petch LA, Burridge K (2000) Integrin engagement suppresses RhoA activity via a c-Src-dependent mechanism. *Curr Biol* **10**: 719-722

Askari JA, Tynan CJ, Webb SE, Martin-Fernandez ML, Ballestrem C, Humphries MJ (2010) Focal adhesions are sites of integrin extension. *The Journal of cell biology* **188**: 891-903

Aumailley M, Krieg T (1996) Laminins: a family of diverse multifunctional molecules of basement membranes. *J Invest Dermatol* **106**: 209-214

Barczyk M, Carracedo S, Gullberg D (2010) Integrins. *Cell and tissue research* **339**: 269-280

Bass MD, Morgan MR, Humphries MJ (2007) Integrins and syndecan-4 make distinct, but critical, contributions to adhesion contact formation. *Soft Matter* **3**: 372-376

Bass MD, Morgan MR, Roach KA, Settleman J, Goryachev AB, Humphries MJ (2008) p190RhoGAP is the convergence point of adhesion signals from alpha 5 beta 1 integrin and syndecan-4. *The Journal of cell biology* **181**: 1013-1026

Bazzoni G, Ma L, Blue ML, Hemler ME (1998) Divalent cations and ligands induce conformational changes that are highly divergent among beta1 integrins. *J Biol Chem* **273**: 6670-6678

Bazzoni G, Rasia M (1998) Effects of an amphipathic drug on the rheological properties of the cell membrane. *Blood Cells Mol Dis* **24**: 552-559

Bazzoni G, Shih DT, Buck CA, Hemler ME (1995) Monoclonal antibody 9EG7 defines a novel beta 1 integrin epitope induced by soluble ligand and manganese, but inhibited by calcium. *J Biol Chem* **270**: 25570-25577

Bernfield M, Gotte M, Park PW, Reizes O, Fitzgerald ML, Lincecum J, Zako M (1999) Functions of cell surface heparan sulfate proteoglycans. *Annu Rev Biochem* **68**: 729-777

Berrier AL, Yamada KM (2007) Cell-matrix adhesion. *J Cell Physiol* **213**: 565-573

Blevins T, Rajeswaran R, Shivaprasad PV, Beknazariants D, Si-Ammour A, Park HS, Vazquez F, Robertson D, Meins F, Jr., Hohn T, Pooggin MM (2006) Four plant Dicers mediate viral small RNA biogenesis and DNA virus induced silencing. *Nucleic Acids Res* **34**: 6233-6246

Bloom L, Ingham KC, Hynes RO (1999) Fibronectin regulates assembly of actin filaments and focal contacts in cultured cells via the heparin-binding site in repeat III13. *Mol Biol Cell* **10**: 1521-1536

Bonini NM, Leiserson WM, Benzer S (1993) The eyes absent gene: genetic control of cell survival and differentiation in the developing *Drosophila* eye. *Cell* **72**: 379-395

Brandt DT, Baarlink C, Kitzing TM, Kremmer E, Ivaska J, Nollau P, Grosse R (2009) SCAI acts as a suppressor of cancer cell invasion through the transcriptional control of beta1-integrin. *Nat Cell Biol* **11**: 557-568

Calalb MB, Polte TR, Hanks SK (1995) Tyrosine phosphorylation of focal adhesion kinase at sites in the catalytic domain regulates kinase activity: a role for Src family kinases. *Mol Cell Biol* **15**: 954-963

Calderwood DA, Shattil SJ, Ginsberg MH (2000) Integrins and actin filaments: reciprocal regulation of cell adhesion and signaling. *J Biol Chem* **275**: 22607-22610

Calderwood DA, Yan B, de Pereda JM, Alvarez BG, Fujioka Y, Liddington RC, Ginsberg MH (2002) The phosphotyrosine binding-like domain of talin activates integrins. *J Biol Chem* **277**: 21749-21758

Calderwood DA, Zent R, Grant R, Rees DJ, Hynes RO, Ginsberg MH (1999) The Talin head domain binds to integrin beta subunit cytoplasmic tails and regulates integrin activation. *J Biol Chem* **274**: 28071-28074

Carey DJ (1997) Syndecans: multifunctional cell-surface co-receptors. *Biochem J* **327 (Pt 1)**: 1-16

Carman CV, Springer TA (2003) Integrin avidity regulation: are changes in affinity and conformation underemphasized? *Curr Opin Cell Biol* **15**: 547-556

Charo IF, Nannizzi L, Phillips DR, Hsu MA, Scarborough RM (1991) Inhibition of fibrinogen binding to GP IIb-IIIa by a GP IIIa peptide. *J Biol Chem* **266**: 1415-1421

Cooper JA (1987) Effects of cytochalasin and phalloidin on actin. *The Journal of cell biology* **105**: 1473-1478

Costa P, Parsons M (2010) New insights into the dynamics of cell adhesions. *International review of cell and molecular biology* **283**: 57-91

Craig WS, Cheng S, Mullen DG, Blevitt J, Pierschbacher MD (1995) Concept and progress in the development of RGD-containing peptide pharmaceuticals. *Biopolymers* **37**: 157-175

Cuvelier D, Thery M, Chu YS, Dufour S, Thiery JP, Bornens M, Nassoy P, Mahadevan L (2007) The universal dynamics of cell spreading. *Curr Biol* **17**: 694-699

Dallas SL, Chen Q, Sivakumar P (2006) Dynamics of assembly and reorganization of extracellular matrix proteins. *Curr Top Dev Biol* **75**: 1-24

Danen EH, Sonneveld P, Brakebusch C, Fassler R, Sonnenberg A (2002) The fibronectin-binding integrins alpha5beta1 and alphavbeta3 differentially modulate RhoA-GTP loading, organization of cell matrix adhesions, and fibronectin fibrillogenesis. *The Journal of cell biology* **159**: 1071-1086

Danen EH, van Rheenen J, Franken W, Huvneers S, Sonneveld P, Jalink K, Sonnenberg A (2005) Integrins control motile strategy through a Rho-cofilin pathway. *The Journal of cell biology* **169**: 515-526

Defilippi P, Olivo C, Venturino M, Dolce L, Silengo L, Tarone G (1999) Actin cytoskeleton organization in response to integrin-mediated adhesion. *Microsc Res Tech* **47**: 67-78

Du XP, Plow EF, Frelinger AL, 3rd, O'Toole TE, Loftus JC, Ginsberg MH (1991) Ligands "activate" integrin alpha IIb beta 3 (platelet GPIIb-IIIa). *Cell* **65**: 409-416

Dubash AD, Wennerberg K, Garcia-Mata R, Menold MM, Arthur WT, Burridge K (2007) A novel role for Lsc/p115 RhoGEF and LARG in regulating RhoA activity downstream of adhesion to fibronectin. *Journal of cell science* **120**: 3989-3998

Duraphe P (2009) Identification and characterization of AUM, a novel human tyrosine phosphatase. *Doctoral thesis submitted to University of Würzburg.*

Dykxhoorn DM, Novina CD, Sharp PA (2003) Killing the messenger: short RNAs that silence gene expression. *Nature reviews Molecular cell biology* **4**: 457-467

Echarri A, Muriel O, Del Pozo MA (2007) Intracellular trafficking of raft/caveolae domains: insights from integrin signaling. *Semin Cell Dev Biol* **18**: 627-637

Echtermeyer F, Streit M, Wilcox-Adelman S, Saoncella S, Denhez F, Detmar M, Goetinck P (2001) Delayed wound repair and impaired angiogenesis in mice lacking syndecan-4. *J Clin Invest* **107**: R9-R14

Elbashir SM, Harborth J, Lendeckel W, Yalcin A, Weber K, Tuschl T (2001) Duplexes of 21-nucleotide RNAs mediate RNA interference in cultured mammalian cells. *Nature* **411**: 494-498

Frantz C, Stewart KM, Weaver VM (2010) The extracellular matrix at a glance. *Journal of cell science* **123**: 4195-4200

Garton AJ, Tonks NK (1999) Regulation of fibroblast motility by the protein tyrosine phosphatase PTP-PEST. *J Biol Chem* **274**: 3811-3818

Gehlsen KR, Argraves WS, Pierschbacher MD, Ruoslahti E (1988) Inhibition of in vitro tumor cell invasion by Arg-Gly-Asp-containing synthetic peptides. *The Journal of cell biology* **106**: 925-930

Geiger B, Volberg T, Ginsberg D, Bitzur S, Sabanay I, Hynes RO (1990) Broad spectrum pan-cadherin antibodies, reactive with the C-terminal 24 amino acid residues of N-cadherin. *Journal of cell science* **97 (Pt 4)**: 607-614

Ginsberg MH, Partridge A, Shattil SJ (2005) Integrin regulation. *Curr Opin Cell Biol* **17**: 509-516

Gohla A, Birkenfeld J, Bokoch GM (2005) Chronophin, a novel HAD-type serine protein phosphatase, regulates cofilin-dependent actin dynamics. *Nat Cell Biol* **7**: 21-29

Goode BL, Eck MJ (2007) Mechanism and function of formins in the control of actin assembly. *Annu Rev Biochem* **76**: 593-627

Grinnell F (1984) Fibronectin and wound healing. *J Cell Biochem* **26**: 107-116

Gumbiner BM (1996) Cell adhesion: the molecular basis of tissue architecture and morphogenesis. *Cell* **84**: 345-357

Hall A (1998) Rho GTPases and the actin cytoskeleton. *Science* **279**: 509-514

Hall A (2005) Rho GTPases and the control of cell behaviour. *Biochem Soc Trans* **33**: 891-895

Hanks SK, Polte TR (1997) Signaling through focal adhesion kinase. *Bioessays* **19**: 137-145

Harborth J, Elbashir SM, Bechert K, Tuschl T, Weber K (2001) Identification of essential genes in cultured mammalian cells using small interfering RNAs. *Journal of cell science* **114**: 4557-4565

Hassid A, Huang S, Yao J (1999) Role of PTP-1B in aortic smooth muscle cell motility and tyrosine phosphorylation of focal adhesion proteins. *Am J Physiol* **277**: H192-198

Hofmann MC, Narisawa S, Hess RA, Millan JL (1992) Immortalization of germ cells and somatic testicular cells using the SV40 large T antigen. *Exp Cell Res* **201**: 417-435

Hooft van Huijsduijnen R (1998) Protein tyrosine phosphatases: counting the trees in the forest. *Gene* **225**: 1-8

Horwitz A, Duggan K, Buck C, Beckerle MC, Burridge K (1986) Interaction of plasma membrane fibronectin receptor with talin--a transmembrane linkage. *Nature* **320**: 531-533

Humphries MJ (2001) Cell-substrate adhesion assays. *Curr Protoc Cell Biol* **Chapter 9**: Unit 9 1

Humphries MJ, Mostafavi-Pour Z, Morgan MR, Deakin NO, Messent AJ, Bass MD (2005) Integrin-syndecan cooperation governs the assembly of signalling complexes during cell spreading. *Novartis Found Symp* **269**: 178-188; discussion 188-192, 223-130

Hunter T (2002) Tyrosine phosphorylation in cell signaling and disease. *Keio J Med* **51**: 61-71

Hunter T (2009) Tyrosine phosphorylation: thirty years and counting. *Curr Opin Cell Biol* **21**: 140-146

Huveneers S, Danen EH (2009) Adhesion signaling - crosstalk between integrins, Src and Rho. *Journal of cell science* **122**: 1059-1069

Huveneers S, Truong H, Fassler R, Sonnenberg A, Danen EH (2008) Binding of soluble fibronectin to integrin alpha5 beta1 - link to focal adhesion redistribution and contractile shape. *Journal of cell science* **121**: 2452-2462

Hynes RO, Destree AT, Wagner DD (1982) Relationships between microfilaments, cell-substratum adhesion, and fibronectin. *Cold Spring Harb Symp Quant Biol* **46 Pt 2**: 659-670

Hynes RO, Yamada KM (1982) Fibronectins: multifunctional modular glycoproteins. *The Journal of cell biology* **95**: 369-377

Ishiguro K, Kadomatsu K, Kojima T, Muramatsu H, Tsuzuki S, Nakamura E, Kusugami K, Saito H, Muramatsu T (2000) Syndecan-4 deficiency impairs focal adhesion formation only under restricted conditions. *J Biol Chem* **275**: 5249-5252

Ishizaki T, Maekawa M, Fujisawa K, Okawa K, Iwamatsu A, Fujita A, Watanabe N, Saito Y, Kakizuka A, Morii N, Narumiya S (1996) The small GTP-binding protein Rho binds to and activates a 160 kDa Ser/Thr protein kinase homologous to myotonic dystrophy kinase. *EMBO J* **15**: 1885-1893

Ishizaki T, Uehata M, Tamechika I, Keel J, Nonomura K, Maekawa M, Narumiya S (2000) Pharmacological properties of Y-27632, a specific inhibitor of rho-associated kinases. *Mol Pharmacol* **57**: 976-983

Iwanicki MP, Vomastek T, Tilghman RW, Martin KH, Banerjee J, Wedegaertner PB, Parsons JT (2008) FAK, PDZ-RhoGEF and ROCKII cooperate to regulate adhesion movement and trailing-edge retraction in fibroblasts. *Journal of cell science* **121**: 895-905

Jamieson JS, Tumbarello DA, Halle M, Brown MC, Tremblay ML, Turner CE (2005) Paxillin is essential for PTP-PEST-dependent regulation of cell spreading and motility: a role for paxillin kinase linker. *Journal of cell science* **118**: 5835-5847

Janiak A, Zemskov EA, Belkin AM (2006) Cell surface transglutaminase promotes RhoA activation via integrin clustering and suppression of the Src-p190RhoGAP signaling pathway. *Mol Biol Cell* **17**: 1606-1619

Jiang P, Enomoto A, Takahashi M (2009) Cell biology of the movement of breast cancer cells: intracellular signalling and the actin cytoskeleton. *Cancer Lett* **284**: 122-130

Jung SK, Jeong DG, Chung SJ, Kim JH, Park BC, Tonks NK, Ryu SE, Kim SJ (2010) Crystal structure of ED-Eya2: insight into dual roles as a protein tyrosine phosphatase and a transcription factor. *The FASEB journal : official publication of the Federation of American Societies for Experimental Biology* **24**: 560-569

Kim JE, Kim DW, Kwak SE, Kwon OS, Choi SY, Kang TC (2008) Potential role of pyridoxal-5'-phosphate phosphatase/chronopin in epilepsy. *Exp Neurol* **211**: 128-140

Kim JE, Kim DW, Kwak SE, Ryu HJ, Yeo SI, Kwon OS, Choi SY, Kang TC (2009) Pyridoxal-5'-phosphate phosphatase/chronopin inhibits long-term potentiation induction in the rat dentate gyrus. *Hippocampus* **19**: 1078-1089

Kimura K, Ito M, Amano M, Chihara K, Fukata Y, Nakafuku M, Yamamori B, Feng J, Nakano T, Okawa K, Iwamatsu A, Kaibuchi K (1996) Regulation of myosin phosphatase by Rho and Rho-associated kinase (Rho-kinase). *Science* **273**: 245-248

Kolokoltsov AA, Weaver SC, Davey RA (2005) Efficient functional pseudotyping of oncoretroviral and lentiviral vectors by Venezuelan equine encephalitis virus envelope proteins. *J Virol* **79**: 756-763

Kontaridis MI, Eminaga S, Fornaro M, Zito CI, Sordella R, Settleman J, Bennett AM (2004) SHP-2 positively regulates myogenesis by coupling to the Rho GTPase signaling pathway. *Mol Cell Biol* **24**: 5340-5352

Kouns WC, Wall CD, White MM, Fox CF, Jennings LK (1990) A conformation-dependent epitope of human platelet glycoprotein IIIa. *J Biol Chem* **265**: 20594-20601

Krendel M, Zenke FT, Bokoch GM (2002) Nucleotide exchange factor GEF-H1 mediates cross-talk between microtubules and the actin cytoskeleton. *Nat Cell Biol* **4**: 294-301

Laemmli UK (1970) Cleavage of structural proteins during the assembly of the head of bacteriophage T4. *Nature* **227**: 680-685

Legate KR, Wickstrom SA, Fassler R (2009) Genetic and cell biological analysis of integrin outside-in signaling. *Genes Dev* **23**: 397-418

Lenter M, Uhlig H, Hamann A, Jeno P, Imhof B, Vestweber D (1993) A monoclonal antibody against an activation epitope on mouse integrin chain beta 1 blocks adhesion of lymphocytes to the endothelial integrin alpha 6 beta 1. *Proc Natl Acad Sci U S A* **90**: 9051-9055

Leung T, Manser E, Tan L, Lim L (1995) A novel serine/threonine kinase binding the Ras-related RhoA GTPase which translocates the kinase to peripheral membranes. *J Biol Chem* **270**: 29051-29054

Li L, Okura M, Imamoto A (2002) Focal adhesions require catalytic activity of Src family kinases to mediate integrin-matrix adhesion. *Mol Cell Biol* **22**: 1203-1217

Lim ST, Chen XL, Lim Y, Hanson DA, Vo TT, Howerton K, Larocque N, Fisher SJ, Schlaepfer DD, Ilic D (2008a) Nuclear FAK promotes cell proliferation and survival through FERM-enhanced p53 degradation. *Mol Cell* **29**: 9-22

Lim Y, Lim ST, Tomar A, Gardel M, Bernard-Trifilo JA, Chen XL, Uryu SA, Canete-Soler R, Zhai J, Lin H, Schlaepfer WW, Nalbant P, Bokoch G, Ilic D, Waterman-Storer C, Schlaepfer DD (2008b) PyK2 and FAK connections to p190Rho guanine nucleotide exchange factor regulate RhoA activity, focal adhesion formation, and cell motility. *The Journal of cell biology* **180**: 187-203

Liu F, Sells MA, Chernoff J (1998a) Protein tyrosine phosphatase 1B negatively regulates integrin signaling. *Curr Biol* **8**: 173-176

Liu F, Sells MA, Chernoff J (1998b) Transformation suppression by protein tyrosine phosphatase 1B requires a functional SH3 ligand. *Mol Cell Biol* **18**: 250-259

Liu S, Calderwood DA, Ginsberg MH (2000) Integrin cytoplasmic domain-binding proteins. *Journal of cell science* **113 (Pt 20)**: 3563-3571

Loosli Y, Luginbuehl R, Snedeker JG (2010) Cytoskeleton reorganization of spreading cells on micro-patterned islands: a functional model. *Philosophical transactions Series A, Mathematical, physical, and engineering sciences* **368**: 2629-2652

Luo BH, Carman CV, Springer TA (2007) Structural basis of integrin regulation and signaling. *Annu Rev Immunol* **25**: 619-647

Machacek M, Hodgson L, Welch C, Elliott H, Pertz O, Nalbant P, Abell A, Johnson GL, Hahn KM, Danuser G (2009) Coordination of Rho GTPase activities during cell protrusion. *Nature* **461**: 99-103

Maekawa M, Ishizaki T, Boku S, Watanabe N, Fujita A, Iwamatsu A, Obinata T, Ohashi K, Mizuno K, Narumiya S (1999) Signaling from Rho to the actin cytoskeleton through protein kinases ROCK and LIM-kinase. *Science* **285**: 895-898

Maher PA (1993) Activation of phosphotyrosine phosphatase activity by reduction of cell-substrate adhesion. *Proc Natl Acad Sci U S A* **90**: 11177-11181

Maschler S, Wirl G, Spring H, Bredow DV, Sordat I, Beug H, Reichmann E (2005) Tumor cell invasiveness correlates with changes in integrin expression and localization. *Oncogene* **24**: 2032-2041

Matsui T, Amano M, Yamamoto T, Chihara K, Nakafuku M, Ito M, Nakano T, Okawa K, Iwamatsu A, Kaibuchi K (1996) Rho-associated kinase, a novel serine/threonine kinase, as a putative target for small GTP binding protein Rho. *EMBO J* **15**: 2208-2216

McGrath JL (2007) Cell spreading: the power to simplify. *Curr Biol* **17**: R357-358

Miner JH, Yurchenco PD (2004) Laminin functions in tissue morphogenesis. *Annu Rev Cell Dev Biol* **20**: 255-284

Mitra SK, Hanson DA, Schlaepfer DD (2005) Focal adhesion kinase: in command and control of cell motility. *Nature reviews Molecular cell biology* **6**: 56-68

Mitra SK, Schlaepfer DD (2006) Integrin-regulated FAK-Src signaling in normal and cancer cells. *Curr Opin Cell Biol* **18**: 516-523

Moffat J, Grueneberg DA, Yang X, Kim SY, Kloepper AM, Hinkle G, Piqani B, Eisenhaure TM, Luo B, Grenier JK, Carpenter AE, Foo SY, Stewart SA, Stockwell BR, Hacohen N, Hahn WC, Lander ES, Sabatini DM, Root DE (2006) A lentiviral RNAi library for human and mouse genes applied to an arrayed viral high-content screen. *Cell* **124**: 1283-1298

Moon SY, Zheng Y (2003) Rho GTPase-activating proteins in cell regulation. *Trends Cell Biol* **13**: 13-22

Nakagawa O, Fujisawa K, Ishizaki T, Saito Y, Nakao K, Narumiya S (1996) ROCK-I and ROCK-II, two isoforms of Rho-associated coiled-coil forming protein serine/threonine kinase in mice. *FEBS Lett* **392**: 189-193

Nakano I, Dougherty JD, Kim K, Klement I, Geschwind DH, Kornblum HI (2007) Phosphoserine phosphatase is expressed in the neural stem cell niche and regulates neural stem and progenitor cell proliferation. *Stem Cells* **25**: 1975-1984

Narumiya S, Tanji M, Ishizaki T (2009) Rho signaling, ROCK and mDia1, in transformation, metastasis and invasion. *Cancer Metastasis Rev* **28**: 65-76

Neel BG, Gu H, Pao L (2003) The 'Shp'ing news: SH2 domain-containing tyrosine phosphatases in cell signaling. *Trends in biochemical sciences* **28**: 284-293

Nobes CD, Hall A (1995) Rho, rac and cdc42 GTPases: regulators of actin structures, cell adhesion and motility. *Biochem Soc Trans* **23**: 456-459

Owen KA, Pixley FJ, Thomas KS, Vicente-Manzanares M, Ray BJ, Horwitz AF, Parsons JT, Beggs HE, Stanley ER, Bouton AH (2007) Regulation of lamellipodial persistence, adhesion

turnover, and motility in macrophages by focal adhesion kinase. *The Journal of cell biology* **179**: 1275-1287

Pandey RN, Rani R, Yeo EJ, Spencer M, Hu S, Lang RA, Hegde RS (2010) The Eyes Absent phosphatase-transactivator proteins promote proliferation, transformation, migration, and invasion of tumor cells. *Oncogene* **29**: 3715-3722

Pankov R, Yamada KM (2002) Fibronectin at a glance. *Journal of cell science* **115**: 3861-3863

Parsons JT, Horwitz AR, Schwartz MA (2010) Cell adhesion: integrating cytoskeletal dynamics and cellular tension. *Nature reviews Molecular cell biology* **11**: 633-643

Patel RS, Odermatt E, Schwarzbauer JE, Hynes RO (1987) Organization of the fibronectin gene provides evidence for exon shuffling during evolution. *EMBO J* **6**: 2565-2572

Pertz O, Hodgson L, Klemke RL, Hahn KM (2006) Spatiotemporal dynamics of RhoA activity in migrating cells. *Nature* **440**: 1069-1072

Pierschbacher MD, Ruoslahti E (1984) Cell attachment activity of fibronectin can be duplicated by small synthetic fragments of the molecule. *Nature* **309**: 30-33

Playford MP, Schaller MD (2004) The interplay between Src and integrins in normal and tumor biology. *Oncogene* **23**: 7928-7946

Priddle H, Hemmings L, Monkley S, Woods A, Patel B, Sutton D, Dunn GA, Zicha D, Critchley DR (1998) Disruption of the talin gene compromises focal adhesion assembly in undifferentiated but not differentiated embryonic stem cells. *The Journal of cell biology* **142**: 1121-1133

Pytela R, Pierschbacher MD, Ruoslahti E (1985) Identification and isolation of a 140 kd cell surface glycoprotein with properties expected of a fibronectin receptor. *Cell* **40**: 191-198

Ren XD, Kiosses WB, Schwartz MA (1999) Regulation of the small GTP-binding protein Rho by cell adhesion and the cytoskeleton. *EMBO J* **18**: 578-585

Ren XD, Kiosses WB, Sieg DJ, Otey CA, Schlaepfer DD, Schwartz MA (2000) Focal adhesion kinase suppresses Rho activity to promote focal adhesion turnover. *Journal of cell science* **113** (Pt 20): 3673-3678

Ridley AJ, Hall A (2004) Snails, Swiss, and serum: the solution for Rac 'n' Rho. *Cell* **116**: S23-25, 22 p following S25

Roca-Cusachs P, Gauthier NC, Del Rio A, Sheetz MP (2009) Clustering of alpha(5)beta(1) integrins determines adhesion strength whereas alpha(v)beta(3) and talin enable mechanotransduction. *Proc Natl Acad Sci U S A* **106**: 16245-16250

Rossman KL, Der CJ, Sondek J (2005) GEF means go: turning on RHO GTPases with guanine nucleotide-exchange factors. *Nature reviews Molecular cell biology* **6**: 167-180

Sastry SK, Rajfur Z, Liu BP, Cote JF, Tremblay ML, Burrridge K (2006) PTP-PEST couples membrane protrusion and tail retraction via VAV2 and p190RhoGAP. *J Biol Chem* **281**: 11627-11636

Schaller MD, Borgman CA, Cobb BS, Vines RR, Reynolds AB, Parsons JT (1992) pp125FAK a structurally distinctive protein-tyrosine kinase associated with focal adhesions. *Proc Natl Acad Sci U S A* **89**: 5192-5196

Schaller MD, Hildebrand JD, Shannon JD, Fox JW, Vines RR, Parsons JT (1994) Autophosphorylation of the focal adhesion kinase, pp125FAK, directs SH2-dependent binding of pp60src. *Mol Cell Biol* **14**: 1680-1688

Schlaepfer DD, Hunter T (1998) Integrin signalling and tyrosine phosphorylation: just the FAKs? *Trends Cell Biol* **8**: 151-157

Schmidt A, Hall A (2002) The Rho exchange factor Net1 is regulated by nuclear sequestration. *J Biol Chem* **277**: 14581-14588

Schoenwaelder SM, Burrridge K (1999) Bidirectional signaling between the cytoskeleton and integrins. *Curr Opin Cell Biol* **11**: 274-286

Schwartz MA, Schaller MD, Ginsberg MH (1995) Integrins: emerging paradigms of signal transduction. *Annu Rev Cell Dev Biol* **11**: 549-599

Schwarzbauer JE, Sechler JL (1999) Fibronectin fibrillogenesis: a paradigm for extracellular matrix assembly. *Curr Opin Cell Biol* **11**: 622-627

Sechler JL, Takada Y, Schwarzbauer JE (1996) Altered rate of fibronectin matrix assembly by deletion of the first type III repeats. *The Journal of cell biology* **134**: 573-583

Shattil SJ, Kim C, Ginsberg MH (2010) The final steps of integrin activation: the end game. *Nature reviews Molecular cell biology* **11**: 288-300

Shen Y, Schaller MD (1999) Focal adhesion targeting: the critical determinant of FAK regulation and substrate phosphorylation. *Mol Biol Cell* **10**: 2507-2518

Sieg DJ, Ilic D, Jones KC, Damsky CH, Hunter T, Schlaepfer DD (1998) Pyk2 and Src-family protein-tyrosine kinases compensate for the loss of FAK in fibronectin-stimulated signaling events but Pyk2 does not fully function to enhance FAK- cell migration. *EMBO J* **17**: 5933-5947

Smith PK, Krohn RI, Hermanson GT, Mallia AK, Gartner FH, Provenzano MD, Fujimoto EK, Goeke NM, Olson BJ, Klenk DC (1985) Measurement of protein using bicinchoninic acid. *Anal Biochem* **150**: 76-85

Snell K, Fell DA (1990) Metabolic control analysis of mammalian serine metabolism. *Adv Enzyme Regul* **30**: 13-32

Sottile J, Hocking DC, Langenbach KJ (2000) Fibronectin polymerization stimulates cell growth by RGD-dependent and -independent mechanisms. *Journal of cell science* **113 Pt 23**: 4287-4299

Stoker AW (2005) Protein tyrosine phosphatases and signalling. *J Endocrinol* **185**: 19-33

Suehiro K, Gailit J, Plow EF (1997) Fibrinogen is a ligand for integrin alpha5beta1 on endothelial cells. *J Biol Chem* **272**: 5360-5366

Takada Y, Ye X, Simon S (2007) The integrins. *Genome Biol* **8**: 215

Takagi J, Petre BM, Walz T, Springer TA (2002) Global conformational rearrangements in integrin extracellular domains in outside-in and inside-out signaling. *Cell* **110**: 599-511

Timpl R (1993) Proteoglycans of Basement-Membranes. *Experientia* **49**: 417-428

Tomar A, Lim ST, Lim Y, Schlaepfer DD (2009) A FAK-p120RasGAP-p190RhoGAP complex regulates polarity in migrating cells. *Journal of cell science* **122**: 1852-1862

Tomar A, Schlaepfer DD (2009) Focal adhesion kinase: switching between GAPs and GEFs in the regulation of cell motility. *Curr Opin Cell Biol* **21**: 676-683

Towbin H, Staehelin T, Gordon J (1979) Electrophoretic transfer of proteins from polyacrylamide gels to nitrocellulose sheets: procedure and some applications. *Proc Natl Acad Sci U S A* **76**: 4350-4354

Travis MA, Humphries JD, Humphries MJ (2003) An unraveling tale of how integrins are activated from within. *Trends in Pharmacological Sciences* **24**: 192-197

Tuschl T (2002) Expanding small RNA interference. *Nat Biotechnol* **20**: 446-448

Tuschl T, Borkhardt A (2002) Small interfering RNAs: a revolutionary tool for the analysis of gene function and gene therapy. *Mol Interv* **2**: 158-167

van Horck FP, Ahmadian MR, Haeusler LC, Moolenaar WH, Kranenburg O (2001) Characterization of p190RhoGEF, a RhoA-specific guanine nucleotide exchange factor that interacts with microtubules. *J Biol Chem* **276**: 4948-4956

Vicente-Manzanares M, Choi CK, Horwitz AR (2009a) Integrins in cell migration--the actin connection. *Journal of cell science* **122**: 199-206

Vicente-Manzanares M, Hodges J, Horwitz AR (2009b) Dendritic Spines: Similarities with Protrusions and Adhesions in Migrating Cells. *Open Neurosci J* **3**: 87-96

Wang YL, Taylor DL (1980) Preparation and characterization of a new molecular cytochemical probe: 5-iodoacetamidofluorescein-labeled actin. *J Histochem Cytochem* **28**: 1198-1206

Watanabe N, Kato T, Fujita A, Ishizaki T, Narumiya S (1999) Cooperation between mDia1 and ROCK in Rho-induced actin reorganization. *Nat Cell Biol* **1**: 136-143

Watanabe N, Madaule P, Reid T, Ishizaki T, Watanabe G, Kakizuka A, Saito Y, Nakao K, Jockusch BM, Narumiya S (1997) p140mDia, a mammalian homolog of *Drosophila* diaphanous, is a target protein for Rho small GTPase and is a ligand for profilin. *EMBO J* **16**: 3044-3056

Webb DJ, Donais K, Whitmore LA, Thomas SM, Turner CE, Parsons JT, Horwitz AF (2004) FAK-Src signalling through paxillin, ERK and MLCK regulates adhesion disassembly. *Nat Cell Biol* **6**: 154-161

Wennerberg K, Rossman KL, Der CJ (2005) The Ras superfamily at a glance. *Journal of cell science* **118**: 843-846

Wolfenson H, Henis YI, Geiger B, Bershadsky AD (2009) The heel and toe of the cell's foot: a multifaceted approach for understanding the structure and dynamics of focal adhesions. *Cell Motil Cytoskeleton* **66**: 1017-1029

Woods A, Couchman JR, Johansson S, Hook M (1986) Adhesion and cytoskeletal organisation of fibroblasts in response to fibronectin fragments. *EMBO J* **5**: 665-670

Xiong JP, Stehle T, Diefenbach B, Zhang R, Dunker R, Scott DL, Joachimiak A, Goodman SL, Arnaout MA (2001) Crystal structure of the extracellular segment of integrin alpha Vbeta3. *Science* **294**: 339-345

Xiong JP, Stehle T, Goodman SL, Arnaout MA (2003) New insights into the structural basis of integrin activation. *Blood* **102**: 1155-1159

Xu J, Wang F, Van Keymeulen A, Herzmark P, Straight A, Kelly K, Takuwa Y, Sugimoto N, Mitchison T, Bourne HR (2003) Divergent signals and cytoskeletal assemblies regulate self-organizing polarity in neutrophils. *Cell* **114**: 201-214

Yamada KM, Geiger B (1997) Molecular interactions in cell adhesion complexes. *Curr Opin Cell Biol* **9**: 76-85

Zaidel-Bar R, Itzkovitz S, Ma'ayan A, Iyengar R, Geiger B (2007a) Functional atlas of the integrin adhesome. *Nat Cell Biol* **9**: 858-867

Zaidel-Bar R, Milo R, Kam Z, Geiger B (2007b) A paxillin tyrosine phosphorylation switch regulates the assembly and form of cell-matrix adhesions. *Journal of cell science* **120**: 137-148

Zhai J, Lin H, Nie Z, Wu J, Canete-Soler R, Schlaepfer WW, Schlaepfer DD (2003) Direct interaction of focal adhesion kinase with p190RhoGEF. *J Biol Chem* **278**: 24865-24873

Zhang EE, Chapeau E, Hagihara K, Feng GS (2004a) Neuronal Shp2 tyrosine phosphatase controls energy balance and metabolism. *Proc Natl Acad Sci U S A* **101**: 16064-16069

Zhang SQ, Yang W, Kontaridis MI, Bivona TG, Wen G, Araki T, Luo J, Thompson JA, Schraven BL, Philips MR, Neel BG (2004b) Shp2 regulates SRC family kinase activity and Ras/Erk activation by controlling Csk recruitment. *Mol Cell* **13**: 341-355

Zhu J, Luo BH, Xiao T, Zhang C, Nishida N, Springer TA (2008) Structure of a complete integrin ectodomain in a physiologic resting state and activation and deactivation by applied forces. *Mol Cell* **32**: 849-861

Zoudilova M, Kumar P, Ge L, Wang P, Bokoch GM, DeFea KA (2007) Beta-arrestin-dependent regulation of the cofilin pathway downstream of protease-activated receptor-2. *J Biol Chem* **282**: 20634-20646

10 Curriculum Vitae

Name:	Ambrish Saxena
Date of Birth:	20.06.1979
Gender:	Male
Nationality:	Indian
Languages:	English, Hindi and German (basic)
Marital Status:	Married
Email:	saxenaambrish@gmail.com , ambrish.saxena@virchow.uni-wuerzburg.de

Education

1997-2000 Bachelor of Science (B. Sc (H) Biochemistry)

Department of Biochemistry,
University of Delhi, New Delhi, India.

2000-2002 Master of Science (M. Sc. Biochemistry)

Department of Biochemistry, **All India Institute of Medical Sciences (AIIMS)**, New Delhi, India.

2009-2011 PhD student in Department of Pharmacology, University of Würzburg, Germany.

Research experience

- 1) Worked from June 2002-Sep. 2003 at **National Institute of Immunology, New Delhi, India** in a Wellcome Trust funded project entitled "Dissecting the functional role of Polyketide Synthases"
- 2) Worked from Oct. 2003-Aug. 2004 at the Institute for Biosynthesis of Neuronal Structures in **Center for Molecular Neurobiology Hamburg (ZMNH)** on extracellular matrix molecules and its interaction with the APP.
- 3) Jan. 2005- 2008, Neurology Department, **University of Düsseldorf**.
Project title: 'Bax inhibitor-1 links Ca²⁺ release from intracellular stores and influx through the

plasma membrane'

- 4) Jan. 2009-Aug. 2009, **Institute for Biochemistry and Mol. Biology II, University of Düsseldorf**. Position funded by DFG SFB 728 with Prof. Dr. A. Gohla as a PhD student.
- 5) Sep. 2009-present, **Institute of Pharmacology and Rudolf Virchow Center for Experimental Biomedicine, University of Würzburg**. Ph.D position funded by DFG, SFB 688 , University of würzburg
Project title: 'Role of AUM, a novel human tyrosine phosphatase, in cell adhesion and migration'
with Prof. Dr. A. Gohla as a PhD student.

Conferences and Symposiums

1. Poster presented at **Euro-phosphatases 2009, EMBO conference**, July 14-18, 2009 Egmond aan Zee, The Netherlands. Poster title "*Characterization of AUM, a novel aspartate-dependent protein tyrosine phosphatase*".
2. Talk at **51st Annual Meeting of the German society for Pharmacology and Toxicology (DGPT)** from March 23 – 25, 2010 Mainz, Germany. Talk title "*Identification and Characterization of AUM, a novel human tyrosine phosphatase*".
3. Poster presented at **International conference on Actin Dynamics**, organized by German society for Cell Biology from September 15-18, 2010 at Jena, Germany. Poster title '*Role of AUM, a novel human tyrosine phosphatase in cell adhesion and spreading*'.
4. Poster presented at **Joint symposium of SFB 688 and 612**, from October 7-8, 2010, Bad Brueckenau, Germany. Poster title '*Role of the tyrosine phosphatase AUM for cell adhesion and spreading*'.

11 Erklärung

Hiermit erkläre ich an Eides statt dass ich die vorliegende Dissertation mit dem Title '*Role of the novel protein tyrosine phosphatase AUM for cell adhesion*' selbständig angefertigt und keine anderes als die von mir angegebenen Quellen und Hilfsmittel verwendet habe.

Weiterhin erkläre ich dass diese dissertation weder in gleicher noch in ähnlicher form bereits ein einem anderen Prüfungsverfahren vorgelegen ist.

Würzburg, November 2011

Amrish Saxena

12 Acknowledgements

The friend in my adversity I shall always cherish most. I can better trust those who helped to relieve the gloom of my dark hours than those who are so ready to enjoy with me the sunshine of my prosperity. - Ulysses S. Grant (18th President of the United States)

I chose to start my acknowledgement with the above words from President Grant. These words truly represent my feelings at this moment and I dedicate these words to my supervisor. I joined Prof. Dr. Antje Gohla at a time when I had lost all hopes and even confidence in myself. It was Antje's brilliant support both professionally and personally that I see this work completed today. I am thankful to Antje for allowing me to work on the novel phosphatase AUM and today I can proudly associate myself with the discovery of a novel enzyme. I am falling short of words to thank the real *Guru* I found after many years of searching. During my stay in her lab she treated me much more than a Ph.D. student in her lab. She made sure that all my wishes are granted in-time without making me even realize what she has gone through to accomplish them. Hearty thanks Antje for all that you have done for me and Salutes to your wonderful spirit towards life.

Another equally important person is Dr. Elisabeth Jeanclos. Without her support and encouragement this work would not have reached the stage that it is now. 'EJ' as we call her in the lab is one of the finest scientist and a wonderful human being I have ever met. It was Elisabeth who actually thought me the real meaning of 'Perfection in science' by the way she conducted her experiments. I learnt from EJ the art of critically analyzing the data. I shall remember her golden words lifetime "Devil lies in the details". Elisabeth thanks for giving me power of selfbelief. I shall never forget the way you cherish and live life. I hope I can live my life the way you taught me during our intense discussions. I do not think that I will get a better dancing partner than you again in life. Thanks for all the fun and science you gave me.

I would also like to thank my second thesis supervisor Prof. Jörg Schultz for kindly accepting this responsibility.

Now I want to thank my lab colleagues who have a lasting impact in this work. First I want to thank Dr. Prashant Duraphe for handing me over such a brilliant and productive project. Annegrit was someone special I met in the lab. She was a constant source of motivation and constructive criticism. Now AUM is in her hands and I am sure she is taking the best care of this enzyme. I would also like to thank Gunnar and Markus (Brother Markus) for all the fun and great time we had together. I did not get much opportunity to work with Gabriela and Angela, but the little time we spent together in the lab touched me deeply. I thank you both for your co-operation during my last days in the lab. Apart from these people I would like to thank Katharina, Melanie and Simon for continuing my work on AUM. I regard your contributions for the success of AUM. Lab would not have been so much fun without our technical support. Kerstin, Karina, Beate and Angelika are not only expert technical support but great human beings as well. I owe all you four

a lot for my success today. I will always miss my morning coffee time that I used to spend with you all in the lab.

My wife Dr. Vasudharani Devanathan is an inseparable part of this thesis. Vasu, is not just a wife rather she is the store-house of all my energy. Without her motivation and courage this day was definitely unachievable. Thanks Vasu for standing by me in hot and cold, day and night. I have no words to thank you for the belief you have in me and my capabilities. If I am a blind man you are my walking stick. This thesis is a result of your long years of patience and confidence in me.

My sister is equally instrumental in completion of this work It was her prayers and support in my every move since childhood that I am able to see this beautiful morning of my long dark night.

In the end I would like to thank my parents. I suppose the word 'thanks' is small for the role they have played in my tough and happy times. Actually I would like to dedicate this work to my mother. It's her never-say-die spirit and principles of life that has led me to this stage that I can again stand after falling from sky. My father actually taught me the meaning of hard work and patience. I really love my mother for her support but I respect my father for inculcating the values of life in me.

My job will remain unfulfilled if I do not appreciate all my friends and well-wishers for their constant support and motivation. I must say that Deutschland is a great country of brainy and disciplined people. I was touched with the extreme simplicity and open-mindedness of the people from this great country.

Lastly I want to celebrate AUM. It is believed that before creation began it was the emptiness or the void. This void is more than nothingness, because everything then existed in a latent state of potentiality. The vibration of "AUM" symbolizes the manifestation of God in form. "AUM" is the reflection of the absolute reality, it is said to be "Adi Anadi", without beginning or the end and embracing all that exists. If one realizes the AUM phosphatase perfectly fits its name.

I close with these motivating lines from Bhagvad Gita.

"you are bound to discharge your duties with devotion. Don't expect the fruits of your deeds. Don't remain idle. Expect nothing in return (for your deeds). He alone gives the results for your deeds. The deeds should go on unmindful of their fruits as anything done for enjoyment enslaves us to desire. Whatever one does with desire binds us to the cycle of birth and death."

- Bhagvad Gita

AUM tat sat



